Selective permeation through modified vinylindene fluoride membranes
by Ronanth Zavaleta

A thesis submitted in partial fulfillment of the requirements for the degree DOCTOR OF PHILOSOPHY in Chemical Engineering
Montana State University
© Copyright by Ronanth Zavaleta (1975)

Abstract:
A permeation apparatus was developed for determining permeability coefficients of gases and mixtures of gases oyer a wide range of temperatures and pressures.

Several chemicals were tested as modifiers for vinylidene fluoride based membranes, primarily for the separation of sulfur dioxide from SO2/N2 mixtures. Sulfolene was found to be a very selective modifier for the separation of sulfur dioxide. The effect of the sulfolene content in the membrane was investigated, and an 18 wt% sulfolene was found to be a good membrane composition. The permeability coefficients for sulfur dioxide, nitrogen, hydrogen, carbon, dioxide, carbon monoxide, oxygen, argon, methane, ethane, ethylene and 1,3 butadiene were determined. The permeability coefficients for SO2 were found to be 4 orders of magnitude greater than those of N2, CO, O2, Ar, CH4, C2H6, C2H4 and 1,3 butadiene; about 3 orders of magnitude greater than those for hydrogen, and about 2 orders of magnitude greater than those for carbon dioxide.

The permeability coefficients for SO2 decrease with increasing temperature. For the other gases studied, except CO2, the coefficients increase with temperature. CO2 shows a mixed behavior. The permeabilities were found to be exponential functions of pressure and temperatures, except for N2, CO and Ar, which are independent of pressure.

Very efficient separations of SO2 from SO2/N2 mixtures were obtained. A permeate containing 95.5 vol. % SO2 was obtained for an exhaust gas SO2 concentration of 5.6 vol. %, with permeate flow rates of about 1 x 10^-3 cc(STP)/cm^2.sec, at O°C and 315 psia upstream pressure. Separation of CO2 from CO2/H2 mixtures was found to be possible. Separation factors of about 2.5 were obtained for CO2.

When working with mixtures of gases a very strong plasticizing effect by the sorbed gas on the membrane was noticed, which, was stronger at lower temperatures, where the deviations from ideality are greater.

SELECTIVE PERMEATION THROUGH MODIFIED VINYLIDENE FLUORIDE MEMBRANES

by

RONANTH ZAVALETA

A thesis submitted in partial fulfillment
of the requirements for the degree

of

DOCTOR OF PHILOSOPHY

in

Chemical Engineering

Approved:

Lloyd Berg
Head, Major Department

J. N. McCandless
Chairman, Examining Committee

Henry L. Parsons
Graduate Dean

MONTANA STATE UNVERSITY
Bozeman, Montana

June, 1975

ACKNOWLEDGMENT

The author wishes to thank the entire staff of the Chemical Engineering Department of Montana State University for their advice, questions and criticisms, which helped guide this investigation.

The author is indebted to Dr. F. P. McCandless, for his advice, assistance and encouragement throughout the course of this project. Thanks goes to James Tillery and Silas Huso who helped in building the apparatus and tracking down various parts and pieces of equipment during the work.

The author gratefully acknowledges financial support, in the form of a scholarship, from the Organization of American States.

The author wishes to thank his mother, whose example and encouragement were fully and unselfishly provided. The author also wishes to thank his wife and son, for their sacrifices and support.

Finally, thanks goes to Sherry Greene for typing this thesis.

TABLE OF CONTENTS

		Page
VITA		ii
ACKNOWLEDGEMENT		iii
LIST OF TABLES		viii
LIST OF FIGURES		ix
ABSTRACT		xii
I.	INTRODUCTION AND PURPOSE	1
II.	REVIEW OF LITERATURE	4
	LIQUID MEMBRANES	4
	MODIFIED NON-LIQUID POLYMERIC MEMBRANES	6
III.	THEORETICAL BACKGROUND	8
	THE NATURE OF THE TRANSPORT PROCESS	8
	TRANSPORT THROUGH A GASEOUS FILM	8
	TRANSPORT THROUGH A POLYMERIC MEMBRANE	11
	DEFINITION OF THE OVERALL MASS TRANSFER COEFFICIENT	16
	DEFINITION OF THE PSEUDO-PERMEABILITY COEFFICIENT	17
	DEFINITION OF THE SEPARATION FACTOR	18
	CHARACTERIZATION OF A GASEOUS SEPARATION	19
IV.	EXPERIMENTAL EQUIPMENT AND PROCEDURES	20
	DESCRIPTION OF EQUIPMENT	20
	1. PERMEATION CELL	20

TABLE OF CONTENTS (Cont).

		Page
2.	CONSTANT TEMPERATURE ENCLOSURE	20
	a. LOW & INTERMEDIATE TEMP. (0-35°C)	23
	b. HIGH TEMPERATURES (35-55°C)	25
3.	PRESSURE MEASUREMENT AND CONTROL	27
4.	FLOW RATE MEASUREMENT	28
5.	ANALYSES SECTION	28
6.	STORAGE AND FEEDING FACILITIES	30
7.	LINES	30
8.	MATERIALS	30
	EXPERIMENTAL PROCEDURE	32
1.	CALIBRATION OF GAS CHROMATOGRAPH	32
2.	CALIBRATION OF EXHAUST GAS ROTAMETER	36
3.	MEMBRANE MANUFACTURE	36
4.	OPERATION PROCEDURE	39
V.	EXPERIMENTAL RESULTS AND DISCUSSION	41
	MEMBRANE MODIFIERS	41
1.	THE DATA	41
2.	DISCUSSION	41
	EFFECT OF THE SULFOLENE CONTENT	46
1.	THE DATA	46
2.	DISCUSSION	46

TABLE OF CONTENTS (Cont).

		Page
	PERMEABILITY COEFFICIENTS FOR SULFUR DIOXIDE	50
	1. THE DATA	50
	2. DISCUSSION	50
	PERMEABILITY COEFFICIENTS FOR NITROGEN, CARBON MONOXIDE AND ARGON.	57
	1. THE DATA	57
	2. DISCUSSION	58
	PERMEABILITY COEFFICIENTS FOR CARBON DIOXIDE	68
	1. THE DATA	68
	2. DISCUSSION	68
	PERMEABILITY COEFFICIENTS FOR OXYGEN, HYDROGEN, METHANE, ETHANE, ETHYLENE, 1-3 BUTADIENE.	75
	1. THE DATA	75
	2. DISCUSSION	75
	SEPARATION OF SO_2/N_2 MIXTURES.	100
	1. THE DATA	100
	2. DISCUSSION	101
	SEPARATION OF CO_2/H_2 MIXTURES.	108
	1. THE DATA	108
	2. DISCUSSION	112
	ANALYSIS OF ERRORS	119
VI.	CONCLUSIONS AND RECOMMENDATIONS.	120

TABLE OF CONTENTS (Cont).

		Page
	CONCLUSIONS	120
	RECOMMENDATIONS	122
VII.	APPENDIX	124
	NOMENCLATURE	125
	SUBSCRIPTS	126
	GREEK LETTERS	126
VIII.	BIBLIOGRAPHY	127

LIST OF TABLES

Table		Page
V-1	Effect of Modifiers in the Performance of Vinylidene Fluoride Membranes	42
V-2	Effect of the Sulfolene Content in the Performance of Vinylidene Fluoride Membranes.	47
V-3	Permeability Coefficient for Sulfur Dioxide.	51
V-4	Permeability Coefficient for Nitrogen.	63
V-5	Permeability Coefficient for Carbon Monoxide	65
V-6	Permeability Coefficient for Argon	67
V-7	Permeability Coefficient for Carbon Dioxide.	69
V-8	Permeability Coefficient for Oxygen.	76
V-9	Permeability Coefficient for Hydrogen.	78
V-10	Permeability Coefficient for Methane	81
V-11	Permeability Coefficient for Ethane.	84
V-12	Permeability Coefficient for Ethylene.	86
V-13	Permeability Coefficient for 1,3 Butadiene	88
V-14	Separation of SO_2/N_2 Mixtures.	102
V-15	Separation of CO_2/H_2 Mixtures Vol % 48.5	109
V-16	Separation of CO_2/H_2 Mixtures Vol % 3.3	111

LIST OF FIGURES

Figure		Page
III-1	Concentration Profiles of i in the Membrane and its Neighborhood	9
IV-1	Simplified Diagram of Permeation Equipment	21
IV-2	Diagram of Permeation Cell	22
IV-3	Constant Temperature Enclosure - Low Temperatures.	24
IV-4	Constant Temperature Enclosure - High Temperatures	26
IV-5	Calibration of Gas Chromatograph. Sample Volume vs. Peak Weight x Attenuation for Nitrogen and Sulfur Dioxide.	34
IV-6	Calibration Curve for Gas Chromatograph. Area Percent of SO_2 Peak vs. SO_2 Volume Percent.	35
IV-7	Calibration of Gas Chromatograph. Sample Volume vs. Peak Weight x Attenuation for Carbon Dioxide.	37
IV-8	Calibration Curve for Rotameter. Flow Rate (STP) vs. Rotameter Reading.	38
V-1	Pseudo-Permeability Coefficient for SO_2 vs. Modifier Content.	43
V-2	Permeate and Exhaust Gas SO_2 Volume % vs. Modifier Content	45
V-3	Pseudo-Permeability Coefficients for SO_2 vs. $10^3/T$ for Various Sulfolene Concentrations in the Membrane	48
V-4	Pseudo-Permeability Coefficients for N_2 vs $10^3/T$ for Various Sulfolene Concentrations in the Membrane	49
V-5	Permeability Coefficient vs. Pressure Differential for Sulfur Dioxide	54
V-6	Permeability Coefficient vs. $10^3/T$ for Sulfur Dioxide.	56
V-7	Permeability Coefficient vs. Pressure Differential for Nitrogen	59

LIST OF FIGURES (Cont).

Figure		Page
V-8	Permeability Coefficient vs. Pressure Differential for Carbon Monoxide	60
V-9	Permeability Coefficient vs. Pressure Differential for Argon	61
V-9A	Permeability Coefficient vs. $10^3/T$ for Carbon Monoxide and Nitrogen	62
V-10	Permeability Coefficient vs. Pressure Differential for Carbon Dioxide	72
V-11	Permeability Coefficient vs. $10^3/T$ for Carbon Dioxide	73
V-12	Permeability Coefficient vs. Pressure Differential for Oxygen	89
V-13	Permeability Coefficient vs. Pressure Differential for Hydrogen	90
V-14	Permeability Coefficient vs. Pressure Differential for Methane	91
V-15	Permeability Coefficient vs. Pressure Differential for Ethane	92
V-16	Permeability Coefficient vs. Pressure Differential for Ethylene	93
V-17	Permeability Coefficient vs. Pressure Differential for 1,3 Butadiene	94
V-18	Permeability Coefficient vs. $10^3/T$ for Oxygen	95
V-19	Permeability Coefficient vs. $10^3/T$ for Hydrogen	96
V-20	Permeability Coefficient vs. $10^3/T$ for Methane	97
V-21	Permeability Coefficient vs. $10^3/T$ for Ethane	98
V-22	Permeability Coefficient vs. $10^3/T$ for Ethylene	99

LIST OF FIGURES (Cont).

Figure		Page
V-23	Pseudo-Permeability Coefficient vs. Partial Pressure Differential for Sulfur Dioxide	104
V-24	Pseudo-Permeability Coefficient vs. Partial Pressure Differential for Nitrogen	105
V-25	Separation Factor α vs. Partial Pressure Differential for Sulfur Dioxide.	106
V-26	Pseudo-Permeability Coefficient vs. Partial Pressure Differential for Carbon Dioxide	113
V-27	Pseudo-Permeability Coefficient vs. Partial Pressure Differential for Hydrogen	114
V-28	Separation Factor α vs. Partial Pressure Differential for Carbon Dioxide.	115
V-29	Pseudo-Permeability Coefficient vs. Partial Pressure Differential for Carbon Dioxide	117
V-30	Pseudo-Permeability Coefficient vs. Partial Pressure Differential for Hydrogen	118

ABSTRACT

A permeation apparatus was developed for determining permeability coefficients of gases and mixtures of gases over a wide range of temperatures and pressures.

Several chemicals were tested as modifiers for vinylidene fluoride based membranes, primarily for the separation of sulfur dioxide from SO_2/N_2 mixtures. Sulfolene was found to be a very selective modifier for the separation of sulfur dioxide. The effect of the sulfolene content in the membrane was investigated, and an 18 wt% sulfolene was found to be a good membrane composition. The permeability coefficients for sulfur dioxide, nitrogen, hydrogen, carbon dioxide, carbon monoxide, oxygen, argon, methane, ethane, ethylene and 1,3 butadiene were determined. The permeability coefficients for SO_2 were found to be 4 orders of magnitude greater than those of N_2, CO, O_2, Ar, CH_4, C_2H_6, C_2H_4 and 1,3 butadiene; about 3 orders of magnitude greater than those for hydrogen, and about 2 orders of magnitude greater than those for carbon dioxide.

The permeability coefficients for SO_2 decrease with increasing temperature. For the other gases studied, except CO_2, the coefficients increase with temperature. CO_2 shows a mixed behavior. The permeabilities were found to be exponential functions of pressure and temperatures, except for N_2, CO and Ar, which are independent of pressure.

Very efficient separations of SO_2 from SO_2/N_2 mixtures were obtained. A permeate containing 95.5 vol. % SO_2 was obtained for an exhaust gas SO_2 concentration of 5.6 vol. %, with permeate flow rates of about 1×10^{-3} cc(STP)/cm^2.sec, at 0°C and 315 psia upstream pressure. Separation of CO_2 from CO_2/H_2 mixtures was found to be possible. Separation factors of about 2.5 were obtained for CO_2.

When working with mixtures of gases a very strong plasticizing effect by the sorbed gas on the membrane was noticed, which was stronger at lower temperatures, where the deviations from ideality are greater.

INTRODUCTION AND PURPOSE

The selective permeation of gases through nonporous polymeric membranes is a potentially effective separation technique that has attracted much attention since the early 1950's. This technique has made considerable progress in recent years in areas such as the development of more permeable and selective membranes, as well as of efficient permeation equipment for large scale operations.

The study of selective permeation is generally motivated by the economic necessity of developing more competitive separation methods. The investigation of carbon dioxide control is perhaps an exception, since it has been aimed towards a reduction in the weight and size of separation equipment used in aerospace missions.

In order to determine the potential usefulness of a gas permeation process, whether in terms of process economics or hardware requirements, it is important to determine the membrane area and the number of stages that are necessary to perform the desired separation. The membrane area requirements are of particular interest from an economic point of view because they determine a large fraction of the investment costs of a large permeation plant. Studies indicate that these costs may constitute as much as 95% of the total costs of a gas permeation process (1, 2).

Sulfur oxides are the most common air pollutants, and result mainly from processes burning high sulfur coal (power generation) and some metallurgical operations such as roasting, smelting and refining of

copper and lead ores. An economic way of separating these oxides from gaseous mixtures is not available yet. The alternative of discontinuing the operations that generate these pollutants seems highly unlikely in view of the limited reserves of other traditional sources of energy and raw materials, and the still distant future of some other non-conventional forms of energy.

It is then necessary to search for improved methods of separation of these oxides, and especially of sulfur dioxide, from the most common mixture of gases, that will probably include nitrogen, oxygen, carbon dioxide, carbon monoxide and probably some hydrocarbons and hydrogen. In an attempt to contribute to the realization of these ultimate goals, this work was undertaken with the following specific objectives in mind:

(1) To design and construct an improved permeation apparatus suitable for the accurate determination of the permeability coefficients of a wide variety of membrane - gaseous mixtures systems, over a broad range of temperatures and pressures.

(2) To determine a membrane composition and manufacturing technique that gives a high selectivity with respect to SO_2.

(3) To investigate over a wide range of temperatures and pressures, the selectivity of the improved membrane with respect to other gases that form mixtures with sulfur dioxide in industrial processes.

(4) To determine operating conditions that give the best separation over the range of temperatures and pressures studied.

(5) To investigate the possibility of performing other gas separations that are of practical interest, by using the membranes developed.

REVIEW OF THE LITERATURE

The best results in the separation of acid gases have been obtained using modified polymeric membranes. Among these:

A. LIQUID MEMBRANES

One of the most successful separations of sulfur dioxide from mixtures containing mainly nitrogen, oxygen and carbon dioxide, has been achieved by means of the so called "liquid membranes". The use of these membranes for gas separations has been disclosed in U. S. Patent No. 3,335,545 Robb et al.(3). Basically the process consists of including a highly selective solvent in the membrane, resulting in a considerable increase in the degree of separation of certain gases. Immobilization or support of the solvent in the membrane can be accomplished in different ways. The liquid can be supported in a non-interacting polymer in such a way to insure that the solvent is the controlling factor. Also, a thin film of the solvent can be supported by a porous, unwet backing having such small holes that the liquid cannot flow through it.

A subsequent improvement over the Robb et al. immobilized liquid membrane was that of Ward et al. U. S. Patent 3,396,510 (4), embodying the phenomenon described as "facilitated transport", applied to the transfer of carbon dioxide, sulfur dioxide and oxygen across liquid membranes. In the case of sulfur dioxide, a large concentration difference of ions HSO_3^- and $SO_3^=$ was used in the immobilized liquid

film. These ions are termed "carrier species" and must be non-volatile and reversible chemically reactive with the gaseous component, the transport of which is being facilitated.

The next step was to look for better solvents for given separations. The U. S. Patent 3,506,186, Ward (5), was issued in the preparation of liquid membranes for sulfur dioxide extraction. Advantage is taken of the high solubility of SO_2 in tetraethylene glycol-dimethyl ether (TEG-DME). The separation is accomplished using a liquid film of this solvent. A suitable film construction employs a thin porous cellulose layer impregnated with the solvent. First a porous membrane of modified cellulose derivation is prepared, hydrolized to cellulose, the hydrolizing agent is leached out and the newly formed cellulose film is impregnated with the liquid glycol.

Preliminary permeability measurements of the immobilized film of TEG-DME have indicated permeability coefficients of about $10{,}000 \times 10^{-9}$ cc(STP). cm/sq cm.sec.cm Hg for SO_2, 3.2×10^{-9} cc(STP). cm/sq cm.sec.cm Hg for N_2 and $105. \times 10^{-9}$ cc(STP).cm/sq cm.sec.cmHg for CO_2 at 25°C. The ratio of permeability coefficients is of about 3100 for the SO_2/N_2 system and of about 95 for the SO_2/CO_2 system. Thus, this membrane is highly selective for SO_2 and has the advantage of being essentially non volatile at room temperature, and with the potential use of glycols of higher molecular weight for higher temperature separations. Ward (5), claims that a permeate of more than 95% SO_2 could be obtained

out of a 10% feed gas, provided the downstream of the liquid membrane be subjected to vacuum or to sweep gas.

B. MODIFIED NON-LIQUID POLYMERIC MEMBRANES

Seibel and McCandless (6) used vinylidene fluoride membranes modified with sulfolane (tetrahydrothiophene 1, 1-dioxide) to separate SO_2 from SO_2/N_2 mixtures. These membranes were made by dissolving vinylidene fluoride and sulfolane in dimethyl formamide. The films were cast on glass plates between thicknesses of masking tape. The solvent was evaporated placing the plates in an electrically heated oven. The membrane was found to be quite selective to SO_2. Maximum separation was achieved with 8% sulfolane in the membrane at 400 psi. The selectivity decreased with increasing temperature. Permeation rate increased with increasing pressure and with increasing amount of sulfolane in the membrane. The greatest separation achieved was with a feed of 12.5% SO_2 at 400 psi and 23°C. The permeate at these conditions was 93.5% SO_2 and the flux, 1.86 $ft^3(STP)/ft^2 day$.

Tajar and Miller (7) studied the permeation of CO_2, O_2 and N_2 through a four component membrane system, polyethylenimine-polyvinyl-butyral-epoxy-water, using a variable pressure technique. To make the membrane the ingredients were dissolved in a compatible mixed solvent system. The films were cast on glass plates, dried in oven and removed from the casting surface by soaking in water. The membrane was found

to be quite selective to CO_2 over O_2 and N_2. The permeability coefficient ratios were of the order of 30:1 or greater, compared to typical ratios for inert membrane systems of the order of 4:1 or 5:1.

In general for all the systems reviewed, it appears that the high selectivity with respect to acid gases is a result of reversible chemical reactions that increase greatly the solubility of these gases in the active ingredient of the membrane (7, 5).

THEORETICAL BACKGROUND

A. THE NATURE OF THE TRANSPORT PROCESS

The permeation of a gaseous mixture through a solid polymeric material includes three different transport stages:

(1) Transport from the gas mixture to the surface of the membrane.

(2) Transport through the membrane.

(3) Transport from the membrane to the stream of permeate.

B. TRANSPORT THROUGH A GASEOUS FILM

The steady state transport of gas A from the bulk stream in the high pressure side of the cell to the surface of the membrane may be treated as the sum of a diffusional contribution and a bulk flow contribution:

$$N_A = c\, D_{AB} \frac{dx_A}{dz} + x_A (N_A + N_B) \qquad \text{III-1}$$

The diffusional contribtuion is proportional to the concentration gradient at the interface, therefore should be roughly proportional to some characteristic composition difference Δx_A between the surface of the membrane and the main stream. The bulk flow contribtuion on the other hand, is independent of any concentration difference (8). It seems adequate to define a local high mass transfer coefficient $k^{\bullet}_{x,loc}$ in terms of the diffusion of species A normal to the interface:

$$J^{*}_{A_z}\Big|_{z=0} = k^{\bullet}_{x,loc}\, \Delta x_A$$

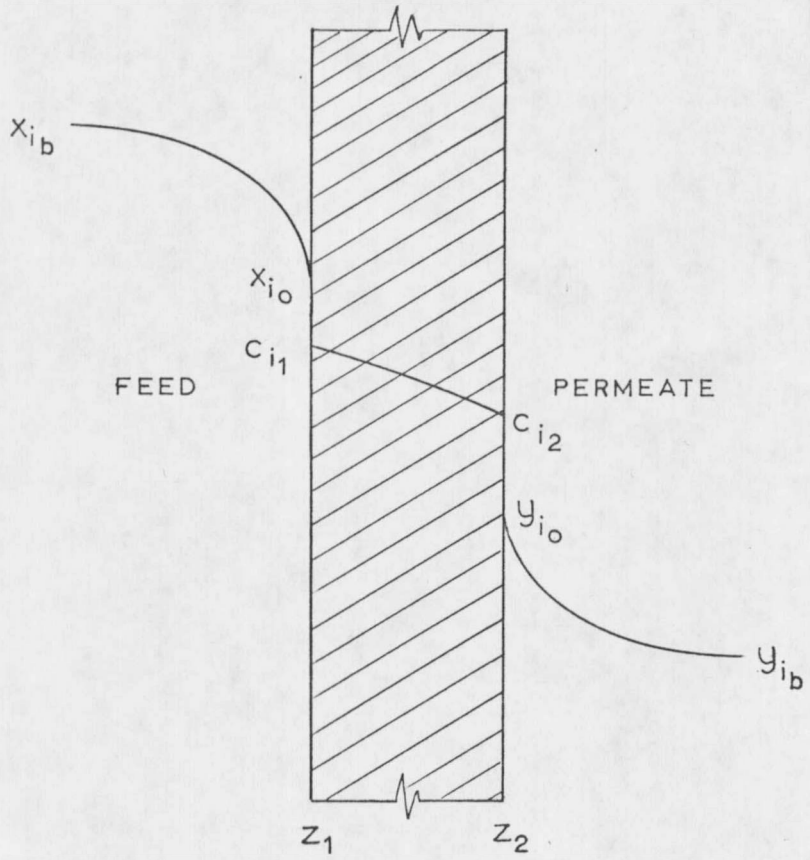

FIGURE III-1. CONCENTRATION PROFILES OF i IN THE MEMBRANE AND ITS NEIGHBORHOOD

Or in terms of the rate of diffusion of species A normal to the interface:

$$N_{A_o} - x_{A_o} (N_{A_o} + N_{B_o}) = k^{\cdot}_{x,loc} \Delta x_A \qquad \text{III-2}$$

The coefficient $k^{\cdot}_{x,loc}$ is a function also of the rate of mass transfer. This effect arises from the distortion of the velocity and concentration profiles by the flow of A and B through the interface (9). For the case of small mass-transfer rates N_{A_o} and N_{B_o}, these effects may be neglected. Thus, a local mass transfer coefficient for this limiting condition is defined by:

$$\lim_{\substack{N_{A_o} \to 0 \\ N_{B_o} \to 0}} \frac{N_{A_o} - x_{A_o} (N_{A_o} + N_{B_o})}{\Delta x_A} = k_{x,loc} \qquad \text{III-3}$$

It has been shown that this coefficient can be used for moderate mass transfer rates instead of $k^{\cdot}_{x,loc}$ (9). For a finite surface A, III-2 can be rewritten:

$$W_A - x_A (W_A + W_B) = k^{\cdot}_x A \Delta x_A$$

or for small mass transfer rates,

$$W_A - x_A (W_A + W_B) = k_x A \Delta x_A \qquad \text{III-4}$$

where, $\Delta x_A = (x_{A_o} - x_{A_b})$

For the case of slow mass transfer in a closed conduit, with known composition, it is convenient to employ a local one phase mass transfer coefficient:

$$dW_A = k_{x,loc}(x_{Ab} - x_{A_o}) + x_{A_o}(dW_A + dW_B) \qquad \text{III-5}$$

or

$$N_{A_o} = k_{x,loc}(x_{Ab} - x_{A_o}) + x_{A_o}(N_{A_o} + N_{B_o}) \qquad \text{III-6}$$

Defining $r = N_{B_o}/N_{A_o}$, equation III-6 can be rewritten:

$$N_{A_o} = \frac{k_{x,loc}(x_{Ab} - x_{A_o})}{1 - x_{A_o}(1 + r)} \qquad \text{III-7}$$

A similar expression can be derived for the gaseous film resistance associated with the permeate, based on the local mass transfer coefficient $k_{y,loc}$:

$$N_{A_o} = \frac{k_{y,loc}(y_{A_o} - y_{Ab})}{1 - y_{A_o}(1 + r)} \qquad \text{III-8}$$

C. TRANSPORT THROUGH A POLYMERIC MEMBRANE

The passage of gas through a polymeric non porous membrane is usually considered to involve three independent physical phenomena:(13)

(1) Solution or sorption of the gas or vapor at one side of the membrane.

(2) Diffusion of the dissolved gas through the membrane.

(3) Re-evaporation or desorption.

The gases are transported through the polymeric nonporous membrane by means of activated diffusion, that is a process that exhibits a large positive activation energy and is quite specific, depending on the solubility of the penetrant in the membrane, as well as the ease of mobility of the penetrant molecule inside the polymer matrix. At any given instant, a penetrant molecule can be visualized as occupying a vacant site existing between adjacent polymer chains. In amorphous polymers above their glass transition temperature, such vacant sites are constantly created and eliminated as a result of the segmental motion of the polymer chains. A penetrant may thus proceed, under the influence of a concentration gradient and the cooperative motion of the chains, from one position to another, thus achieving a finite jump in the direction imposed by the concentration gradient. The overall travel of the particle consists then of a series of steps or diffusional jumps. Thus, the energy of activation for diffusion can be associated with the energy required for vacant site formation against the cohesive forces interacting among the chains, in addition to the energy required to force the diffusing molecule through the surrounding chain network.

The motion of the penetrant molecule inside the polymer matrix is strongly affected by the way in which the molecule is held inside the solid and by the molecular environment in which diffusion takes

place. These two factors are associated with the solubility of the penetrating substance in the polymer.

The solubility of a penetrant in a polymeric material can be ascribed to the tendency of the penetrant to distribute itself between two phases. Due to interactions between the penetrant and the polymer, some mixing of the polymer and the penetrant phases will normally occur, with a subsequent increase in the entropy of the system (10). The solutions of penetrants by a solid polymer is referred as "sorption" in the permeation literature, to include both, absorption and adsorption mechanisms. Adsorption includes only the surfaces of the solid, both external and internal. The internal surface would include not only regions comprising pores and pinholes, but also regions on groups of molecules, or even single macromolecules. The total internal surface available for adsorption for a penetrant with a given molecular size and shape would then depend upon the configuration of the macromolecules to form sites of the proper magnitude and shape. The adsorption of a penetrant into these sites is further characterized by the magnitude of the forces interacting between the penetrant and substrate. If these forces are weak and non specific, such as van der Waals forces the process is defined as "physical adsorption". On the contrary, if the forces of interaction are strong and specific, the process may exhibit heats of sorption comparable to those of chemical bond formation and is referred as "chemisorption". The penetrant is

attached firmly to the site and is not readily removable on desorption, leading to hysteresis effects.

Absorption, on the other hand, occurs when the penetrant-polymer system forms a random mixture, similar to an actual solution. This random mixture may be evenly distributed throughout the solid phase, or may exist only in the amorphous regions of a semi-crystalline polymer (11).

Addition of plasticizers or modifiers to a polymer increases the diffusivity of a given gas or vapor. This increase is attributed to the increase in polymer segmental mobility as a result of lower cohesive forces between chains (12). The solubility may also be greatly increased by the addition of modifiers. This increase is sometimes attributed to reversible chemical reactions taking place between the modifier and the penetrant (7, 5). The combined effect is a marked increase in the permeation rate.

The presence of crystalline regions in a semi-crystalline polymer has a strong negative effect on the rate of diffusion of penetrants through the polymer. The principal effects are: a reduction in the available volume for diffusion; the tortuosity involved in by-passing crystallites; the decrease in the mobility of amorphous chain segments as a result of the presence of crystalline regions which may act as crosslinks.

The permeation process is generally slow. Thus, the use of an

equilibrium relationship between the concentrations of sorbed gas and the partial pressures at the interfaces appears to be justified. Henry's law can then be assumed to apply,

$$c_A = mp_A \qquad \text{III-9}$$

The diffusion process is described by Fick's law:

$$N_A = -D_A \frac{d\,c_A}{d_z} \qquad \text{III-10}$$

If an average value of the diffusivity D_A is considered, equation III-10 can be integrated subject to the following boundary conditions:

$$\begin{aligned} z &= z_1 & c_A &= c_{A1} \\ z &= z_2 & c_A &= c_{A2} \end{aligned} \qquad \text{III-11}$$

to give,

$$N_A = \frac{D_A}{\Delta_z} (c_{A1} - c_{A2}) \qquad \text{III-12}$$

From equation III-9 and III-12:

$$N_A = \frac{D_A}{\Delta z} (m_1(p_{A_1})_o - m_2(p_{A_2})_o) \qquad \text{III-13}$$

If the Henry's law constant is assumed to be a function only of temperature and both membrane surfaces are at the same temperature, then

$$m_1 = m_2 = m$$

and:

$$N_A = \frac{D_A\, m}{\Delta z} \left[(p_{A_1})_o - (p_{A_2})_o \right] \qquad \text{III-14}$$

The permeability coefficient P is defined as

$$P_A = D_A\, m = \frac{N_A\, \Delta z}{(p_{A_1})_o - (p_{A_2})_o} \qquad \text{III-15}$$

$$\text{But } (p_{A_1})_o = P_1\, x_{A_o} \qquad (p_{A_2})_o = P_2\, y_{A_o} \qquad \text{III-16}$$

From III-14 and III-16,

$$N_A = \frac{D_A\, m}{\Delta z} \left(P_1\, x_{A_o} - P_2\, y_{A_o} \right) \qquad \text{III-17}$$

D. DEFINITION OF THE OVERALL MASS TRANSFER COEFFICIENT

At steady state the molar fluxes defined by equations III-7, III-8 and III-14 have to be the same. Thus:

$$N_A = \frac{k_{x,loc}\,(x_{A_b} - x_{A_o})}{1 - x_{A_o}(1 + r)} = \frac{k_{y,loc}\,(y_{A_o} - y_{A_b})}{1 - y_{A_o}(1 + r)} = \frac{D_A\, m}{\Delta z} \left(P_1 x_{A_o} - P_2 y_{A_o} \right) \qquad \text{III-18}$$

That can be expressed as;

$$N_A = K \left[(p_{A_1})_b - (p_{A_2})_b \right] \qquad \text{III-19}$$

where,

$$K = \frac{1}{\frac{P_1[1-x_{A_o}(1+r)]}{k_{x,loc}} + \frac{\Delta z}{D_A m} + \frac{P_2[1-y_{A_o}(1+r)]}{k_{y,loc}}} \qquad \text{III-20}$$

is the overall mass transfer coefficient. For the case of permeation of only one gas or vapor, $k_{x,loc}$ and $k_{y,loc}$ become infinite and equation III-20 reduces to III-17, since the pressure of the penetrant is the same in the interface and in the bulk stream.

E. DEFINITION OF THE PSEUDO-PERMEABILITY COEFFICIENT

Equations III-19 and III-20 describe the permeation phenomena for mixtures of gases or vapors. The equilibrium compositions x_{Ao} and y_{Ao} are included in these expressions, together with the Henry's law constant m and $k_{y,loc}$. When these variables of the system are not available, there is still the need of an expression that includes the significant parameters of the transport phenomena taking place, and permits the correlation of experimental data. Thus a "pseudo-permeability coefficient" for component i of a gaseous mixture is defined as follows:

$$\pi_i = \frac{N_i \Delta z}{(p_{i1})_b - (p_{i2})_b} \qquad \text{III-21}$$

that is similar to equation III-15, the only difference being the driving force employed, that for the case of equation III-21 is the difference

in partial pressures of the bulk streams at both sides of the membrane, while in equation III-15 the interfacial partial pressures, resulting from the equilibrium at the interface, are considered. It follows that,

$$(p_{i1})_b - (p_{i2})_b > (p_{i1})_o - (p_{i2})_o \qquad \text{III-22}$$

and

$$\pi_i < P_i \qquad \text{III-23}$$

Even though equation III-21 is not adequate to predict the performance of a membrane based on experimental data, since several relevant mass transport variables have been neglected, it nevertheless proves useful for comparative analyses while working with gaseous mixtures and for correlation of experimental data.

It can be seen from equation III-21, that a pseudo permeability coefficient for each component of a gaseous mixture can be obtained.

F. DEFINITION OF THE SEPARATION FACTOR

The actual local or point separation factor α_i of component i in a gaseous mixture is defined as:

$$\alpha_i = \frac{y_i / (1 - y_i)}{x_i / (1 - x_i)} \qquad \text{III-24}$$

For a case in which perfect mixing can be assumed, the local separation factor α_i has a constant value for any point in the membrane and is identical to the overall separation factor.

G. CHARACTERIZATION OF A GASEOUS SEPARATION

The separation factor gives an idea of the selectivity of a membrane with respect to a component of a gaseous mixture. The higher the separation factor, the higher the selectivity. However, no information is derived from the separation factor concerning the rate of permeation. This rate is directly related to the pseudo-permeability coefficients of the components of the mixture, from which all the relevant information can be obtained. To characterize a binary separation, the pseudo permeabilities for the two components of the mixture must be reported, or the pseudo permeability coefficient of one component and the overall separation factor. In both cases, the separation process is defined.

EXPERIMENTAL EQUIPMENT AND PROCEDURES

A. DESCRIPTION OF EQUIPMENT

The arrangement of the experimental equipment used in the permeation studies is shown schematically in Figure IV-1. The equipment consists of the following basic parts: gas storage and feeding facilities, the constant temperature enclosure - permeation cell system, pressure measurement and control facilities, flow rate measurement equipment and the analyses section. A description of the individual components follows.

(1) Permeation Cell

A diagram of the permeation cell is shown in Figure IV-2. It is fabricated from two stainless steel blank flanges, 5/8 in. thick and 4.5 in. in diameter. Two cavities were machined in the flanges for the feed circulation and membrane support. The membrane is supported by a porous stainless steel disk covered with filter paper and is sealed between two teflon gaskets and clamped shut by eight equally spaced bolts. The gasket openings and hence exposed membrane surface, have an area of 21.2 cm^2. The cell has provisions for the insertion of thermocouple probes to both, the high and low pressure sides of the membrane.

(2) Constant Temperature Enclosure

The constant temperature enclosure was made from a piece of 18 in.

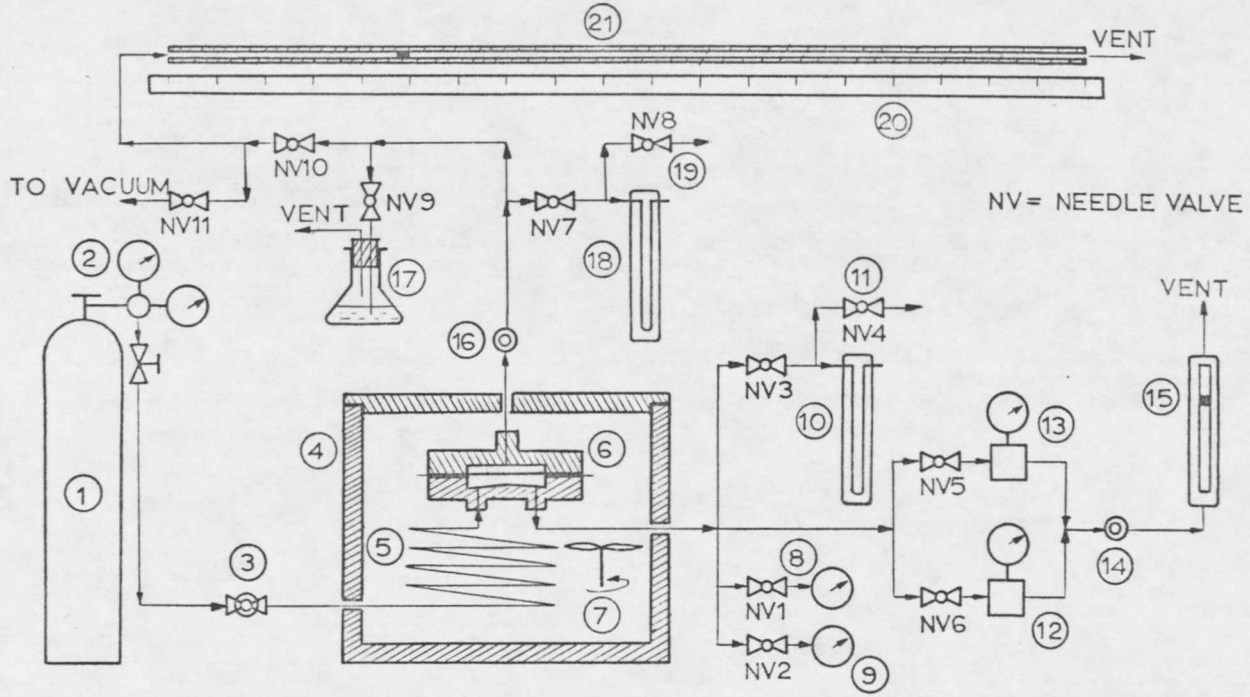

(1) GAS CYLINDER (2) PRESSURE REGULATOR (3) METERING NEEDLE VALVE (4) CONSTANT TEMPERATURE ENCLOSURE (5) HEAT EXCHANGER (6) PERMEATION CELL (7) HIGH SPEED FAN (8) HIGH PRESSURE GAUGE (9) INTERMEDIATE PRESSURE GAUGE (10) LOW PRESSURE MERCURY MANOMETER (11) PRESSURE RELIEF VALVE (12) BACK PRESSURE (HIGH & INTERMEDIATE PRESSURES) REGULATOR (13) BACK PRESSURE REGULATOR (LOW PRESSURE) (14) SAMPLING SEPTUM (VENT GAS) (15) ROTAMETER (16) SAMPLING SEPTUM (PERMEATE) (17) OIL SEAL (18) OIL MANOMETER (19) PRESSURE RELIEF VALVE (20) LENGTH MEASUREMENT (21) CALIBRATED CAPILLARY TUBE

FIGURE IV-1. SIMPLIFIED DIAGRAM OF PERMEATION EQUIPMENT

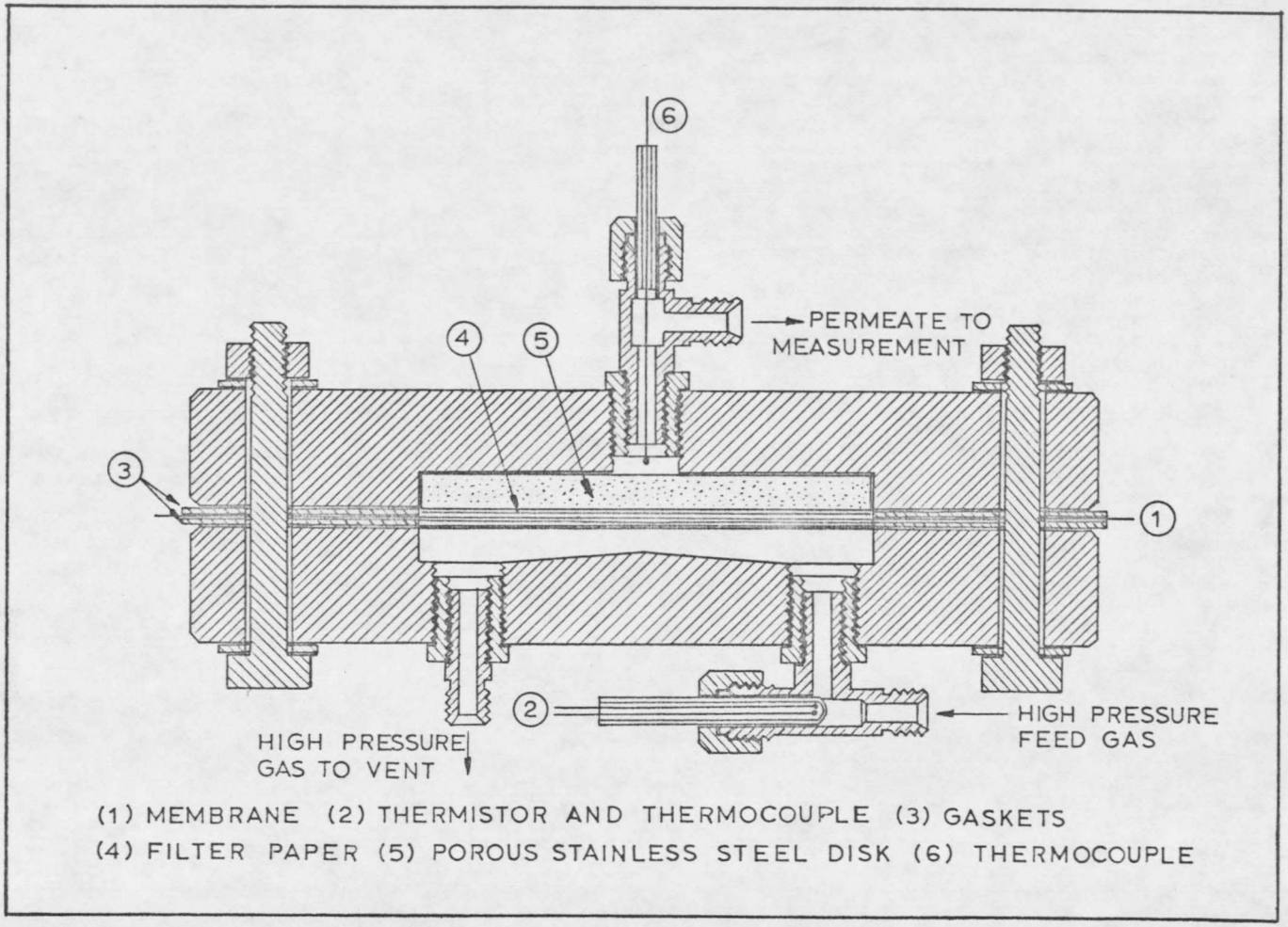

FIGURE IV-2. DIAGRAM OF PERMEATION CELL

diameter by 12 in. high asbestos pipe, sealed at the bottom and with a tight fitting asbestos board lid. The wall, top and bottom were further insulated with fiberglass.

Depending on the range of temperatures to be used there are two arrangements of the constant temperature enclosure.

a. Low and Intermediate Temperatures (0-35°C)

The arrangement of the equipment for this case is shown diagramatically in Figure IV-3. A tank 11 in. high and 12 in. diameter is placed inside the enclosure. The permeation cell is mounted in the tank, together with a 60 ft. coil of 1/8 in. stainless steel tubing to insure the same temperature for the feed gas and surrounding medium. The tank is filled up with an ice-water mixture for runs at 0°C. Ice is added periodically to the tank to insure that uniform temperature is maintained. For runs at temperatures in the range of 10-35°C, the tank is connected to a Neslab Instruments constant bath temperature unit, equipped for control to within $\pm$ 0.1°C and with circulation of the bath liquid. Cold water is used for cooling purposes (4-6°C) through the heat exchanger coil built in the unit. The cooling water flow rate is measured with a rotameter. Heating is provided by a 100Ω resistance contained in a quartz coil. This heater is connected to the temperature controller. The water tank is equipped with a

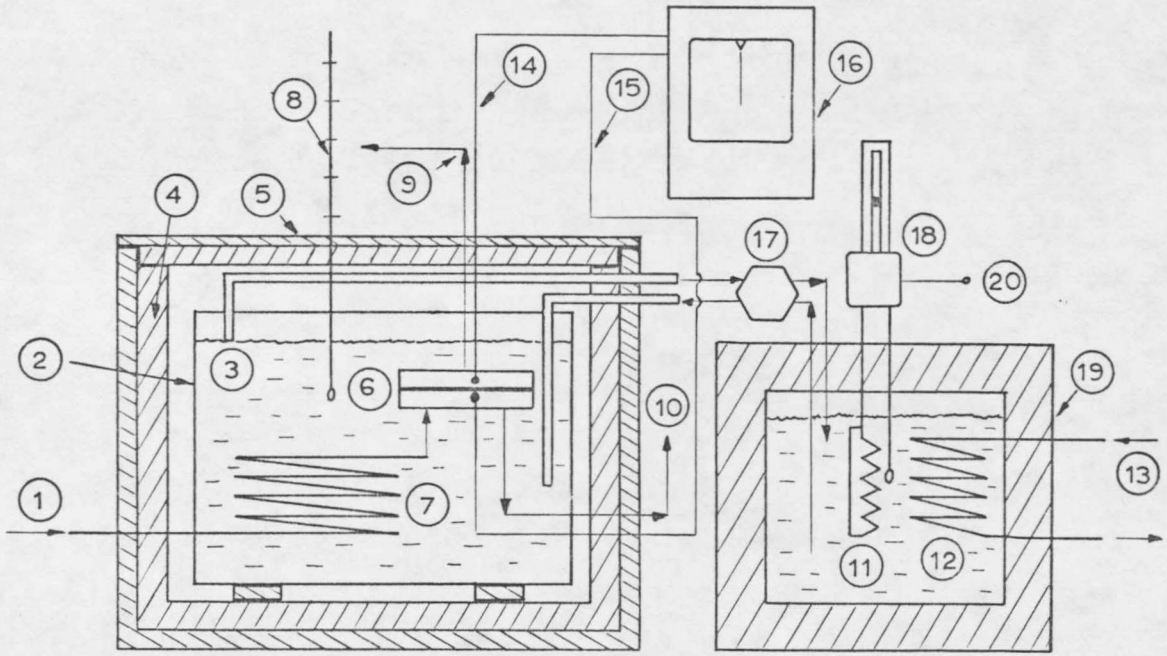

(1) GAS FEED (2) WATER TANK (3) LEVEL CONTROLLER (4) THERMAL INSULATION (5) CONSTANT TEMPERATURE ENCLOSURE (6) PERMEATION CELL (7) HEAT EXCHANGER COIL (8) THERMOMETER (9) PERMEATE (10) EXHAUST GAS (11) HEATER (12) COOLING COIL (13) COOLING WATER (14), (15) THERMOCOUPLE PROBES (16) TEMPERATURE RECORDER (17) RECIRCULATING PUMP (18) THERMOREGULATOR-THERMOMETER (19) RECIRCULATION CONSTANT TEMPERATURE BATH (20) POWER SUPPLY

FIGURE IV-3. CONSTANT TEMPERATURE ENCLOSURE - LOW TEMPERATURES

level controller that works coupled with the constant water temperature unit. A mercury therometer (sensitive to 0.1°C) is placed in the tank. The temperature of the water in the tank was found to be very uniform, probably because of the active circulation provided by the recirculating pump.

An iron - constantan thermocouple probe for temperature measurement is mounted in a thermowell in a tee at the gas inlet to the high pressure side of the cell. Another iron - constantan thermocouple probe is mounted in the low pressure side of the permeation cell, very close to the porous stainless steel disk, as shown in Figure IV-2. The temperatures were recorded in a Speedomax Type G Leeds & Northrup Co. recorder with a range of 0-200 °C, and with multiple input.

b. High Temperatures (35 - 55°C)

The arrangement of the equipment for this case is shown in Figure IV-4. The permeation cell is mounted in the enclosure together with a 60 ft. coil of 1/8 in. stainless steel tubing to insure the same temperature in the feed and surrounding medium. Two 500 watt heaters are placed in the bottom of the enclosure and covered with a piece of asbestos board to shield the permeation cell and heat exchanger coil from direct exposure to the heaters. The input to one of these heaters is controlled by a Powerstat

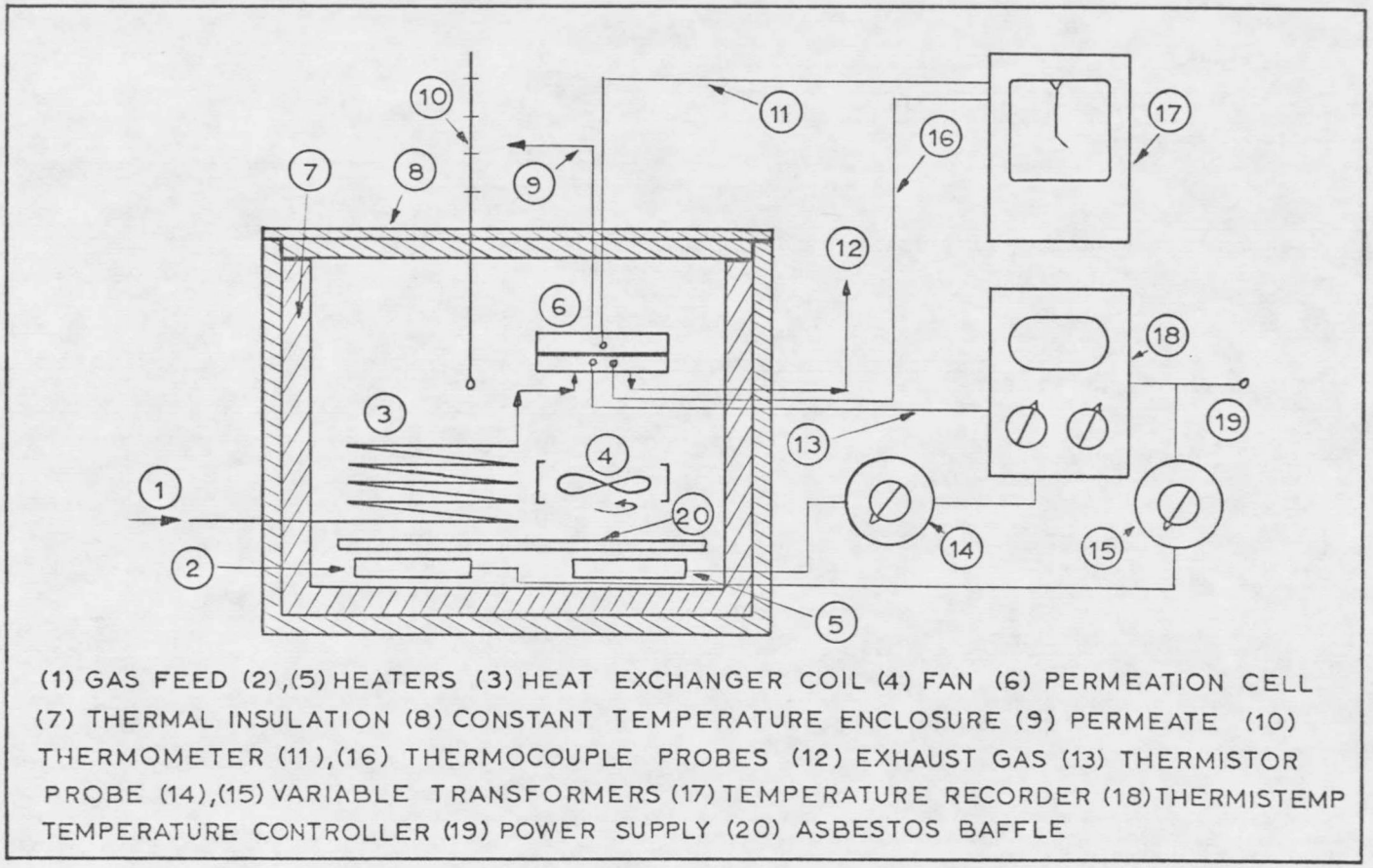

FIGURE IV-4. CONSTANT TEMPERATURE ENCLOSURE - HIGH TEMPERATURES

(The Superior Electric Co.) variable transformer, while the input to the other heater is controlled by a Thermistemp Model 63 thermistor temperature controller through another Powerstat (The Superior Electric Co.) variable transformer. The thermistor probe together with the thermocouple for temperature measurement are mounted in a thermowell in a tee at the gas inlet to the high pressure side of the permeation cell. Another thermocouple probe is mounted in the low pressure side of the cell, very close to the porous stainless steel disk, as shown in Figure IV-2. The temperatures are recorded in a Speedomax Type G (Leeds and Northrup) recorder with multiple input. A high speed Pamotor Model 4500 24w fan is mounted on the asbestos baffle to maintain a constant temperature throughout. A mercury thermometer (sensitive to 0.1°C) is used to determine the temperature of the enclosure. The temperature was found to be quite uniform throughout.

(3) Pressure Measurement and Control

Since the range of pressures required in the high pressure side of the cell is very wide (1 - 750 psig) a multiple system of pressure measurement and control is necessary. For low pressures, a 24 in. mercury manometer is used, together with a low flow rate, low pressure Grove Model No. 155 back pressure regulator. For intermediate pressures

a Weksler Instruments Phosphor Bronze gauge is used. This gauge has a 0 to 100 psig range. For high pressures an Acragage gauge with a 0-700 psig range is used. For the intermediate and high pressure range the control is provided by a Grove Mighty Mite back pressure regulator.

The pressure in the low pressure (permeate) side of the cell is measured with a calibrated 14 inch oil manometer.

(4) Flow Rate Measurement

The rate of permeation is determined by timing the movement of a small slug of mercury inside a 45 in. calibrated pyrex capillary tube. Two capillary tubes of different internal diameters were used depending on the permeation rate. These tubes were calibrated by determining the weight of mercury required to fill a given length of tube. The volumes per unit length of tubing are 0.017743 and 0.0452 cc/cm. When the rate of permeation is not being measured, the permeate is vented through an oil seal. The mercury slug is moved back into reading position by means of vacuum. A set of needle valves avoids the flooding of the lines with oil when the slug is being pulled back.

The flow rate of exhaust gas is measured by a low flow rate calibrated rotameter with a range of 0.2 - 6 liters (STP)/hour.

(5) Analyses Section

A Varian Aerograph Series 1400 thermal conductivity gas

chromatograph coupled with a Sargent Model SR recorder are used to analyze $SO_2 - N_2$ and $CO_2 - H_2$ mixtures, operating under the following conditions:

SO_2/N_2

Column: 6 feet x 1/8 in. stainless steel tubing packed with Porapak Q-S (Waters Associates, Inc.)

Column Temperature - 120°C

Detector Temperature - 110°C

Carrier Flow - 25 cc/min.

Detector Current - 150 ma.

Carrier gas: Helium

CO_2/H_2

Column: 9 ft. x 1/8 in. stainless steel packed with Porapak N (Waters Associates, Inc.)

Column Temperature - 80°C

Detector Temperature - 125°C

Carrier Flow - 25 cc/min

Detector Current - 150 ma.

Carrier Gas: Helium

In both cases, the chromatograph was calibrated using known gas mixtures. Duplicate analyses of gas samples of known compositions

indicated an accuracy of about $\pm$ 1% of the absolute amount present.

(6) Storage and Feeding Facilities

High pressure cylinders are used to store the gases, vapors and mixtures that are fed to the permeation cell. The feed flow rate is controlled by pressure regulators and a micro needle valve that can provide constant feed rate of as low as 200 cc/hour.

(7) Lines

The lines connecting the different parts of the apparatus consist of 1/8 in. fluorinated polyethylene tubing (low pressures) and 1/8 in. stainless steel tubing (high pressures).

(8) Materials

1. Vinylidene Fluoride - The membranes used in this study are made of vinylidene fluoride, to which the modifier and the solvent are added and the solution formed cast into membranes. The resin is commercially available under the trade name of Kynar, Grade 301 and manufactured by the Penwalt Corp. No antioxidants are used.

2. Sulfolene - The sulfolene was purchased from the Phillips Petroleum Company in 1 lb. containers.

3. Dimethyl Formamide - Used as a solvent for the resin (vinylidene fluoride) and the modifier to form a solution from which the membrane is cast. The dimethyl formamide used was purchased from

The Baker Chemical Company, Baker grade (BP 150-152).

4. Sulfur Dioxide - Technical grade, purchased from The Matheson Company in cylinders with net weight of 40 lbs.

5. Carbon Dioxide - Laboratory grade, purchased from the Chemetron Company in cylinders with net weight of 40 lbs.

6. Nitrogen - Laboratory grade, purchased from the Chemetron Company in cylinders containing 285 cu ft (STP).

7. Hydrogen - Laboratory grade, purchased from the Chemetron Company in cylinders containing 285 cu ft (STP).

8. Oxygen - Laboratory grade, purchased from the Chemetron Company in cylinders containing 285 cu ft (STP).

9. Carbon Monoxide - Technical grade, purchased from the Matheson Company in cylinders containing 285 cu ft (STP).

10. Ethylene - Laboratory grade, purchased from the Matheson Company in cylinders with a net weight of 4-1/2 lb.

11. Ethane - Laboratory grade, purchased from the Matheson Company in cylinders with a net weight of 3 lbs.

12. Methane - Laboratory grade, purchased from the Matheson Company in cylinders at 2000 psi and 40 cu ft (STP).

13. 1-3 Butadiene - Purchased from the Matheson Company in cylinders containing 2 lb net weight.

14. 3-Methyl Sulfolene - Purchased from the Phillips Petroleum Company in 1 lb. containers.

15. p - Aminophenyl Sulfone - Purchased from the Aldrich Chemical Company in 100 gr. containers, purity 99% (mp 175-177°F).

16. Phenyl Sulfone - Purchased from the Aldrich Chemical Company in 100 gr. containers, purity 97% (mp 123-125°F).

17. 4,4 Sulfonyl Diphenol - Purchased from the Aldrich Chemical Company in 100 gr. containers, purity 98% (mp 245-247°F).

18. Tetrahydro - 3 - Thiophenamine 1,1 - Dioxide - Technical grade, purchased from the Aldrich Chemical Company in 50 gr. containers (bp 154°F).

19. Oil - Used in the oil seal and oil manometer was purchased from Van Waters and Rogers (Pump oil). (Sg 0.97).

20. Gas Mixtures - Gas mixtures are prepared as follows: an adequate cylinder is evacuated using a vacuum pump. The cylinder is pressured up with the solute to the required pressure. The diluent gas is then added until the chosen pressure is reached. The cylinder is placed close to a heater that is periodically turned on and off to accelerate the mixing process, for a least a week. The mixtures so prepared are found to be very uniform in composition. This gas mixture is analyzed using a calibrated chromatograph.

B. EXPERIMENTAL PROCEDURE

(1) Calibration of Gas Chromatograph

The Porapak Q-S 6 feet column for analyses of SO_2/N_2 mixtures was

calibrated as follows:

Samples of different sizes of pure SO_2 and nitrogen from the cylinder were taken with a 0.5 cc precision syringe (Precision Sampling Corp) through a silicon rubber septum mounted on a low pressure regulator (10 psig). Samples were injected to the gas chromatograph for analyses under the same conditions of temperature and pressure (Pressure 25.3 in Hg, Temp. 24°C). The runs were repeated several times to insure reproducibility, that was found to be very good. The SO_2 and N_2 peaks were then copied on a Xerox copying machine and the resulting peaks were cut off and their weight determined in a Mettler precision balance (Sensitivity to 1×10^{-4} gr). This calibration data appears in Figure IV-5 as a function of the product peak weight x chromatograph attenuation. The chromatograph response is quite linear. Straight lines were fitted to both the SO_2 and N_2 using the least squares technique. The resulting equations were combined to give an analytical expression of the volume percent of SO_2 as a function of the SO_2 peak area percent. This calibration curve is shown in Figure IV-6, together with the experimental points used.

The 9 ft. Porapak-N column for the analyses of CO_2/H_2 was calibrated to determine only the absolute amount of CO_2 in a sample. CO_2 samples were injected to the chromatograph and photo copies were made of the peaks obtained. The volume of the sample was plotted as a function of the product peak weight x attenuation, as shown in

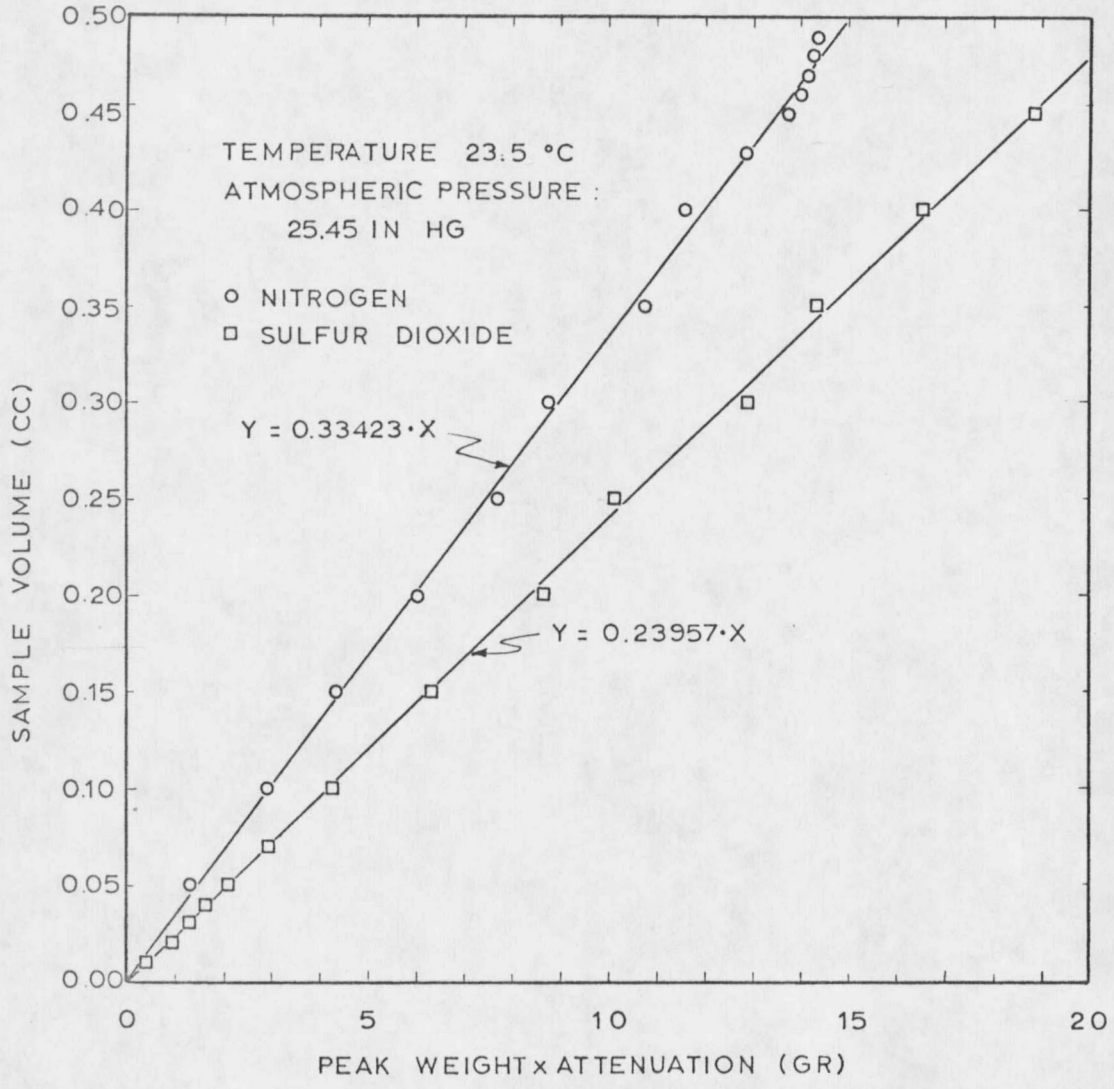

FIGURE IV-5. CALIBRATION OF GAS CHROMATOGRAPH SAMPLE VOLUME VS. PEAK WEIGHT x ATTENUATION FOR NITROGEN AND SULFUR DIOXIDE

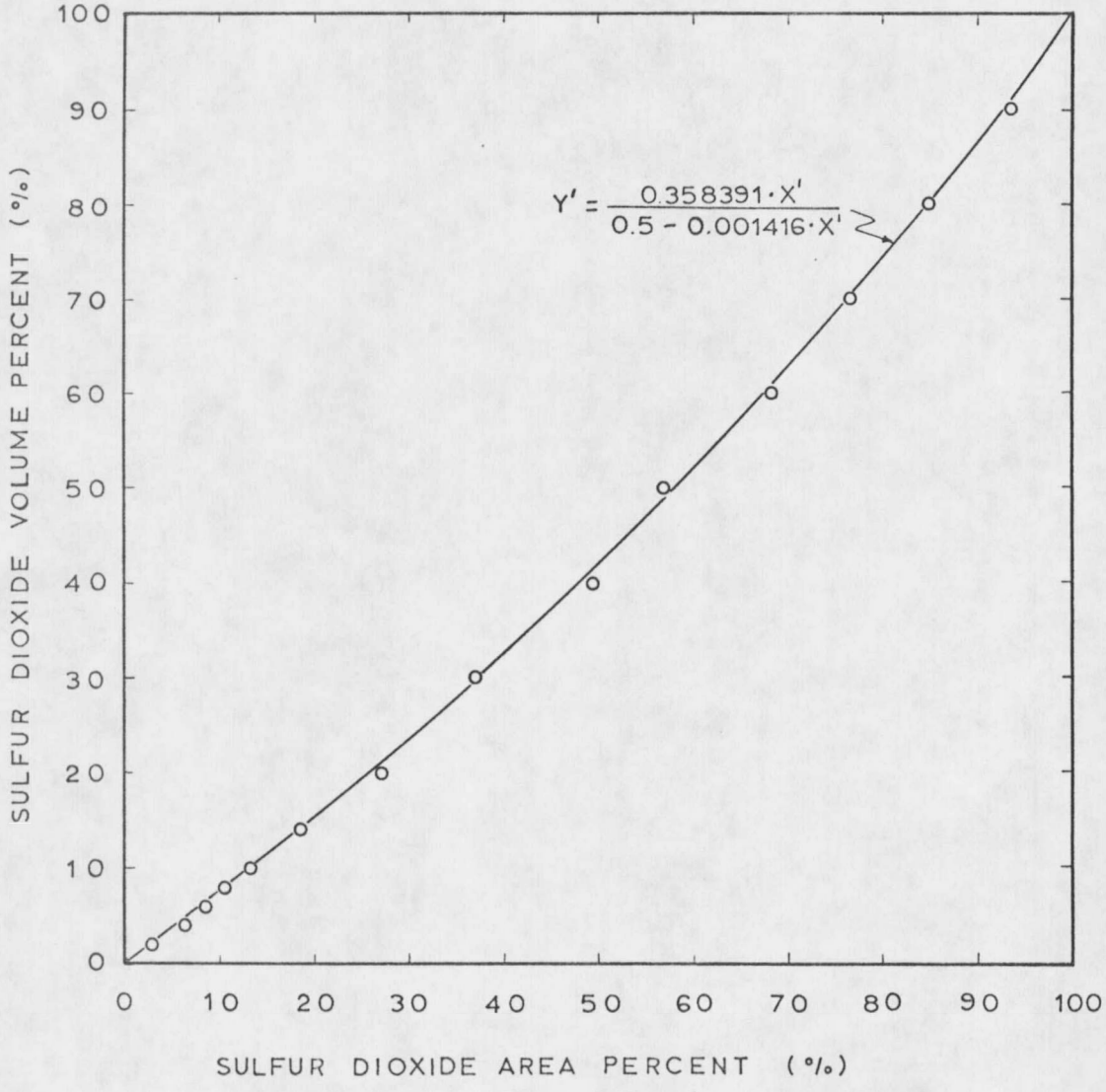

FIGURE IV-6. CALIBRATION CURVE FOR GAS CHROMATOGRAPH AREA PERCENT OF SO_2 PEAK VS. SO_2 VOLUME PERCENT

Figure IV-7. The paper used in the copies is Xerox standard copying paper (4024 Dual-purpose white, 75 g/m^2). In this case only an approximate analysis is possible because the separation of H_2 is rather erratic for this system. The CO_2 percent is determined by dividing the cc obtained from the calibration curve by the volume of the sample that is subject to analysis.

(2) Calibration of Exhaust Gas Rotameter

This low flow rate rotameter was calibrated against a wet test meter at room temperature (23.5°C). Corrections were made to account for the increase in humidity of the gas. The calibration curve is shown in Figure IV-8 together with the experimental data used.

(3) Membrane Manufacture

Membranes are made as follows:

A pyrex beaker is cleaned carefully and weighed in a Mettler balance (sensitivity 1×10^{-4} gr). The membrane modifier and vinylidene fluoride are added in appropriate amounts. The composition of the membrane on a solvent free basis is determined by weight differences. Dimethyl formamide is added in a ratio of 5.7 cc dimethyl formamide/gr vinylidene fluoride. The mixture is stirred with a glass rod for about ten minutes. The beaker is then tightly covered with polyethylene film and placed in an oven at about 100°C until complete dissolution is achieved. The films are then cast on a

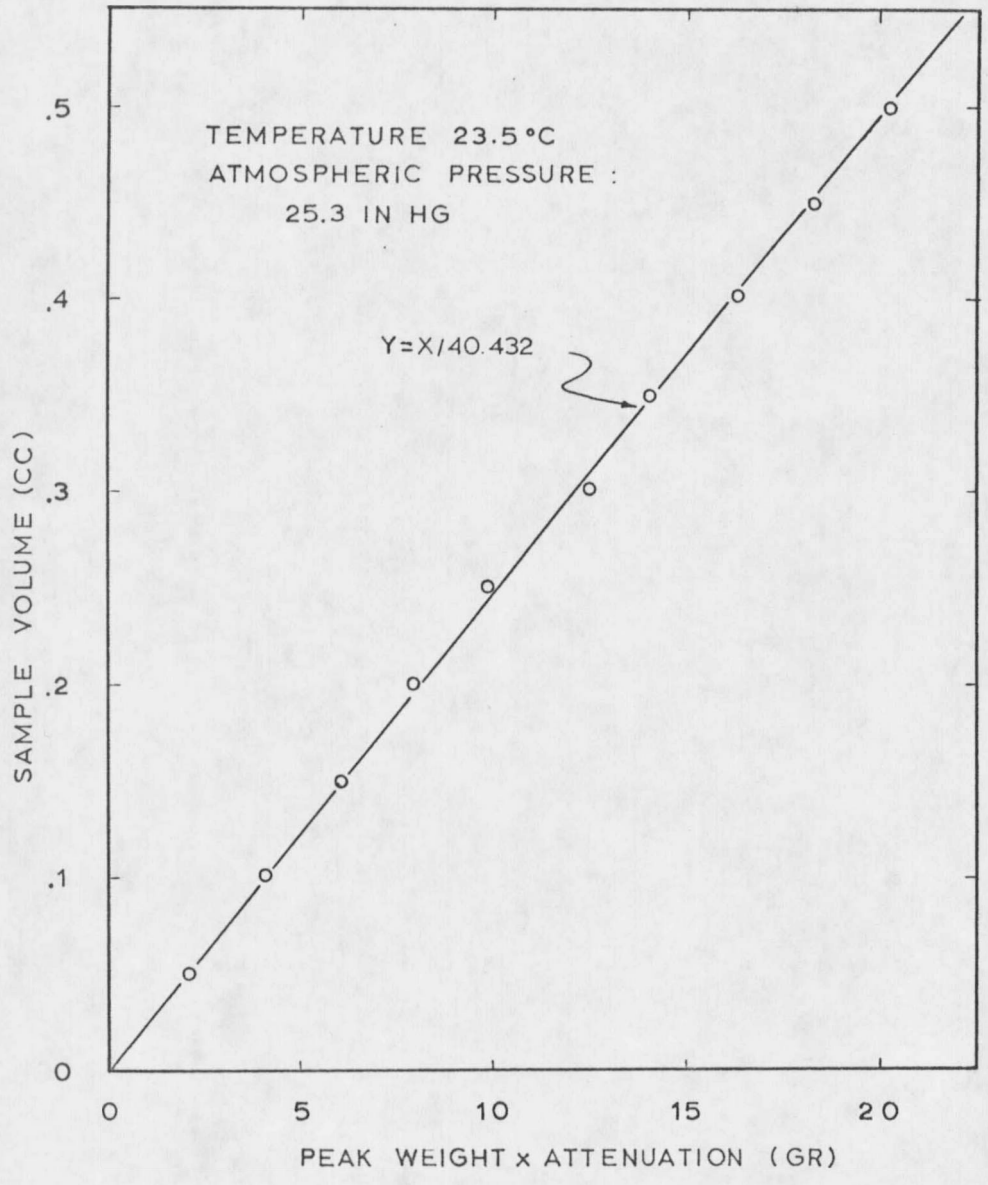

FIGURE IV-7 CALIBRATION OF GAS CHROMATOGRAPH
SAMPLE VOLUME VS PEAK WEIGHT x ATTENUATION
FOR CARBON DIOXIDE

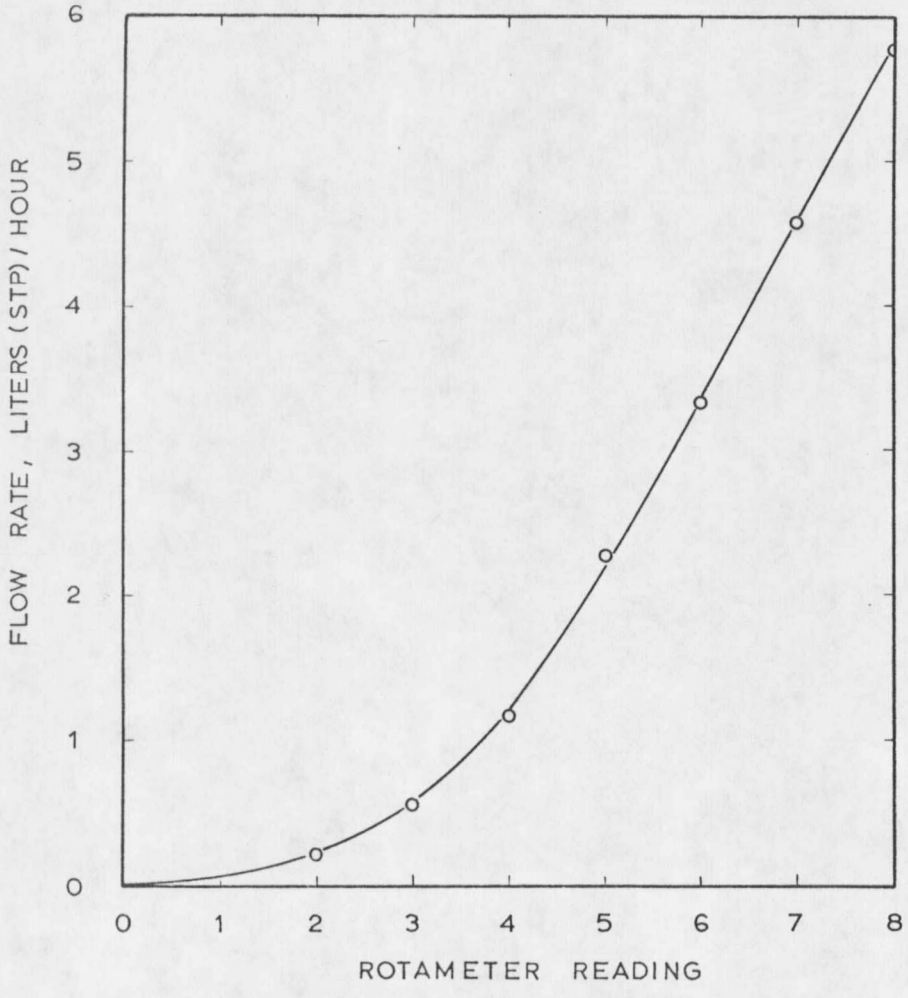

FIGURE IV-8. CALIBRATION CURVE FOR ROTAMETER.
FLOW RATE (STP) VS. ROTAMETER READING

9.5 x 5 x 3/16 in. glass plate by pouring the solution on the glass plate and distributing it evenly by drawing a glass rod down the plate with the rod resting on the masking tape. The glass plate is then placed in a ventilated electrically heated oven to evaporate the solvent. Membrane thickness is about one mil for three thicknesses of tape, and about two mils for six thicknesses of tape. The drying time is 20 minutes at 110°C for one mil membranes. For two mil membranes, the drying time is of 30 minutes at 125°C. Ventilation is provided by connecting a vacuum line to the oven. The plate is cooled to room temperature before stripping the film from the plate for mounting in the test cell. The surface of the membrane that was in contact with the glass plate is mounted facing the high pressure side of the cell.

(4) Operation Procedure

The following steps are followed before starting a permeation experiment:

i) The membrane is mounted in the test cell and the pressure at the high pressure side of the membrane, is increased to 700 psig with nitrogen, to test for possible leaks. The permeability coefficient for nitrogen is very low when using vinylidene fluoride based membranes. A high flow rate indicates a possible leak.

ii) The temperature of the cell is brought to the desired level

by setting the temperature controller. Final adjustments are made using the permeation cell thermocouple and the enclosure mercury thermometer.

iii) The pressure in the cell is brought to the desired level by setting the back pressure regulator and by opening the feed micro-needle valve to the flow rate of gas desired.

iv) The system is allowed to run until no further change is detected in the permeation rate or in the permeate or exhaust gas compositions.

v) The permeate flow rate is measured and the permeate and exhaust streams analyzed.

EXPERIMENTAL RESULTS AND DISCUSSION

A. MEMBRANE MODIFIERS

(1) The Data

In order to ascertain the effect of the modifer content in the membrane permeation rate and selectivity, the pseudo permeabilities for SO_2 and N_2 were determined using a 6.5% SO_2/N_2 mixture and different compositions of membranes. Room temperature was maintained (about 24°C) and a pressure of about 400 psig for all the runs. All the membranes were 1 mil thick. The data are presented in Table V-1.

(2) Discussion

The following chemicals have been added to vinylidene fluoride membranes in order to try to improve their permeation characteristics with respect to SO_2:

- Sulfolene
- 3-Methyl sulfolene
- p-Aminophenyl sulfone
- Phenyl sulfone
- 4,4 Sulfonyl diphenol
- Tetrahydro - 3 - Thiophenamine 1,1 - Dioxide

In Figure V-1, the pseudo-permeability coefficients of SO_2 are shown as functions of the modifier weight percent on a solvent free basis. It can be seen that the pseudo-permeability coefficients for sulfolene/vinylidene fluoride membranes are about two orders of

TABLE V-1. EFFECT OF MODIFIERS IN THE PERFORMANCE OF VINYLIDENE FLUROIDE MEMBRANES

Membrane Thickness: 1 mil P_1 = 412.3 psia P_2 = 12.36 psia

Run No	Modifier	Wt.% Modif.	Temp °C	% SO_2 Perm.	% SO_2 Vent	Flux x 10^5 cc(STP) (cm^{2}sec) SO_2	Flux x 10^5 cc(STP) (cm^{2}sec) N_2	π cc.cm/sec cm^2.cmHg π x 10^7 SO_2	π cc.cm/sec cm^2.cmHg π x 10^{11} N_2
1	3-Methyl Sulfolene	5	24.4	79.50	6.28	2.39	.617	.00733	.790
2	3-Methyl Sulfolene	10	24.	81.37	5.89	10.2	2.34	0.0353	2.98
3	3-Methyl Sulfolene	15	24.6	87.19	5.07	29.2	4.29	.142	5.41
4	None	-	24.6	80.46	6.31	2.17	.527	0.00664	.675
5	None	-	24.4	76.24	6.16	1.45	.452	0.00447	.579
6	3-Methyl Sulfolene	20	24.5	86.82	5.53	35.54	5.39	.145	6.83
9	P-Aminophenyl Sulfone	3	23.5	72.89	5.53	1.284	.475	0.00455	.604
11	P-Aminophenyl Sulfone	7	23.9	78.67	5.67	1.63	.442	0.00587	.562
12	Phenyl Sulfone	10	24.9	81.	5.69	1.55	.364	0.00566	.462
14	Phenyl Sulfone	15	24.1	83.48	5.74	1.66	.382	0.00612	.417
16	4,4 Sulfonyl Diphenol	10	24.4	77.18	5.55	1.464	.432	0.00538	.549
18	Sulfolene	10	25.	76.31	5.36	21.1	6.55	0.0817	8.31
20	Sulfolene	20	24.8	93.32	5.98	192.	13.7	.719	17.4
21	Sulfolene	15	24.	87.11	5.03	126.	18.6	.619	23.5
23	Tetrahydro-3-Thiophenamine 1,1 Dioxide	15	25.2	65.90	5.44	3.22	1.72	0.0114	2.19
24	Sulfolene	10	25.7	84.49	5.09	17.7	3.25	0.0832	4.19

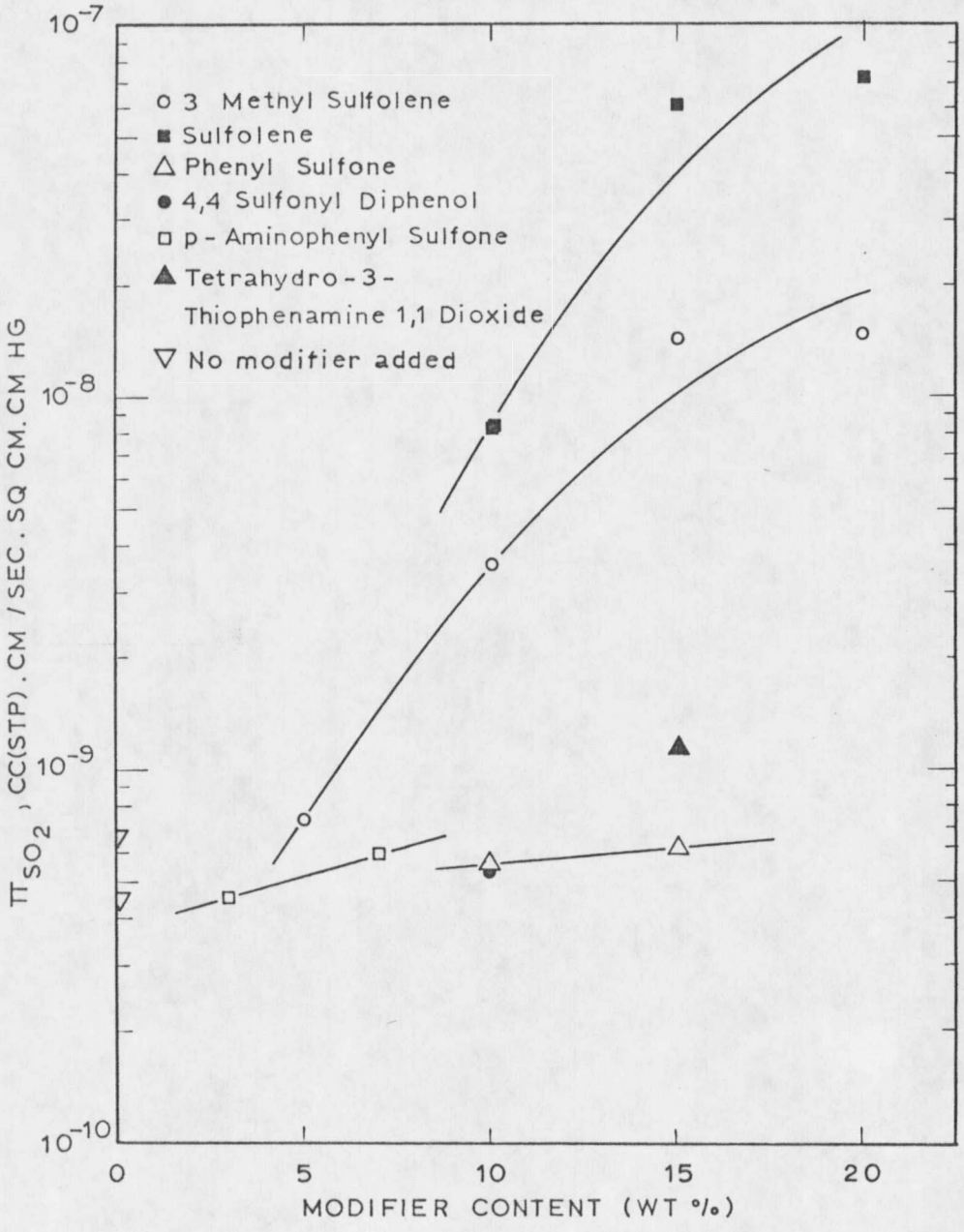

FIGURE V-1. PSEUDO PERMEABILITY COEFFICIENT FOR SO_2 VS. MODIFIER CONTENT

magnitude greater than those of the other systems, with the exception of 3-methyl sulfolene modified membranes, that show coefficients of the same order of magnitude, but still considerably lower than those obtained with sulfolene membranes.

In Figure V-2, the permeate and exhaust gas SO_2 concentrations have been plotted as functions of the modifier content on a solvent free basis. It can be seen that the SO_2 content in both, permeate and exhaust streams, shows no big differences for all the systems. However, the highest concentration of SO_2 in the permeate was obtained with sulfolene modified membranes. But even in the cases in which no modifier was added, the selectivity with respect to SO_2 was still quite high. This suggests that the solvent used (dimethyl formamide) is itself a modifier that gives the membrane some selectivity with respect to SO_2. This effect is probably responsible, at least in part, for the selectivity of other membranes, and it may be more important in systems of low pseudo-permeability coefficients.

What makes sulfolene the best modifier tested, is the high permeate flow rates obtained by its use. Because of this, a more detailed investigation of the properties of the sulfolene/vinylidene fluoride system has been carried out. The discussion of these results follows.

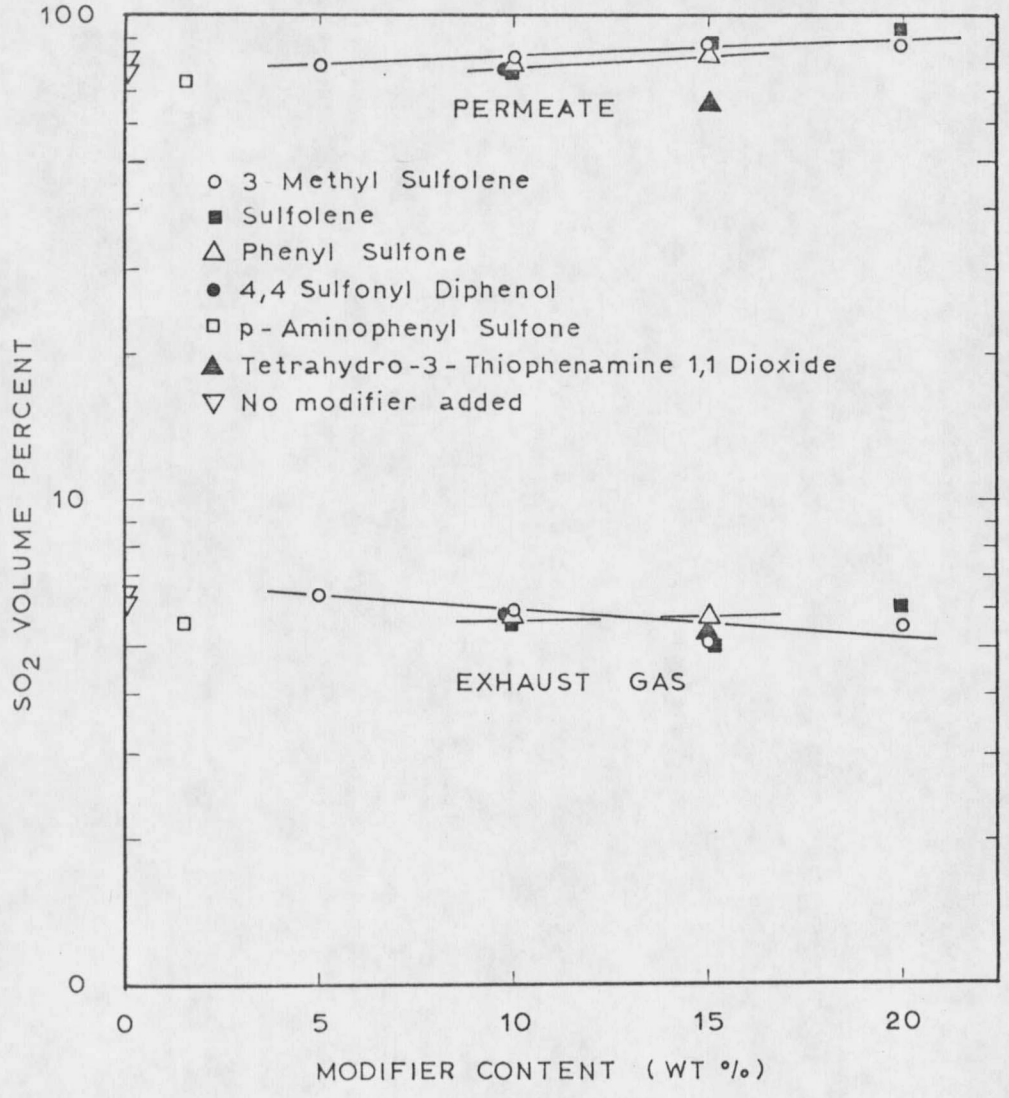

FIGURE V-2. PERMEATE AND EXHAUST GAS SO_2 VOLUME % VS. MODIFIER CONTENT

B. EFFECT OF THE SULFOLENE CONTENT

(1) The Data

In order to determine the effect of the concentration of sulfolene on the performance of the membrane for the N_2/SO_2-sulfolene/vinylidene fluoride system, permeation experiments at a pressure of about 500 psig were made in the 0°C to 46°C temperature range. A 6.5% SO_2/N_2 mixture was used for all the runs.

All the membranes were 1 mil thick. The data are presented in Table V-2.

(2) Discussion

The pseudo-permeability coefficient of SO_2 increases with the concentration of sulfolene in the membrane for all the temperatures investigated, as shown in Figure V-3. These coefficients show also a strong dependence on temperature, being higher at lower temperatures.

The pseudo-permeability coefficients for N_2 were also determined and are shown in Figure V-4. In this case, the coefficients do not show a strong dependence on modifier concentration in the membrane. The higher values were obtained at higher temperatures. It can be seen from Figure V-3 that the higher the sulfolene content in the membrane the higher the SO_2 pseudo-permeability coefficient. But it was found that membranes with higher sulfolene contents were prone to developing leaks. A 25% sulfolene 1 mil thick membrane was extremely

TABLE V-2. EFFECT OF THE SULFOLENE CONTENT IN THE PERFORMANCE OF VINYLDENE FLUROIDE MEMBRANES

Membrane Thickness: 1 mil.

Run No.	Wt.% Sufolene	Temp. °C	P_1 (psia)	P_2 (psia)	$\%SO_2$ Perm	% SO_2 Vent	Flux x 10^3 cc(STP) / cm^2 sec SO_2	Flux x 10^3 cc(STP) / cm^2 sec N_2	π cc.cm/sec.cm^2 cm.Hg $SO_2 x 10^8$	π cc.cm/sec.cm^2 cm.Hg $N_2 x 10^9$
25-1	15.	0.0	410.3	12.347	78.81	3.21	.261	0.070	3.72	0.087
25-2	15.	22.0	406.3	12.351	61.71	4.50	.214	.133	.986	.170
25-3	15.	35.5	406.3	12.351	50.19	4.65	.178	.177	.691	.228
25-4	15.	46.5	406.3	12.354	41.09	4.72	.157	.225	.546	.291
26-1	20.	0.0	410.3	12.354	80.81	3.11	.461	.109	8.165	.136
26-2	20.	22.5	410.3	12.351	65.43	4.08	.273	.144	1.55	.182
28-1	17.50	0.0	410.3	12.361	82.62	3.30	.360	0.076	5.331	0.094
28-2	17.50	22.7	410.3	12.351	66.72	4.31	.229	.114	1.191	144
28-3	17.50	32.5	414.3	12.351	59.953	4.21	.184	.123	.900	.154
28-4	17.50	43.0	414.3	12.351	50.30	4.23	.160	.158	.694	.198
30-1	10.	0.0	414.3	12.372	80.61	3.71	.303	.730	2.77	0.090
30-2	10.	22.0	414.3	12.372	60.13	4.65	.168	.111	.699	.140
30-3	10.	33.0	416.5	12.528	39.12	4.92	.128	.199	.404	.252
30-4	10.	43.50	417.4	12.498	30.03	5.09	.120	.280	.337	.355

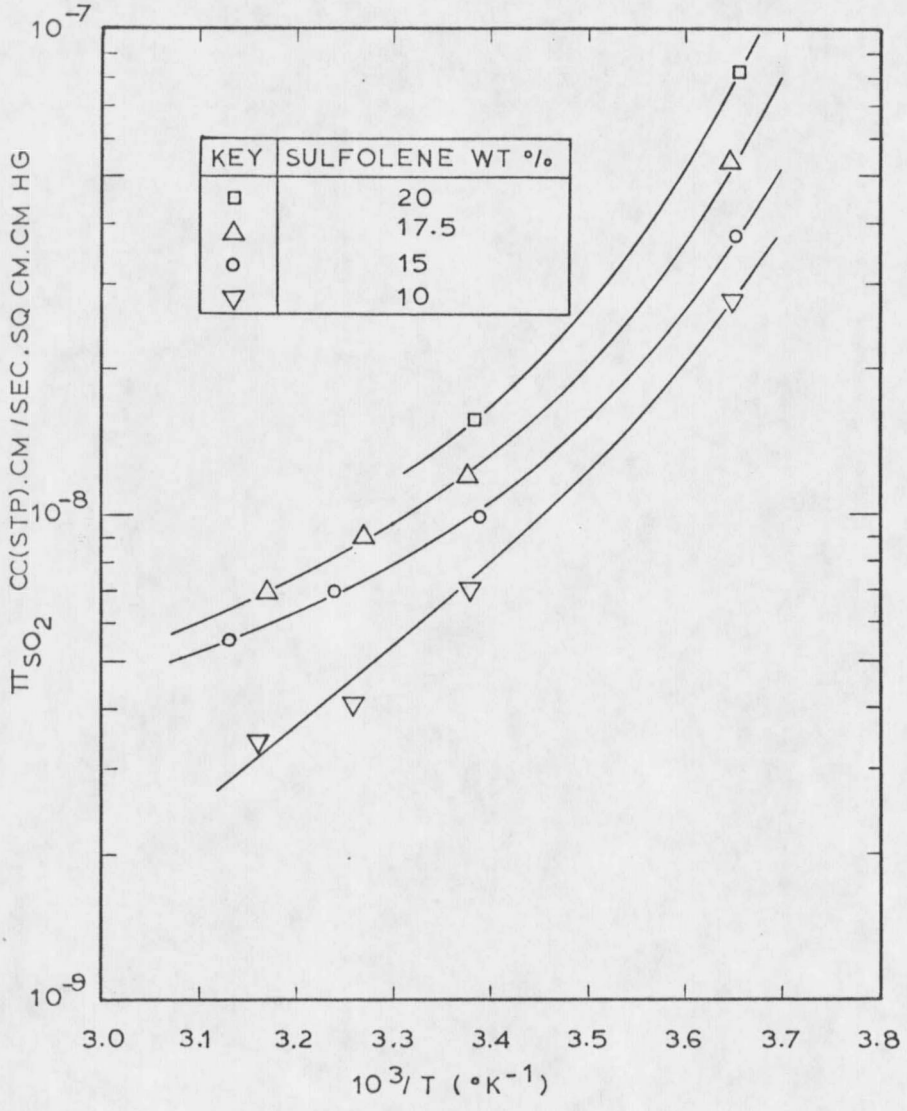

FIGURE V-3. PSEUDO PERMEABILITY COEFFICIENTS FOR SO_2 VS. $10^3/T$ FOR VARIOUS SULFOLENE CONCENTRATIONS IN THE MEMBRANE

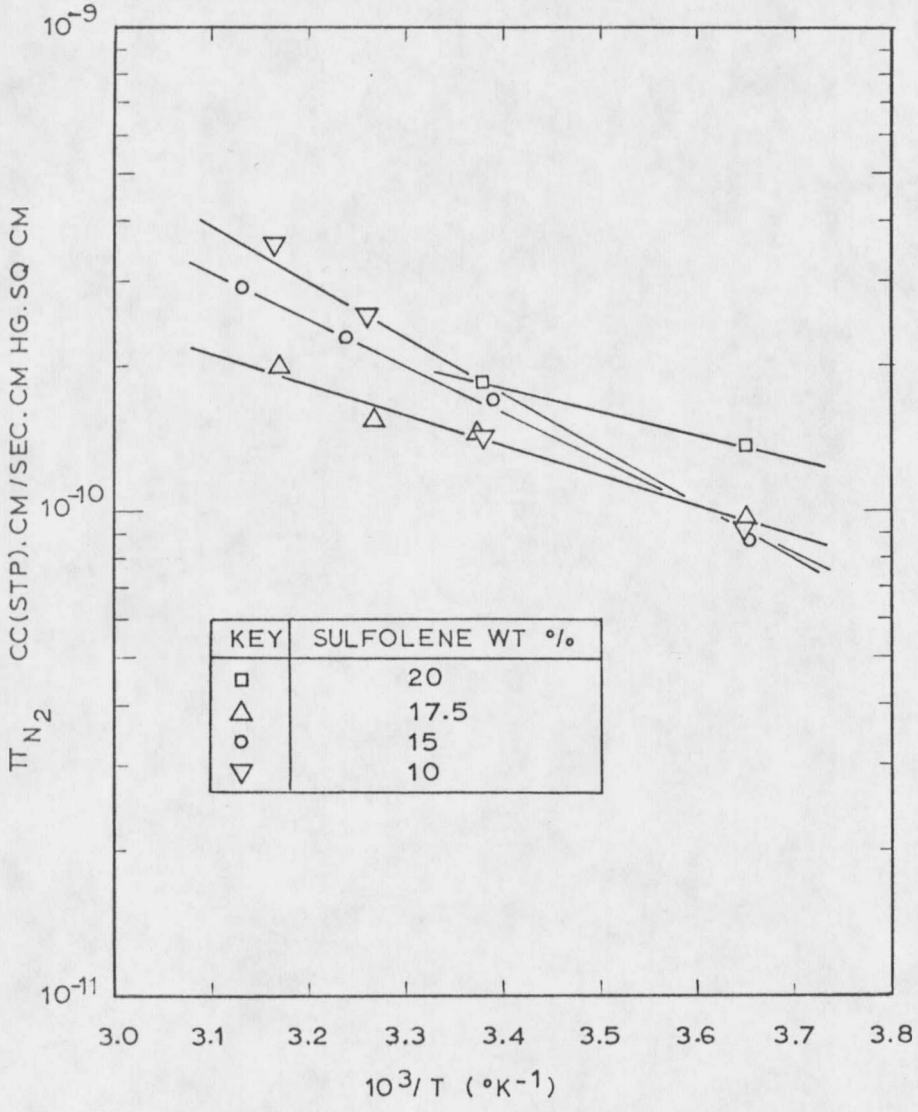

FIGURE V-4. PSEUDO PERMEABILITY COEFFICIENTS FOR N_2 VS. $10^3/T$ FOR VARIOUS SULFOLENE CONCENTRATIONS IN THE MEMBRANE

difficult to make. Even with the 20% sulfolene membrane some problems were encountered, especially at higher temperatures. It was also found that an 18% sulfolene membrane could be made without much trouble and that its performance was quite consistent. It was further found that increasing the thickness of the membrane to 2 mils, the membrane was more durable and that the reproducibility of the results was improved, increasing at the same time the performance of the membrane.

It was decided to study in more detail these improved sulfolene membranes.

C. PERMEABILITY COEFFICIENTS FOR SULFUR DIOXIDE

(1) The Data

The permeability coefficients for SO_2 were determined in the 0°C to 55°C temperature range and in the pressure range of 1 psig to about 40 psig. The membrane used contained 18 wt% sulfolene on a solvent free basis and had a thickness of 2 mils. The data are presented in Table V-3.

(2) Discussion

The permeability coefficient of SO_2 shows a strong dependence on both, temperature and pressure, as shown in Figure V-5. The coefficient increases with decreasing temperature and with increasing pressure. The maximum value, $P = 0.518 \times 10^{-6}$ $cc(STP).cm/sec.cm^2.cmH_g$, was obtained at the highest pressure tested for the lowest temperature runs

TABLE V-3. PERMEABILITY COEFFICIENTS FOR SULFUR DIOXIDE

Sulfolene in Membrane: 18 wt.% Thickness: 2 mils.

Run No.	Temp. °C	P_1 (psia)	P_2 (psia)	Flux cc(STP)/ cm^2 sec	P cc(STP)cm/ $sec.cm^2 cmH_g$
35-1	0.0	13.3	12.36		$.207 \times 10^{-6}$
35-2	0.0	13.9	12.36		$.235 \times 10^{-6}$
35-3	0.0	14.4	12.37		$.249 \times 10^{-6}$
35-4	0.0	14.9	12.37		$.268 \times 10^{-6}$
35-5	0.0	15.3	12.37		$.279 \times 10^{-6}$
35-6	0.0	15.9	12.37		$.295 \times 10^{-6}$
35-7	0.0	16.3	12.38		$.314 \times 10^{-6}$
35-8	0.0	16.9	12.38		$.341 \times 10^{-6}$
35-9	0.0	17.5	12.38		$.362 \times 10^{-6}$
35-10	0.0	17.8	12.38		$.376 \times 10^{-6}$
35-11	0.0	18.4	12.39		$.405 \times 10^{-6}$
35-12	0.0	19.0	12.42		$.441 \times 10^{-6}$
35-13	0.0	19.6	12.42		$.472 \times 10^{-6}$
35-14	0.0	19.8	12.42		$.484 \times 10^{-6}$
35-15	0.0	20.3	12.43		$.518 \times 10^{-6}$
40-1	14.5	13.3	12.30	$.475 \times 10^{-4}$	$.452 \times 10^{-7}$
40-2	14.5	14.3	12.30	$.112 \times 10^{-3}$	$.556 \times 10^{-7}$
40-3	14.5	15.3	12.30	$.197 \times 10^{-3}$	$.637 \times 10^{-7}$
40-4	14.5	16.3	12.30	$.285 \times 10^{-3}$	$.694 \times 10^{-7}$
40-5	14.5	17.3	12.31	$.396 \times 10^{-3}$	$.780 \times 10^{-7}$
40-6	14.5	18.2	12.31	$.524 \times 10^{-3}$	$.869 \times 10^{-7}$
40-7	14.5	19.4	12.32	$.706 \times 10^{-3}$	$.986 \times 10^{-7}$
40.8	14.5	20.3	12.32	$.884 \times 10^{-3}$	$.108 \times 10^{-6}$
40-9	14.5	21.2	12.32	$.106 \times 10^{-2}$	$.117 \times 10^{-6}$
40-10	14.5	22.2	12.32	$.124 \times 10^{-2}$	$.124 \times 10^{-6}$

TABLE V-3 (Cont).

Run No.	Temp. °C	P_1 (Psia)	P_2 (Psia)	FLUX cc(STP)/ cm^2 sec	P cc(STP)cm/ sec.cm^2 cmH_g
40-11	14.5	23.3	12.32	$.151 \times 10^{-2}$	$.136 \times 10^{-6}$
40-12	14.5	24.2	12.33	$.173 \times 10^{-2}$	$.143 \times 10^{-6}$
40-13	14.5	25.6	12.33	$.215 \times 10^{-2}$	$.160 \times 10^{-6}$
40-14	14.5	27.6	12.33	$.282 \times 10^{-2}$	$.182 \times 10^{-6}$
40-15	14.5	29.6	12.33	$.362 \times 10^{-2}$	$.207 \times 10^{-6}$
40-16	14.5	31.6	12.34	$.460 \times 10^{-2}$	$.235 \times 10^{-6}$
41-1	25.1	14.5	12.51	$.260 \times 10^{-4}$	$.126 \times 10^{-7}$
41-2	25.1	16.4	12.51	$.620 \times 10^{-4}$	$.156 \times 10^{-7}$
41-3	25.1	18.6	12.51	$.121 \times 10^{-3}$	$.195 \times 10^{-7}$
41-4	25.1	20.5	12.51	$.186 \times 10^{-3}$	$.229 \times 10^{-7}$
41-5	25.1	22.6	12.52	$.286 \times 10^{-3}$	$.280 \times 10^{-7}$
41-6	25.1	24.4	12.52	$.397 \times 10^{-3}$	$.328 \times 10^{-7}$
41-7	25.1	26.8	12.52	$.596 \times 10^{-3}$	$.411 \times 10^{-7}$
41-8	25.1	28.7	12.53	$.785 \times 10^{-3}$	$.478 \times 10^{-7}$
41-9	25.1	30.7	12.53	$.105 \times 10^{-3}$	$.569 \times 10^{-7}$
41-10	25.1	32.7	12.53	$.131 \times 10^{-3}$	$.641 \times 10^{-7}$
41-11	25.1	34.9	12.53	$.170 \times 10^{-2}$	$.750 \times 10^{-7}$
41-12	25.1	36.8	12.53	$.211 \times 10^{-2}$	$.856 \times 10^{-7}$
41-13	25.1	38.9	12.53	$.266 \times 10^{-2}$	$.992 \times 10^{-7}$
41-14	25.1	40.8	12.54	$.324 \times 10^{-2}$	$.113 \times 10^{-6}$
41-15	25.1	42.9	12.54	$.397 \times 10^{-2}$	$.129 \times 10^{-6}$
41-16	25.1	44.9	12.55	$.478 \times 10^{-2}$	$.145 \times 10^{-6}$
41-17	25.1	46.9	12.55	$.560 \times 10^{-2}$	$.160 \times 10^{-6}$
41-18	25.1	48.7	12.55	$.653 \times 10^{-2}$	$.178 \times 10^{-6}$
42-1	35.0	16.5	12.41	$.371 \times 10^{-4}$	$.885 \times 10^{-8}$
42-2	35.0	20.5	12.41	$.104 \times 10^{-3}$	$.127 \times 10^{-7}$

TABLE V-3 (Cont).

Run No.	Temp °C	P_1 (Psia)	P_2 (Psia)	Flux cc(STP)/ cm^2 sec.	P cc(STP)cm/ $sec.cm^2 cmH_g$
42-3	35.0	24.4	12.41	$.200 \times 10^{-3}$	$.164 \times 10^{-7}$
42-4	35.0	28.7	12.52	$.362 \times 10^{-3}$	$.220 \times 10^{-7}$
42-5	35.0	32.8	12.52	$.583 \times 10^{-3}$	$.283 \times 10^{-7}$
42-6	35.0	36.8	12.53	$.871 \times 10^{-3}$	$.353 \times 10^{-7}$
42-7	35.0	41.8	12.53	$.146 \times 10^{-2}$	$.489 \times 10^{-7}$
42-8	35.0	47.7	12.54	$.205 \times 10^{-2}$	$.608 \times 10^{-7}$
42-9	35.0	49.5	12.47	$.259 \times 10^{-2}$	$.688 \times 10^{-7}$
44-1	45.8	16.3	12.40	$.293 \times 10^{-4}$	$.733 \times 10^{-8}$
44-2	45.9	22.5	12.40	$.105 \times 10^{-3}$	$.102 \times 10^{-7}$
44-3	45.9	27.7	12.40	$.199 \times 10^{-3}$	$.127 \times 10^{-7}$
44-4	46.1	32.6	12.40	$.314 \times 10^{-3}$	$.152 \times 10^{-7}$
44-5	45.8	37.5	12.40	$.489 \times 10^{-3}$	$.191 \times 10^{-7}$
44-6	45.9	42.3	12.41	$.718 \times 10^{-3}$	$.236 \times 10^{-7}$
44-7	45.9	49.9	12.41	$.128 \times 10^{-2}$	$.335 \times 10^{-7}$
45-1	55.0	17.3	12.39	$.354 \times 10^{-4}$	$.703 \times 10^{-8}$
45-2	55.0	22.6	12.40	$.891 \times 10^{-4}$	$.859 \times 10^{-8}$
45-3	55.0	27.4	12.40	$.154 \times 10^{-3}$	$.100 \times 10^{-7}$
45-4	55.0	32.4	12.40	$.235 \times 10^{-3}$	$.115 \times 10^{-7}$
45-5	55.0	37.9	12.40	$.349 \times 10^{-3}$	$.134 \times 10^{-7}$
45-6	55.0	42.3	12.40	$.471 \times 10^{-3}$	$.154 \times 10^{-7}$
45-7	55.0	50.0	12.41	$.761 \times 10^{-3}$	$.199 \times 10^{-7}$

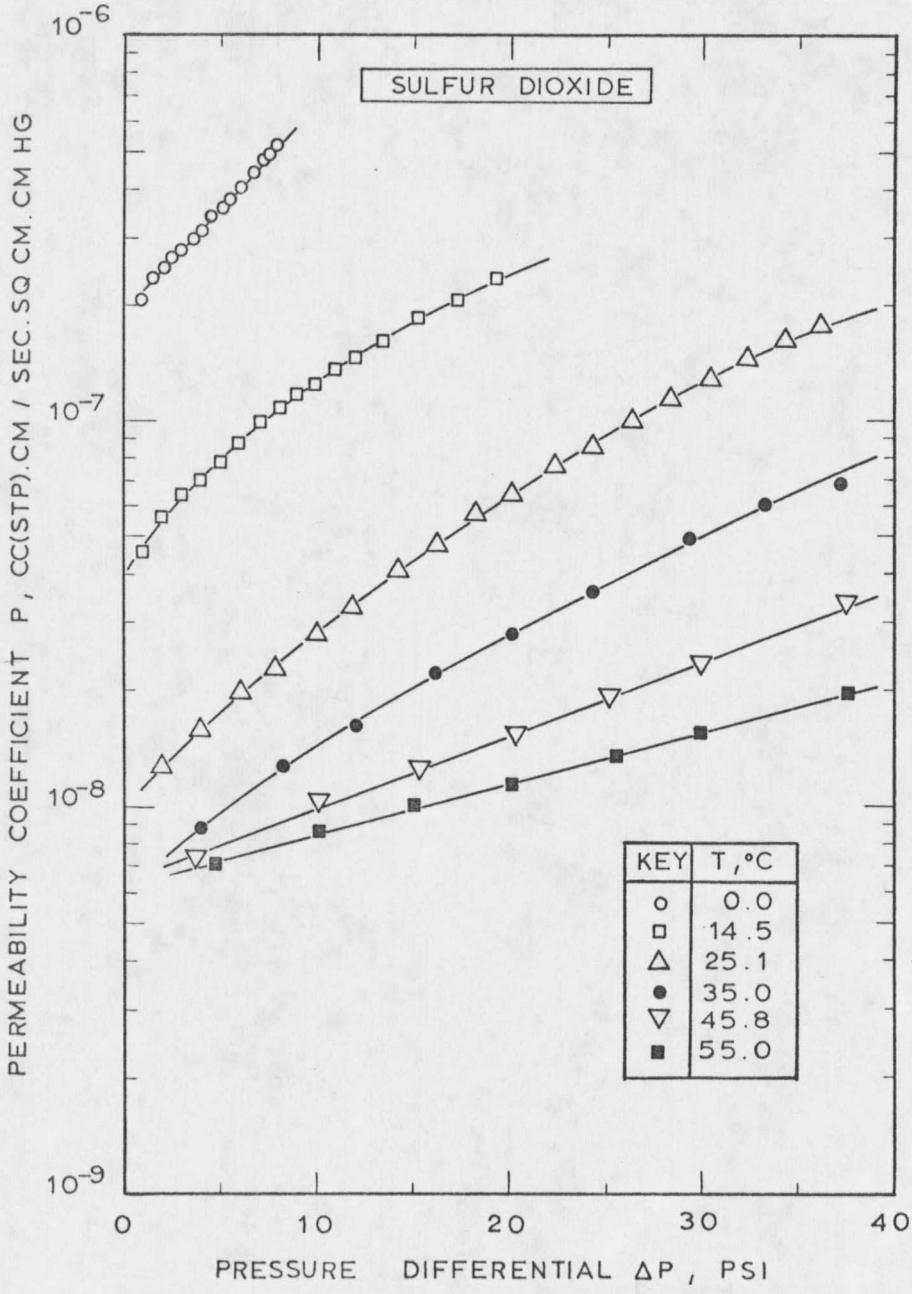

FIGURE V-5. PERMEABILITY COEFFICIENT VS. PRESSURE DIFFERENTIAL FOR SULFUR DIOXIDE

(about 8 psig and 0°C). In Figure V-6 selected values extracted from Figure V-5 are plotted as functions of the reciprocal value of the absolute temperature, keeping the pressure differential across the membrane as a parameter. Again, the permeability coefficient shows a highly non linear dependence on pressure and temperature, and an Arrhenius-type relationship, typical of other permeation systems, is not suitable to correlate the data in this case.

The behavior of the SO_2-Sulfolene/Vinylidene Fluoride system can probably be explained in terms of the solubility and diffusivity of SO_2 in the membrane. The solubility of the gas or vapor in a solid or liquid increases with lower temperatures. On the other hand, the diffusivity generally decreases with decreasing temperature. Depending on how strongly the solubility and diffusivity depend on temperature, the permeability coefficient, that is the product of both, will follow either the solubility or diffusivity behavior with respect to temperature. Thus, it is possible to speak of "solubility controlled" or "diffusivity controlled" permeation processes. According to Figure V-5, the permeation of SO_2 through sulfolene modified vinylidene fluoride membranes appears to be a "solubility controlled" permeation process. While lowering the temperature, the effect of the decrease of the SO_2 diffusivity in the membrane is more than compensated by the increase of SO_2 concentration, the net effect being an increase of permeate flux and of the permeability coefficient. There is also the

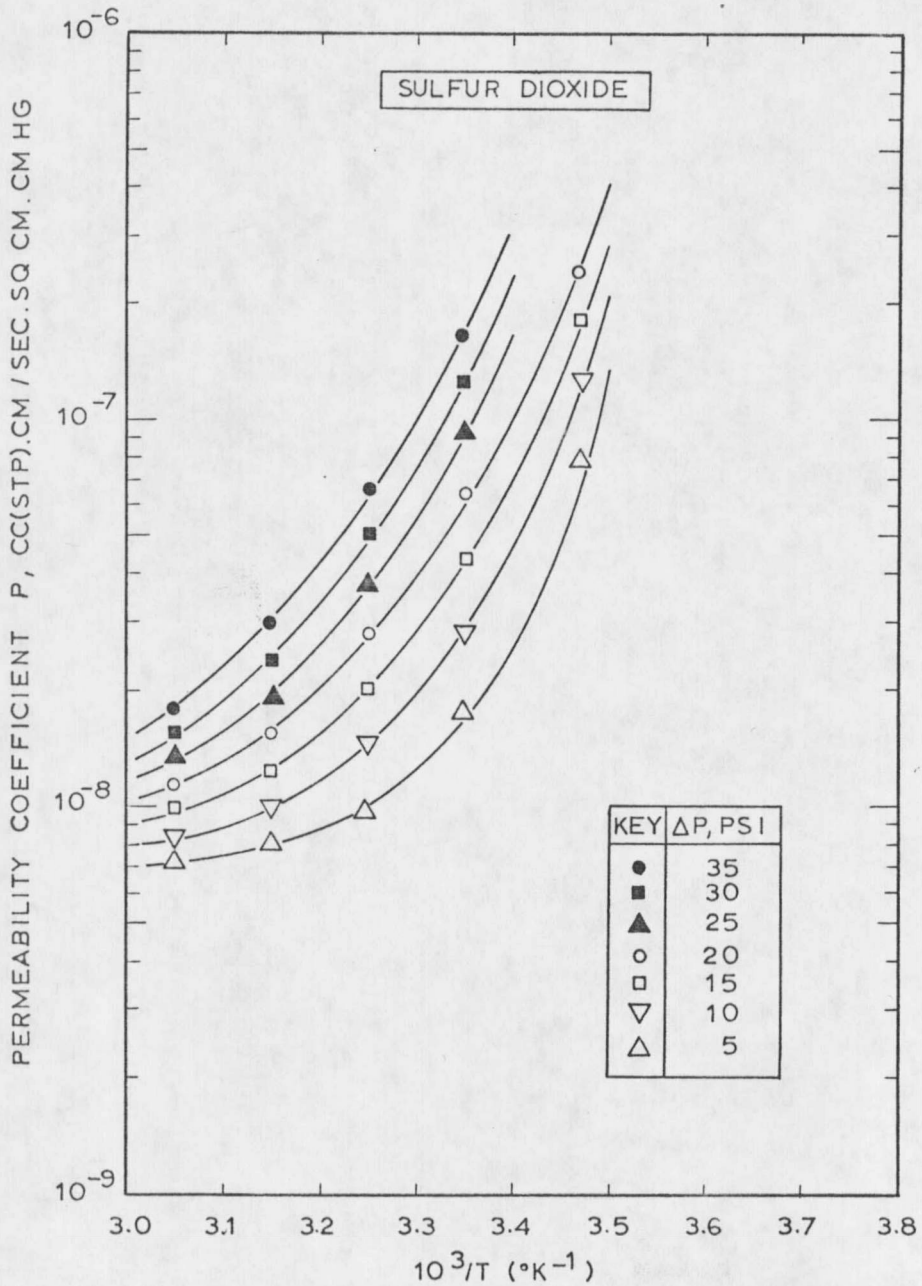

FIGURE V-6. PERMEABILITY COEFFICIENT VS. $10^3/T$ FOR SULFUR DIOXIDE

possibility of the diffusivity increasing with increased sorbed gas concentration. This effect that has been demonstrated by Stannet et al (14). In their work organic vapors of methyl bromide, isobutylene, benzene and n-hexane were used. The increase of diffusivity with the sorbed gas concentration is considered due largely to the plasticizing effect of the solute on the membrane.

The pressure dependence of the permeability coefficient can probably be explained in terms of a pressure dependent solubility of SO_2 in the membrane. Also the increase of sorbed gas concentration with pressure can result in an increase of the diffusivity due to the plasticizing effect of the penetrant on the membrane.

The effect of pressure on the permeability coefficient shown in Figure V-5 may be accounted for by the exponential equation $P = P_o e^{(k_1 P_1 + k_2 P_1^2)}$ for temperatures up to 35°C. For higher temperatures, the system behaves more "ideally" and an exponential equation $P = P_o e^{k_1 P_1}$ describes the pressure dependence of the permeability coefficient.

D. PERMEABILITY COEFFICIENTS FOR NITROGEN, CARBON MONOXIDE AND ARGON

(1) The Data

The permeability coefficients for N_2 and CO were determined in the 0°C to 55°C temperature range and in the pressure range of about 200 psig to 700 psig. The coefficients for argon were only determined

in the 400 psig to 700 psig pressure range and at 0°C. The membrane used contained 18 wt% sulfolene on a solvent free basis and had a thickness of 2 mils. The data are presented in Table V-4 to Table V-6.

(2) Discussion

The permeability coefficient for N_2, CO and Ar were found to be independent of pressure, as shown in Figure V-7 to Figure V-9. The coefficients for N_2 and CO increase with temperature. In Figure V-9A selected values extracted from Figure V-7 and Figure V-8 were plotted as functions of the reciprocal value of the absolute temperatures. It can be seen that an exponential expression of the form $P=P_o e^{-k_1/T}$ can be used to correlate the data for nitrogen and carbon monoxide. The permeability coefficients for the three gases studied are extremely low, especially at lower temperatures. This is probably due to the high crystallinity degree of the vinylidene fluoride resin and to low solubilities of the gases in sulfolene. The temperature function of the permeability coefficients, that follows an Arrhenius-type expression, is probably determined by the diffusivity dependence on temperature. The permeation processes for these gases seem to be diffusivity controlled. Plasticizing effects due to the concentration of penetrant in the membrane are not apparent. The systems behave ideally.

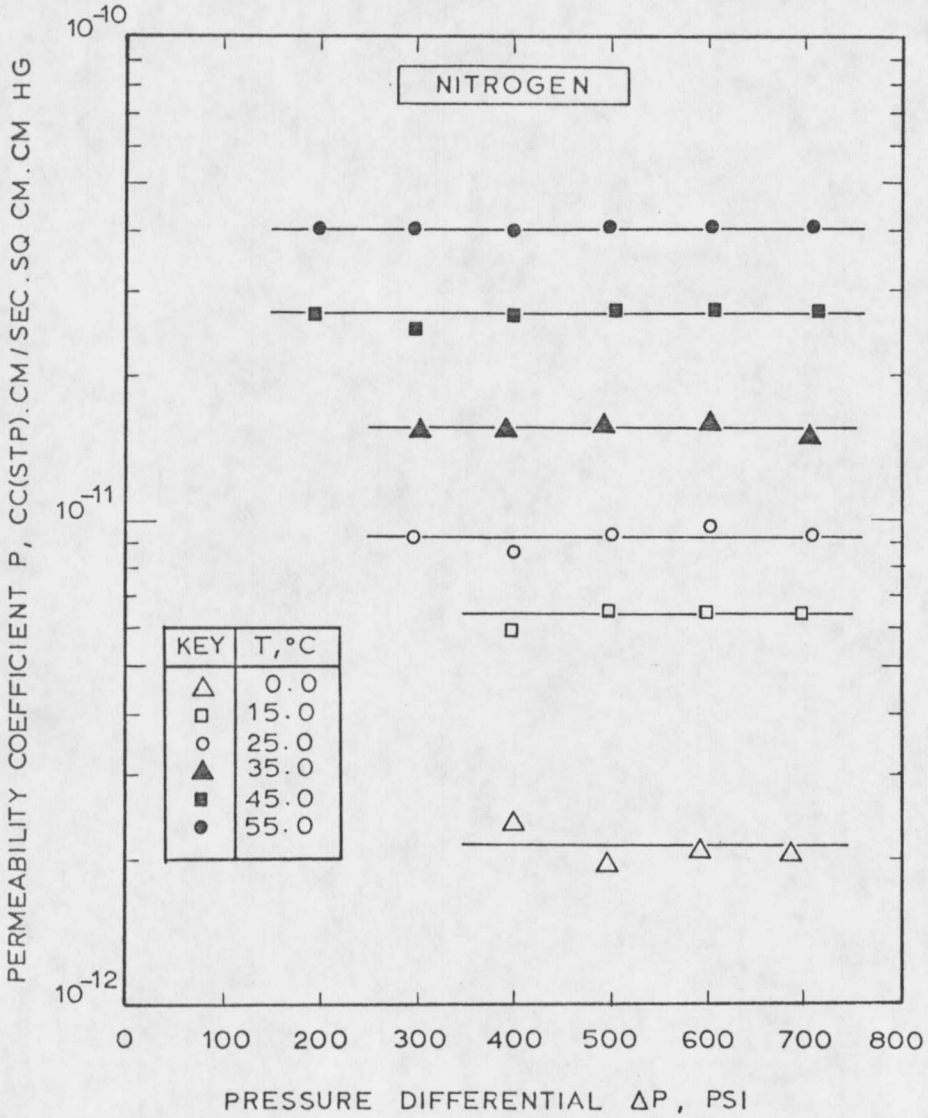

FIGURE V-7. PERMEABILITY COEFFICIENT VS. PRESSURE DIFFERENTIAL FOR NITROGEN

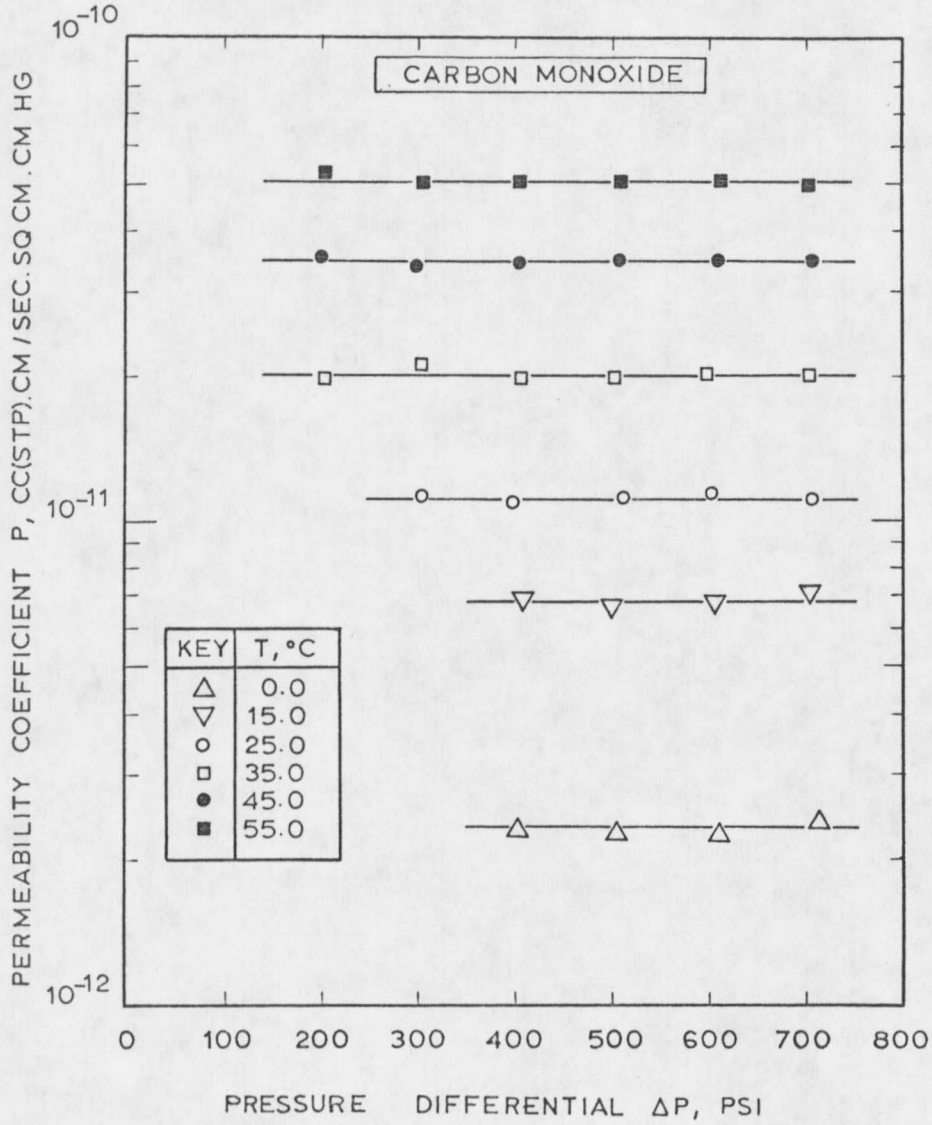

FIGURE V-8. PERMEABILITY COEFFICIENT VS. PRESSURE DIFFERENTIAL FOR CARBON MONOXIDE

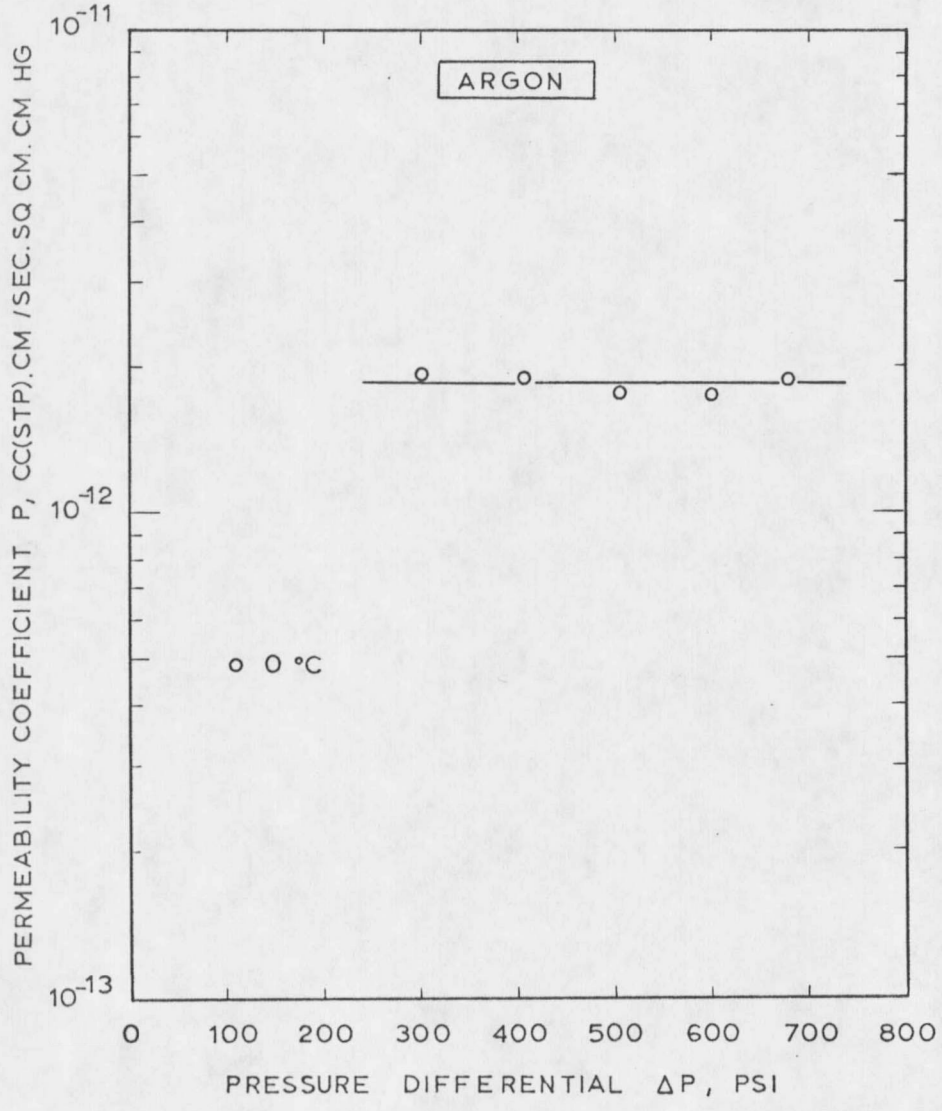

FIGURE V-9. PERMEABILITY COEFFICIENT VS. PRESSURE DIFFERENTIAL FOR ARGON

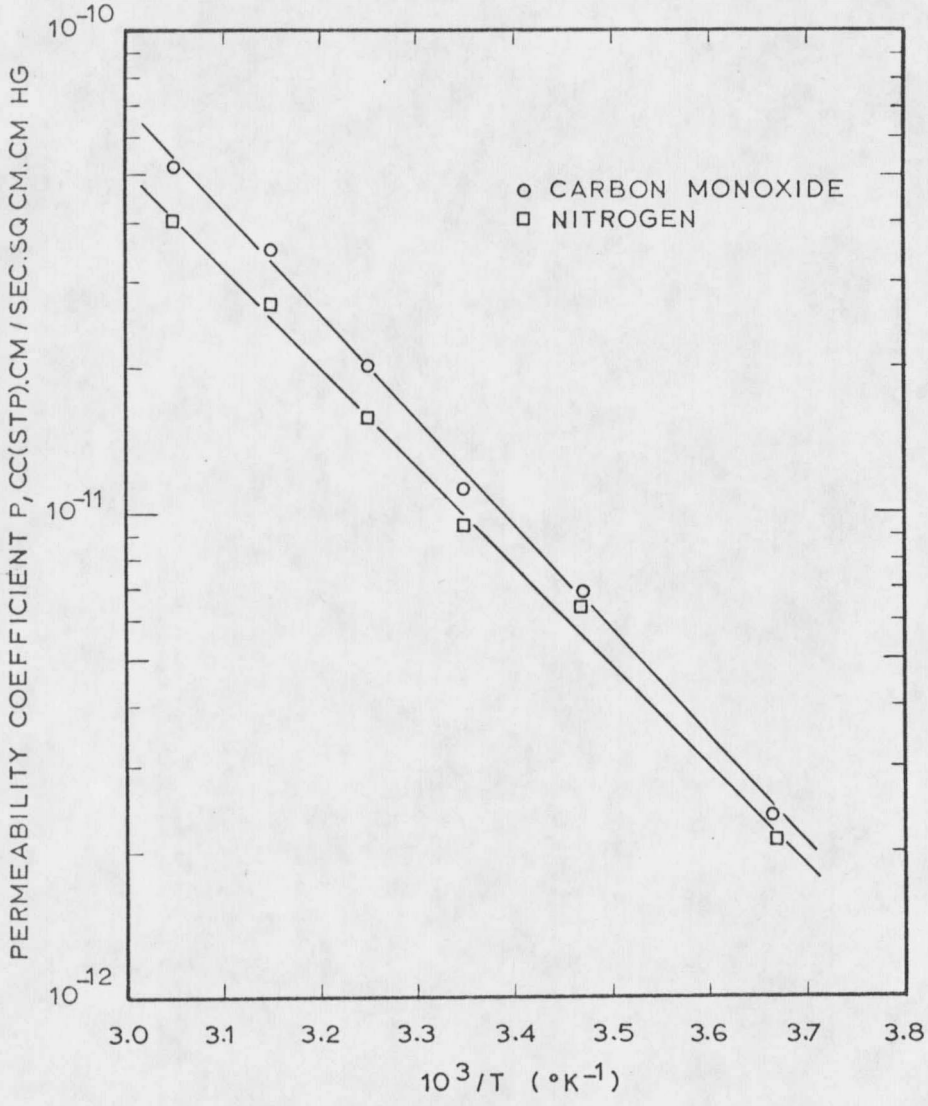

FIGURE V-9A. PERMEABILITY COEFFICIENT VS. $10^3/T$ FOR CARBON MONOXIDE AND NITROGEN

TABLE V-4. PERMEABILITY COEFFICIENTS FOR NITROGEN

Sulfolene in Membrane: 18 wt.% Thickness: 2 mils.

Run No	Temp. °C	P_1 (Psia)	P_2 (Psia)	Flux cc(STP)/ cm^2 sec.	P cm.cc(STP)/ sec.cm^2.cmHg
53-1	0.0	702.5	12.53	$.143 \times 10^{-5}$	$.203 \times 10^{-11}$
53-2	0.0	605.5	12.53	$.124 \times 10^{-5}$	$.205 \times 10^{-11}$
53-3	0.0	509.5	12.53	$.984 \times 10^{-6}$	$.194 \times 10^{-11}$
53-4	0.0	412.5	12.52	$.957 \times 10^{-6}$	$.235 \times 10^{-11}$
54-1	15.0	711.4	12.48	$.455 \times 10^{-5}$	$.639 \times 10^{-11}$
54-2	15.0	612.4	12.49	$.393 \times 10^{-5}$	$.644 \times 10^{-11}$
54-3	15.0	513.4	12.49	$.329 \times 10^{-5}$	$.645 \times 10^{-11}$
54-4	15.0	412.4	12.49	$.240 \times 10^{-5}$	$.590 \times 10^{-11}$
55-1	25.0	720.4	12.44	$.670 \times 10^{-5}$	$.930 \times 10^{-11}$
55-2	25.0	615.4	12.44	$.592 \times 10^{-5}$	$.965 \times 10^{-11}$
55-3	25.0	514.4	12.44	$.476 \times 10^{-5}$	$.932 \times 10^{-11}$
55-4	25.0	413.4	12.43	$.348 \times 10^{-5}$	$.852 \times 10^{-11}$
55-5	25.0	310.4	12.43	$.281 \times 10^{-5}$	$.925 \times 10^{-11}$
56-1	35.0	717.5	12.53	$.107 \times 10^{-4}$	$.149 \times 10^{-10}$
56-2	35.0	613.5	12.53	$.962 \times 10^{-5}$	$.157 \times 10^{-10}$
56-3	35.0	505.5	12.53	$.783 \times 10^{-5}$	$.156 \times 10^{-10}$
56-4	35.0	406.5	12.52	$.608 \times 10^{-5}$	$.152 \times 10^{-10}$
56-5	35.0	315.5	12.52	$.468 \times 10^{-5}$	$.152 \times 10^{-10}$
57-1	45.0	727.3	12.39	$.197 \times 10^{-4}$	$.271 \times 10^{-10}$
57-2	45.0	618.3	12.39	$.171 \times 10^{-4}$	$.277 \times 10^{-10}$
57-3	45.0	515.3	12.39	$.138 \times 10^{-4}$	$.270 \times 10^{-10}$
57-4	45.0	412.3	12.39	$.108 \times 10^{-4}$	$.265 \times 10^{-10}$
57-5	45.0	313.3	12.39	$.760 \times 10^{-5}$	$.248 \times 10^{-10}$
57-6	45.0	209.3	12.38	$.545 \times 10^{-5}$	$.272 \times 10^{-10}$

TABLE V-4 (Cont).

Run No.	Temp. °C	P_1 (Psia)	P_2 (Psia)	Flux cc(STP)/ cm^2 sec.	P cm.cc(STP)/ sec.cm^2.cmH_g
58-1	55.0	722.3	12.39	$.291 \times 10^{-4}$	$.403 \times 10^{-10}$
58-2	55.0	614.3	12.39	$.248 \times 10^{-4}$	$.404 \times 10^{-10}$
58-3	55.0	512.3	12.40	$.204 \times 10^{-4}$	$.401 \times 10^{-10}$
58-4	55.0	413.3	12.39	$.164 \times 10^{-4}$	$.403 \times 10^{-10}$
58-5	55.0	310.3	12.39	$.122 \times 10^{-4}$	$.403 \times 10^{-10}$
58-6	55.0	213.3	12.39	$.828 \times 10^{-5}$	$.405 \times 10^{-10}$

TABLE V-5. PERMEABILITY COEFFICIENTS FOR CARBON MONOXIDE

Sulfolene in Membrane: 18 wt.% Thickness: 2 mils

Run No.	Temp °C	P_1 (Psia)	P_2 (Psia)	Flux cc(STP)/ cm^2 sec.	P cm.cc(STP)/ $sec.cm^2.cmH_g$
59-1	0.0	727.3	12.40	$.173 \times 10^{-5}$	$.238 \times 10^{-11}$
59-2	0.0	622.3	12.40	$.139 \times 10^{-5}$	$.224 \times 10^{-11}$
59-3	0.0	515.3	12.40	$.115 \times 10^{-5}$	$.224 \times 10^{-11}$
59-4	0.0	420.3	12.40	$.954 \times 10^{-6}$	$.230 \times 10^{-11}$
60-1	15.0	715.4	12.46	$.435 \times 10^{-5}$	$.608 \times 10^{-11}$
60-2	15.0	616.4	12.46	$.357 \times 10^{-5}$	$.581 \times 10^{-11}$
60-3	15.0	510.4	12.46	$.284 \times 10^{-5}$	$.561 \times 10^{-11}$
60-4	15.0	420.4	12.46	$.244 \times 10^{-5}$	$.587 \times 10^{-11}$
61-1	25.0	717.4	12.49	$.790 \times 10^{-5}$	$.110 \times 10^{-10}$
61-2	25.0	616.4	12.49	$.705 \times 10^{-5}$	$.115 \times 10^{-10}$
61-3	25.0	522.4	12.49	$.695 \times 10^{-5}$	$.134 \times 10^{-10}$
61-4	25.0	412.4	12.49	$.544 \times 10^{-5}$	$.134 \times 10^{-10}$
61-5	25.0	317.4	12.49	$.392 \times 10^{-5}$	$.126 \times 10^{-10}$
62-1	35.0	720.4	12.49	$.187 \times 10^{-4}$	$.259 \times 10^{-10}$
62-2	35.0	611.4	12.49	$.157 \times 10^{-4}$	$.257 \times 10^{-10}$
62-3	35.0	514.4	12.49	$.131 \times 10^{-4}$	$.257 \times 10^{-10}$
62-4	35.0	419.4	12.49	$.106 \times 10^{-4}$	$.256 \times 10^{-10}$
62-5	35.0	312.4	12.49	$.826 \times 10^{-4}$	$.270 \times 10^{-10}$
62-6	35.0	214.4	12.49	$.515 \times 10^{-4}$	$.250 \times 10^{-10}$
63-1	45.0	718.5	12.54	$.246 \times 10^{-4}$	$.342 \times 10^{-10}$
63-2	45.0	622.5	12.54	$.216 \times 10^{-4}$	$.348 \times 10^{-10}$
63-3	45.0	524.5	12.54	$.182 \times 10^{-4}$	$.349 \times 10^{-10}$
63-4	45.0	420.5	12.54	$.140 \times 10^{-4}$	$.339 \times 10^{-10}$
63-5	45.0	312.5	12.54	$.102 \times 10^{-4}$	$.335 \times 10^{-10}$

TABLE V-5 (Cont).

Run No.	Temp. °C	P_1 (Psia)	P_2 (Psia)	Flux cc(STP)/ cm^2 sec.	P cm.cc(STP)/ $sec.cm^2.cmH_g$
63-5	45.0	214.5	12.54	$.725 \times 10^{-5}$	$.353 \times 10^{-10}$
64-1	55.0	714.5	12.55	$.354 \times 10^{-4}$	$.495 \times 10^{-10}$
64-2	55.0	622.5	12.54	$.314 \times 10^{-4}$	$.506 \times 10^{-10}$
64-3	55.0	520.5	12.54	$.262 \times 10^{-4}$	$.506 \times 10^{-10}$
64-4	55.0	414.5	12.54	$.204 \times 10^{-4}$	$.500 \times 10^{-10}$
64-5	55.0	316.5	12.53	$.156 \times 10^{-4}$	$.505 \times 10^{-10}$
64-5	55.0	217.5	12.53	$.110 \times 10^{-4}$	$.526 \times 10^{-10}$

TABLE V-6. PERMEABILITY COEFFICIENTS FOR ARGON

Sulfolene in Membrane: 18 wt.% Thickness: 2 mils

Run No	Temp. °C	P_1 (Psia)	P_2 (Psia)	Flux cc(STP)/ cm^2 sec.	P cm.cc(STP)/ sec.cm^2.cmH_g
46-1	0.0	692.4	12.45	$.128 \times 10^{-5}$	$.185 \times 10^{-11}$
46-2	0.0	612.4	12.44	$.107 \times 10^{-5}$	$.175 \times 10^{-11}$
46-3	0.0	518.4	12.45	$.909 \times 10^{-6}$	$.177 \times 10^{-11}$
46-4	0.0	416.4	12.44	$.768 \times 10^{-6}$	$.187 \times 10^{-11}$
46-5	0.0	313.4	12.44	$.581 \times 10^{-6}$	$.190 \times 10^{-11}$

E. PERMEABILITY COEFFICIENTS FOR CARBON DIOXIDE

(1) The Data

The permeability coefficients for carbon dioxide were determined in the 0°C to 55°C temperature range, and in the pressure range of about 100 psig to 700 psig. The membrane used contained 18 wt% sulfolene on a solvent free basis and had a thickness of 2 mils. The data are presented in Table V-7.

(2) Discussion

The permeability coefficients for carbon dioxide show a strong dependence on both, temperature and pressure, as shown in Figure V-10. Selected values extracted from Figure V-10 are plotted in Figure V-11 as functions of the reciprocal values of the absolute temperatures, keeping the pressure differential as a parameter. Again, the pressure and temperature dependence follow a rather complex pattern. The data may be correlated by exponential expressions of the form

$$P = P_o e^{(k_1 P_1 + k_2 P_1^2)}.$$

In general, the coefficients are one order of magnitude lower than those of SO_2, but still about two orders of magnitude higher than those of the N_2, CO, Ar group. The highest value, $P = 0.4 \times 10^{-8}$ cc(STP). $cm/sec.cm^2 cmH_g$, was obtained at 15.1°C and 681 psia.

The behavior of the CO_2-sulfolene/vinylidene fluoride system can probably be explained in terms of the solubility and diffusivity of

TABLE V-7. PERMEABILITY COEFFICIENTS FOR CARBON DIOXIDE

Sulfolene in Membrane: 18 wt. % Thickness: 2 Mils

Run No.	Temp. °C	P_1 (Psia)	P_2 (Psia)	Flux cc(STP)/ cm^2 sec.	P cm.cc(STP)/ sec.cm^2.cmH_g
47-1	0.0	474.3	12.34	$.126 \times 10^{-2}$	$.269 \times 10^{-8}$
47-2	0.0	409.3	12.33	$.814 \times 10^{-3}$	$.201 \times 10^{-8}$
47-3	0.0	362.3	12.33	$.517 \times 10^{-3}$	$.145 \times 10^{-8}$
47-4	0.0	310.3	12.33	$.309 \times 10^{-3}$	$.102 \times 10^{-8}$
47-5	0.0	262.3	12.33	$.170 \times 10^{-3}$	$.667 \times 10^{-9}$
47-6	0.0	208.3	12.32	$.802 \times 10^{-4}$	$.402 \times 10^{-9}$
47-7	0.0	159.3	12.32	$.328 \times 10^{-4}$	$.219 \times 10^{-9}$
47-8	0.0	110.3	12.32	$.111 \times 10^{-4}$	$.111 \times 10^{-9}$
48-1	15.1	681.3	12.34	$.277 \times 10^{-2}$	$.407 \times 10^{-8}$
48-2	15.1	635.3	12.33	$.240 \times 10^{-2}$	$.379 \times 10^{-8}$
48-3	15.1	583.3	12.33	$.191 \times 10^{-2}$	$.329 \times 10^{-8}$
48-4	15.1	509.3	12.33	$.129 \times 10^{-2}$	$.255 \times 10^{-8}$
48-5	15.1	461.3	12.33	$.935 \times 10^{-3}$	$.204 \times 10^{-8}$
48-6	15.1	412.3	12.33	$.653 \times 10^{-3}$	$.160 \times 10^{-8}$
48-7	15.1	361.3	12.32	$.423 \times 10^{-3}$	$.119 \times 10^{-8}$
48-8	15.1	312.3	12.32	$.267 \times 10^{-3}$	$.874 \times 10^{-9}$
48-9	15.1	262.3	12.32	$.160 \times 10^{-3}$	$.630 \times 10^{-9}$
48-10	15.1	212.3	12.31	$.939 \times 10^{-4}$	$.462 \times 10^{-9}$
48-11	15.1	114.3	12.31	$.252 \times 10^{-4}$	$.243 \times 10^{-9}$
49-1	25.0	714.3	12.34	$.231 \times 10^{-2}$	$.323 \times 10^{-8}$
49-2	25.0	668.3	12.34	$.197 \times 10^{-2}$	$.295 \times 10^{-8}$
49-3	25.0	615.3	12.33	$.163 \times 10^{-2}$	$.266 \times 10^{-8}$
49-4	25.0	565.3	12.33	$.130 \times 10^{-2}$	$.231 \times 10^{-8}$
49-5	25.0	512.3	12.33	$.992 \times 10^{-3}$	$.195 \times 10^{-8}$

TABLE V-7 (Cont).

Run No.	Temp. °C	P_1 (Psia)	P_2 (Psia)	Flux cc(STP)/ cm^2 sec.	P cm.cc(STP)/ sec.cm^2.cmH_g
49-6	25.0	409.3	12.33	$.540 \times 10^{-3}$	$.134 \times 10^{-8}$
49-7	25.0	309.3	12.32	$.268 \times 10^{-3}$	$.885 \times 10^{-9}$
49-8	25.0	212.3	12.32	$.110 \times 10^{-3}$	$.541 \times 10^{-9}$
49-9	25.0	112.3	12.31	$.338 \times 10^{-4}$	$.332 \times 10^{-9}$
50-1	35.0	702.3	12.38	$.193 \times 10^{-2}$	$.275 \times 10^{-8}$
50-2	35.0	665.3	12.38	$.172 \times 10^{-2}$	$.259 \times 10^{-8}$
50-3	35.0	615.3	12.38	$.147 \times 10^{-2}$	$.239 \times 10^{-8}$
50-4	35.0	565.3	12.38	$.118 \times 10^{-2}$	$.209 \times 10^{-8}$
50-5	35.0	509.3	12.38	$.932 \times 10^{-3}$	$.184 \times 10^{-8}$
50-6	35.0	417.3	12.37	$.584 \times 10^{-3}$	$.142 \times 10^{-8}$
50-7	35.0	310.3	12.37	$.303 \times 10^{-3}$	1.000×10^{-9}
50-8	35.0	212.3	12.37	$.117 \times 10^{-3}$	$.577 \times 10^{-9}$
50-9	35.0	112.3	12.36	$.439 \times 10^{-4}$	$.431 \times 10^{-9}$
51-1	44.8	712.3	12.39	$.199 \times 10^{-2}$	$.280 \times 10^{-8}$
51-2	44.8	665.3	12.39	$.167 \times 10^{-2}$	$.251 \times 10^{-8}$
51-3	44.8	610.3	12.38	$.143 \times 10^{-2}$	$.235 \times 10^{-8}$
51-4	44.8	564.3	12.38	$.121 \times 10^{-2}$	$.215 \times 10^{-8}$
51-5	44.8	516.3	12.38	$.975 \times 10^{-3}$	$.190 \times 10^{-8}$
51-6	44.8	415.3	12.38	$.600 \times 10^{-3}$	$.146 \times 10^{-8}$
51-7	44.8	312.3	12.37	$.338 \times 10^{-3}$	$.110 \times 10^{-8}$
51-8	44.8	212.3	12.37	$.164 \times 10^{-3}$	$.805 \times 10^{-9}$
51-9	44.8	111.3	12.37	$.627 \times 10^{-4}$	$.622 \times 10^{-9}$
52-1	55.0	722.3	12.39	$.199 \times 10^{-2}$	$.275 \times 10^{-8}$
52-2	55.0	659.3	12.38	$.165 \times 10^{-2}$	$.250 \times 10^{-8}$
52-3	55.0	615.3	12.38	$.145 \times 10^{-2}$	$.236 \times 10^{-8}$
52-4	55.0	515.3	12.38	$.990 \times 10^{-3}$	$.193 \times 10^{-8}$

TABLE V-7 (Cont).

Run No.	Temp. °C	P_1 (Psia)	P_2 (Psia)	Flux cc(STP)/ cm^2 sec.	P cm.cc(STP)/ sec.cm^2.cmH_g
52-5	55.0	417.3	12.38	$.672 \times 10^{-3}$	$.163 \times 10^{-8}$
52-6	55.0	322.3	12.37	$.416 \times 10^{-3}$	$.132 \times 10^{-8}$
52-7	55.0	215.3	12.37	$.211 \times 10^{-3}$	$.102 \times 10^{-8}$
52-8	55.0	122.3	12.37	$.752 \times 10^{-4}$	$.740 \times 10^{-9}$

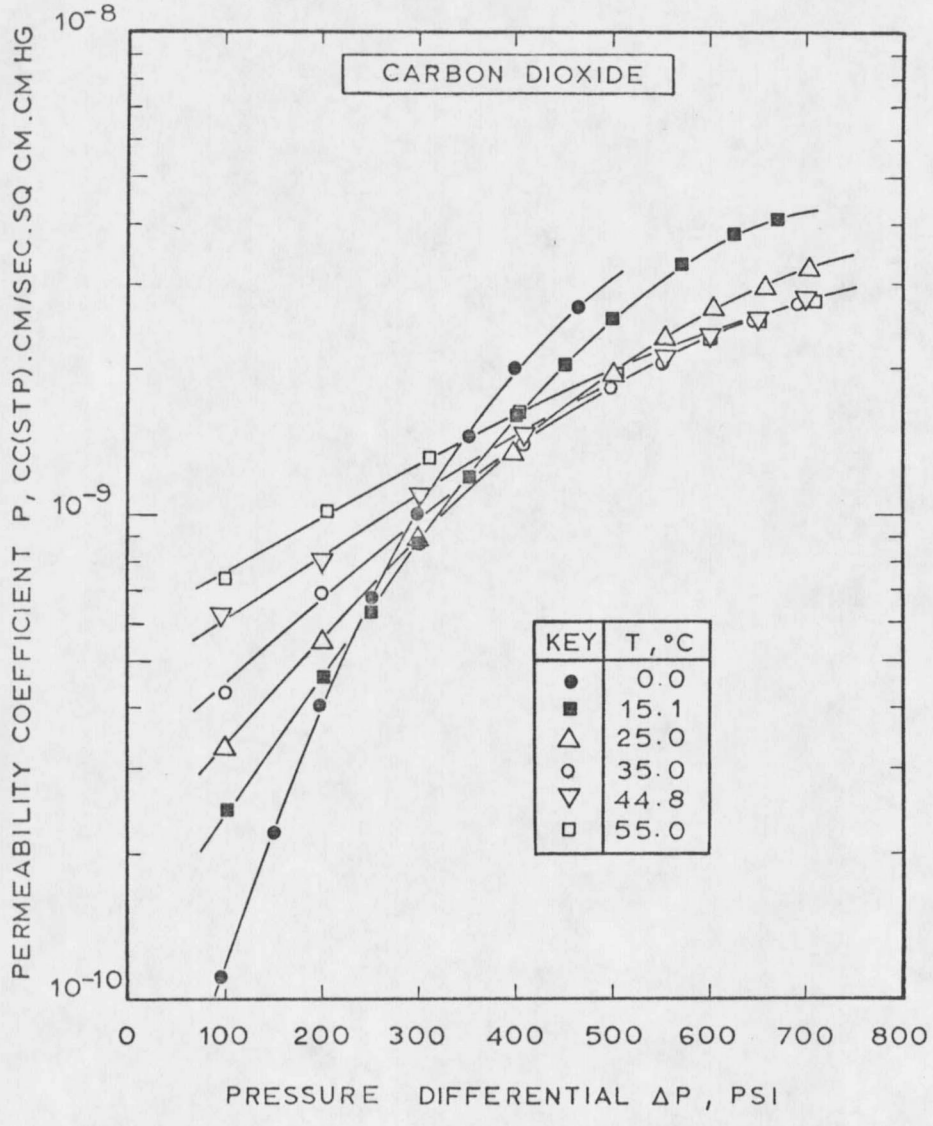

FIGURE V-10. PERMEABILITY COEFFICIENT VS. PRESSURE DIFFERENTIAL FOR CARBON DIOXIDE

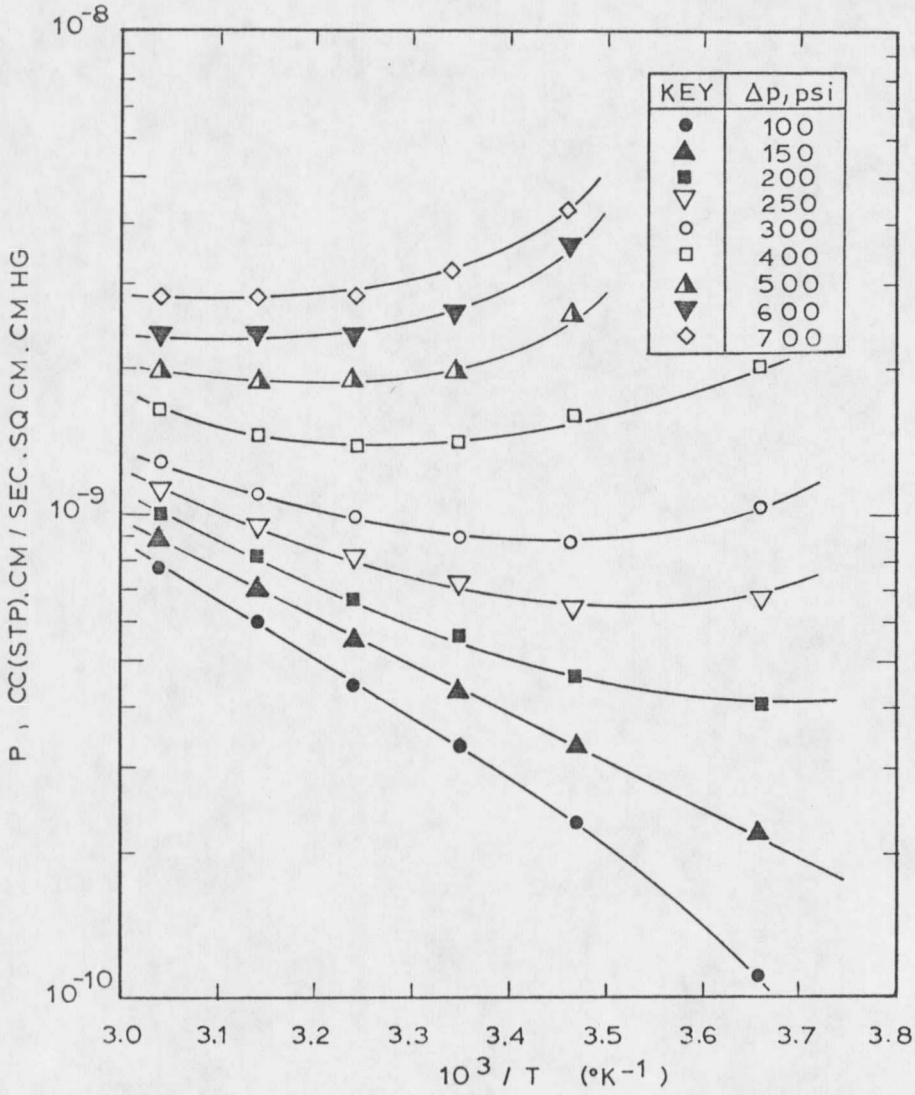

FIGURE V-11. PERMEABILITY COEFFICIENT VS. 10^3/ T FOR CARBON DIOXIDE

CO_2 in the membrane. The permeability coefficient is a highly nonlinear function of pressure, especially at lower temperatures, which may be due to a strong dependence of the solubility on pressure and to the plasticizing effect associated with the higher concentration of sorbed gas in the membrane, which tends to increase the diffusivity. As the pressure decreases, the concentration of the penetrant decreases together with the plasticizing effect associated with it. Because of this combined mechanism, the permeability coefficient drop could be quite drastic, as appears in Figure V-10. At higher temperatures, the pressure dependence of the permeability coefficient, even though it shows the same trend, is not as strong. This may be due to the fact that the solubility and the coupled plasticizing effect diminish with temperature, while there may be a considerable increase in the diffusivity with the increasing temperature. The net effect is a milder dependence of the permeability coefficient on the pressure, especially at low pressures, where the effect of the increasing diffusivity is stronger than the effect of the decreasing solubility. Thus, at low pressure, a net increase in permeability coefficients is achieved with increasing temperatures. At higher pressure, the effect of the solubility (apparently a strong function of pressure) is predominant and an increase in temperature causes a decrease in the permeability coefficients. Therefore, it appears that the system under investigation shows a mixed behavior, is diffusivity controlled at low pressures, and

solubility controlled at higher pressures, for the range of temperatures studied. This explains the intersections of the experimental curves shown in Figure V-10 and the rather complex patterin shown in Figure V-11 where the permeability coefficients shows minima for some temperatures.

F. PERMEABILITY COEFFICIENT FOR OXYGEN, HYDROGEN, METHANE, ETHANE, ETHYLENE, 1-3 BUTADIENE

(1) The Data

The permeability coefficients for oxygen and ethylene were determined in the 0°C to 55°C temperature range, and in the 200 psig to 700 psig pressure range. For hydrogen, methane and ethane the temperatures and pressure ranges considered were about 15°C to 55°C and 200 psig to 700 psig respectively. For 1-3 Butadiene the temperature range considered was 38°C to 55°C with a pressure range of 10 psig to about 30 psig. The data are presented in Table V-8 to Table V-13. The membrane used contained 18 wt% solfolene on a solvent free basis and had a thickness of 2 mils.

(2) Discussion

The permeability coefficients for all the gases in this group are pressure dependent, as shown in Figure V-12 to Figure V-17. Selected values extracted from these figures are plotted in Figure V-18 to Figure V-22 as functions of the reciprocal values of the absolute temperatures, keeping the pressure differential across the membrane as a parameter.

TABLE V-8. PERMEABILITY COEFFICIENTS FOR OXYGEN

Sulfolene in Membrane: 18 wt.% Thickness: 2 mils.

Run No.	Temp. °C	P_1 (Psia)	P_2 (Psia)	Flux cc(STP)/ cm^2 sec.	P cm.cc(STP)/ sec.cm^2.cmH_g
65-1	0.0	715.3	12.35	$.215 \times 10^{-5}$	$.300 \times 10^{-11}$
65-2	0.0	613.3	12.35	$.177 \times 10^{-5}$	$.290 \times 10^{-11}$
65-3	0.0	511.3	12.35	$.115 \times 10^{-5}$	$.226 \times 10^{-11}$
65-4	0.0	412.3	12.35	$.760 \times 10^{-6}$	$.187 \times 10^{-11}$
66-1	15.0	719.3	12.38	$.667 \times 10^{-5}$	$.928 \times 10^{-11}$
66-2	15.0	622.3	12.38	$.550 \times 10^{-5}$	$.886 \times 10^{-11}$
66-3	15.0	515.3	12.38	$.401 \times 10^{-5}$	$.784 \times 10^{-11}$
66-4	15.0	400.3	12.37	$.261 \times 10^{-5}$	$.662 \times 10^{-11}$
66-5	15.0	315.3	12.38	$.183 \times 10^{-5}$	$.593 \times 10^{-11}$
67-1	25.0	707.3	12.38	$.104 \times 10^{-4}$	$.148 \times 10^{-10}$
67.2	25.0	611.3	12.38	$.825 \times 10^{-5}$	$.135 \times 10^{-10}$
67-3	25.0	515.3	12.38	$.671 \times 10^{-5}$	$.131 \times 10^{-10}$
67-4	25.0	422.3	12.38	$.481 \times 10^{-5}$	$.115 \times 10^{-10}$
67-5	25.0	312.3	12.38	$.322 \times 10^{-5}$	$.105 \times 10^{-10}$
67-6	25.0	212.3	12.38	$.209 \times 10^{-5}$	$.103 \times 10^{-10}$
68-1	35.0	722.3	12.38	$.194 \times 10^{-4}$	$.268 \times 10^{-10}$
6802	35.0	615.3	12.38	$.148 \times 10^{-4}$	$.241 \times 10^{-10}$
68-3	35.0	514.3	12.38	$.120 \times 10^{-4}$	$.235 \times 10^{-10}$
68-4	35.0	410.3	12.38	$.933 \times 10^{-5}$	$.230 \times 10^{-10}$
68-5	35.0	316.3	12.38	$.749 \times 10^{-5}$	$.242 \times 10^{-10}$
68-6	35.0	214.3	12.38	$.412 \times 10^{-5}$	$.200 \times 10^{-10}$
69-1	45.0	714.3	12.35	$.326 \times 10^{-4}$	$.456 \times 10^{-10}$
69-2	45.0	614.3	12.35	$.262 \times 10^{-4}$	$.428 \times 10^{-10}$
69-3	45.0	518.3	12.35	$.214 \times 10^{-4}$	$.415 \times 10^{-10}$

TABLE V-8 (Cont).

Run No.	Temp. °C	P_1 (Psia)	P_2 (Psia)	Flux cc(STP)/ cm^2 sec.	P cm.cc(STP)/ $sec.cm^2.cmH_g$
69-4	45.0	414.3	12.35	$.155 \times 10^{-4}$	$.378 \times 10^{-10}$
69-5	45.0	312.3	12.35	$.115 \times 10^{-4}$	$.376 \times 10^{-10}$
69-6	45.0	210.3	12.35	$.670 \times 10^{-5}$	$.333 \times 10^{-10}$
70-1	55.0	722.3	12.35	$.537 \times 10^{-4}$	$.743 \times 10^{-10}$
70-2	55.0	612.3	12.35	$.428 \times 10^{-4}$	$.700 \times 10^{-10}$
70-3	55.0	519.3	12.35	$.339 \times 10^{-4}$	$.656 \times 10^{-10}$
70-4	55.0	415.3	12.35	$.258 \times 10^{-4}$	$.630 \times 10^{-10}$
70-5	55.0	312.3	12.35	$.178 \times 10^{-4}$	$.582 \times 10^{-10}$
70-6	55.0	208.3	12.35	$.108 \times 10^{-4}$	$.554 \times 10^{-10}$

TABLE V-9. PERMEABILITY COEFFICIENTS FOR HYDROGEN

Sulfolene in Membrane: 18 wt. % Thickness: 2 mils.

Run No.	Temp. °C	P_1 (Psia)	P_2 (Psia)	Flux cc(STP)/ cm^2 sec.	P cm.cc(STP)/ sec.cm^2.$cmHg$
93-1	11.0	727.5	12.54	$.119 \times 10^{-4}$	$.164 \times 10^{-10}$
93-2	11.0	727.5	12.54	$.121 \times 10^{-4}$	$.166 \times 10^{-10}$
93-3	11.0	614.5	12.54	$.793 \times 10^{-5}$	$.129 \times 10^{-10}$
93-5	11.0	614.5	12.54	$.816 \times 10^{-5}$	$.132 \times 10^{-10}$
93-5	11.0	512.5	12.54	$.559 \times 10^{-5}$	$.110 \times 10^{-10}$
93-6	11.0	512.5	12.54	$.565 \times 10^{-5}$	$.111 \times 10^{-10}$
93-7	11.0	412.5	12.54	$.423 \times 10^{-5}$	$.104 \times 10^{-10}$
93-8	11.0	412.5	12.54	$.373 \times 10^{-5}$	$.916 \times 10^{-11}$
93-9	11.0	412.5	12.54	$.359 \times 10^{-5}$	$.882 \times 10^{-11}$
93-10	11.0	412.5	12.54	$.352 \times 10^{-5}$	$.865 \times 10^{-11}$
94-1	15.0	720.5	12.59	$.136 \times 10^{-4}$	$.189 \times 10^{-10}$
94-2	15.0	720.5	12.59	$.140 \times 10^{-4}$	$.194 \times 10^{-10}$
94-3	15.0	613.5	12.59	$.992 \times 10^{-4}$	$.162 \times 10^{-10}$
94-4	15.0	613.5	12.59	$.100 \times 10^{-4}$	$.164 \times 10^{-10}$
94-5	15.0	510.5	12.59	$.831 \times 10^{-5}$	$.164 \times 10^{-10}$
94-6	15.0	510.5	12.59	$.799 \times 10^{-4}$	$.157 \times 10^{-10}$
94-7	15.0	510.5	12.59	$.785 \times 10^{-5}$	$.155 \times 10^{-10}$
94-8	15.0	412.5	12.59	$.608 \times 10^{-5}$	$.147 \times 10^{-10}$
94-9	15.0	412.5	12.59	$.585 \times 10^{-5}$	$.143 \times 10^{-10}$
95-1	25.0	720.5	12.59	$.318 \times 10^{-4}$	$.442 \times 10^{-10}$
95-2	25.0	720.5	12.59	$.323 \times 10^{-4}$	$.449 \times 10^{-10}$
95-3	25.0	615.5	12.59	$.266 \times 10^{-4}$	$.433 \times 10^{-10}$
95-4	25.0	615.5	12.59	$.268 \times 10^{-4}$	$.436 \times 10^{-10}$
95-5	25.0	510.5	12.59	$.201 \times 10^{-4}$	$.397 \times 10^{-10}$
95-6	25.0	510.5	12.59	$.202 \times 10^{-4}$	$.399 \times 10^{-10}$

TABLE V-9 (Cont).

Run No	Temp °C	P_1 (Psia)	P_2 (Psia)	Flux cc(STP)/ cm^2 sec.	P cm.cc(STP)/ $sec.cm^2.cmHg$
95-7	25.0	408.5	12.59	$.116 \times 10^{-4}$	$.289 \times 10^{-10}$
95-8	25.0	408.5	12.59	$.116 \times 10^{-4}$	$.287 \times 10^{-10}$
95-9	25.0	408.5	12.59	$.115 \times 10^{-4}$	$.286 \times 10^{-10}$
96-1	35.0	727.5	12.60	$.616 \times 10^{-4}$	$.847 \times 10^{-10}$
96-2	35.0	727.5	12.60	$.613 \times 10^{-4}$	$.843 \times 10^{-10}$
96-3	35.0	727.5	12.60	$.616 \times 10^{-4}$	$.847 \times 10^{-10}$
96-4	35.0	614.5	12.60	$.482 \times 10^{-4}$	$.787 \times 10^{-10}$
96-5	35.0	614.5	12.60	$.489 \times 10^{-4}$	$.799 \times 10^{-10}$
96-6	35.0	614.5	12.60	$.465 \times 10^{-4}$	$.759 \times 10^{-10}$
96-7	35.0	509.5	12.60	$.358 \times 10^{-4}$	$.707 \times 10^{-10}$
96-8	35.0	509.5	12.60	$.368 \times 10^{-4}$	$.727 \times 10^{-10}$
96-9	35.0	509.5	12.60	$.366 \times 10^{-4}$	$.723 \times 10^{-10}$
96-10	35.0	407.5	12.60	$.238 \times 10^{-4}$	$.591 \times 10^{-10}$
96-11	35.0	407.5	12.60	$.227 \times 10^{-4}$	$.566 \times 10^{-10}$
96-12	35.0	407.5	12.60	$.231 \times 10^{-4}$	$.576 \times 10^{-10}$
96-13	35.0	312.5	12.60	$.145 \times 10^{-4}$	$.474 \times 10^{-10}$
96-14	35.0	312.5	12.60	$.148 \times 10^{-4}$	$.484 \times 10^{-10}$
96-15	35.0	312.5	12.60	$.145 \times 10^{-4}$	$.474 \times 10^{-10}$
97-1	45.0	732.3	12.38	$.113 \times 10^{-3}$	$.155 \times 10^{-9}$
97-2	45.0	732.3	12.38	$.117 \times 10^{-3}$	$.160 \times 10^{-9}$
97-3	45.0	732.3	12.38	$.114 \times 10^{-3}$	$.156 \times 10^{-9}$
97-4	45.0	614.3	12.38	$.953 \times 10^{-4}$	$.155 \times 10^{-9}$
97-5	45.0	614.3	12.38	$.918 \times 10^{-4}$	$.150 \times 10^{-9}$
97-6	45.0	614.3	12.38	$.945 \times 10^{-4}$	$.154 \times 10^{-9}$
97-7	45.0	614.3	12.38	$.942 \times 10^{-4}$	$.154 \times 10^{-9}$
97-8	45.0	510.3	12.38	$.660 \times 10^{-4}$	$.130 \times 10^{-9}$

TABLE V-9 (Cont).

Run No	Temp °C	P_1 (Psia)	P_2 (Psia)	Flux cc(STP)/ cm^2 sec.	P cm.cc(STP)/ $sec.cm^2.cmH_g$
97-9	45.0	510.3	12.38	$.657 \times 10^{-4}$	$.130 \times 10^{-9}$
97-10	45.0	415.3	12.38	$.489 \times 10^{-4}$	$.119 \times 10^{-9}$
97-11	45.0	415.3	12.38	$.487 \times 10^{-4}$	$.119 \times 10^{-9}$
97-12	45.0	312.3	12.38	$.316 \times 10^{-4}$	$.103 \times 10^{-9}$
97-13	45.0	312.3	12.38	$.312 \times 10^{-4}$	$.102 \times 10^{-9}$
97-14	45.0	312.3	12.38	$.307 \times 10^{-4}$	$.100 \times 10^{-9}$
97-15	45.0	312.3	12.38	$.313 \times 10^{-4}$	$.103 \times 10^{-9}$
97-16	45.0	212.3	12.38	$.209 \times 10^{-4}$	$.103 \times 10^{-9}$
97-17	45.0	212.3	12.38	$.208 \times 10^{-4}$	$.102 \times 10^{-9}$
98-1	55.0	722.3	12.38	$.171 \times 10^{-3}$	$.237 \times 10^{-9}$
98-2	55.0	722.3	12.38	$.170 \times 10^{-3}$	$.235 \times 10^{-9}$
98-3	55.0	722.3	12.38	$.178 \times 10^{-3}$	$.246 \times 10^{-9}$
98-4	55.0	615.3	12.38	$.136 \times 10^{-3}$	$.221 \times 10^{-9}$
98-5	55.0	615.3	12.38	$.133 \times 10^{-3}$	$.217 \times 10^{-9}$
98-6	55.0	511.3	12.38	$.105 \times 10^{-3}$	$.207 \times 10^{-9}$
98-7	55.0	510.3	12.38	$.109 \times 10^{-3}$	$.215 \times 10^{-9}$
98-8	55.0	412.3	12.38	$.758 \times 10^{-4}$	$.186 \times 10^{-9}$
98-9	55.0	412.3	12.38	$.824 \times 10^{-4}$	$.202 \times 10^{-9}$
98-10	55.0	412.3	12.38	$.782 \times 10^{-4}$	$.192 \times 10^{-9}$
98-11	55.0	312.3	12.38	$.562 \times 10^{-4}$	$.184 \times 10^{-9}$
98-12	55.0	312.3	12.38	$.567 \times 10^{-4}$	$.186 \times 10^{-9}$
98-13	55.0	209.3	12.38	$.308 \times 10^{-4}$	$.154 \times 10^{-9}$
98-14	55.0	209.3	12.38	$.305 \times 10^{-4}$	$.152 \times 10^{-9}$

TABLE V-10. PERMEABILITY COEFFICIENTS FOR METHANE

Sulfolene in Membrane: 18 wt. % Thickness: 2 mils.

Run No.	Temp. °C	P_1 (Psia)	P_2 (Psia)	Flux cc(STP)/ cm^2 sec.	P cm.cc(STP)/ $sec.cm^2.cmHg$
85-1	15.0	713.5	12.60	$.190 \times 10^{-5}$	$.266 \times 10^{-11}$
85-2	15.0	713.5	12.60	$.208 \times 10^{-5}$	$.291 \times 10^{-11}$
85-3	15.0	713.5	12.60	$.207 \times 10^{-5}$	$.290 \times 10^{-11}$
85-4	15.0	613.5	12.60	$.717 \times 10^{-5}$	$.280 \times 10^{-11}$
85-5	15.0	613.5	12.60	$.158 \times 10^{-5}$	$.258 \times 10^{-11}$
85-6	15.0	513.5	12.60	$.122 \times 10^{-5}$	$.239 \times 10^{-11}$
85-7	15.0	513.5	12.60	$.125 \times 10^{-5}$	$.246 \times 10^{-11}$
85-8	15.0	407.5	12.60	$.947 \times 10^{-5}$	$.236 \times 10^{-11}$
85-9	15.0	407.5	12.60	$.860 \times 10^{-6}$	$.214 \times 10^{-11}$
86-1	25.0	713.5	12.52	$.372 \times 10^{-5}$	$.521 \times 10^{-11}$
86-2	25.0	713.5	12.52	$.359 \times 10^{-5}$	$.503 \times 10^{-11}$
86-3	25.0	612.5	12.52	$.280 \times 10^{-5}$	$.458 \times 10^{-11}$
86-4	25.0	612.5	12.52	$.228 \times 10^{-5}$	$.374 \times 10^{-11}$
86-5	25.0	612.5	12.52	$.242 \times 10^{-5}$	$.397 \times 10^{-11}$
86-6	25.0	513.5	12.52	$.181 \times 10^{-5}$	$.355 \times 10^{-11}$
86-7	25.0	513.5	12.52	$.363 \times 10^{-5}$	$.515 \times 10^{-11}$
86-6	25.0	513.5	12.52	$.239 \times 10^{-5}$	$.468 \times 10^{-11}$
86-9	25.0	513.5	12.52	$.232 \times 10^{-5}$	$.455 \times 10^{-11}$
86-10	25.0	414.5	12.52	$.156 \times 10^{-5}$	$.381 \times 10^{-11}$
86-11	25.0	414.5	12.52	$.169 \times 10^{-5}$	$.414 \times 10^{-11}$
86-12	25.0	414.5	12.52	$.131 \times 10^{-5}$	$.321 \times 10^{-11}$
86-13	25.0	414.5	12.52	$.134 \times 10^{-5}$	$.329 \times 10^{-11}$
86-14	25.0	312.5	12.52	$.104 \times 10^{-5}$	$.341 \times 10^{-11}$
86-15	25.0	312.5	12.52	$.104 \times 10^{-5}$	$.342 \times 10^{-11}$

TABLE V-10 (Cont).

Run No	Temp. °C	P_1 (Psia)	P_2 (Psia)	Flux cc(STP)/ cm^2 sec.	P cm.cc(STP)/ $sec.cm^2.cmHg$
87-1	35.0	722.4	12.43	$.638 \times 10^{-5}$	$.883 \times 10^{-11}$
87-2	35.0	722.4	12.43	$.712 \times 10^{-5}$	$.985 \times 10^{-11}$
87-3	35.0	722.4	12.43	$.711 \times 10^{-5}$	$.984 \times 10^{-11}$
87-4	35.0	614.4	12.43	$.587 \times 10^{-5}$	$.959 \times 10^{-11}$
87-5	35.0	614.4	12.43	$.573 \times 10^{-5}$	$.935 \times 10^{-11}$
87-6	35.0	614.4	12.43	$.620 \times 10^{-5}$	$.101 \times 10^{-10}$
87-7	35.0	515.4	12.43	$.476 \times 10^{-5}$	$.930 \times 10^{-11}$
87-8	35.0	515.4	12.43	$.503 \times 10^{-5}$	$.983 \times 10^{-11}$
87-9	35.0	515.4	12.43	$.517 \times 10^{-5}$	$.101 \times 10^{-10}$
87-10	35.0	515.4	12.43	$.486 \times 10^{-5}$	$.950 \times 10^{-11}$
87-11	35.0	410.4	12.43	$.381 \times 10^{-5}$	$.940 \times 10^{-11}$
87-12	35.0	410.4	12.43	$.381 \times 10^{-5}$	$.942 \times 10^{-11}$
87-13	35.0	410.4	12.43	$.392 \times 10^{-5}$	$.968 \times 10^{-11}$
87-14	35.0	312.4	12.43	$.271 \times 10^{-5}$	$.888 \times 10^{-11}$
87-15	35.0	312.4	12.43	$.305 \times 10^{-5}$	$.999 \times 10^{-11}$
87-16	35.0	312.4	12.43	$.288 \times 10^{-5}$	$.943 \times 10^{-11}$
88-1	45.0	724.4	12.43	$.143 \times 10^{-4}$	$.198 \times 10^{-10}$
88-2	45.0	724.4	12.43	$.160 \times 10^{-4}$	$.221 \times 10^{-10}$
88-3	45.0	724.4	12.43	$.160 \times 10^{-4}$	$.220 \times 10^{-10}$
88-4	45.0	616.4	12.43	$.127 \times 10^{-4}$	$.206 \times 10^{-10}$
88-5	45.0	616.4	12.43	$.128 \times 10^{-4}$	$.208 \times 10^{-10}$
88-6	45.0	513.4	12.43	$.989 \times 10^{-5}$	$.194 \times 10^{-10}$
88-7	45.0	513.4	12.43	$.112 \times 10^{-4}$	$.221 \times 10^{-10}$
88-8	45.0	513.4	12.43	$.102 \times 10^{-4}$	$.199 \times 10^{-10}$
88-9	45.0	513.4	12.43	$.883 \times 10^{-5}$	$.173 \times 10^{-10}$
88-10	45.0	513.4	12.43	$.987 \times 10^{-5}$	$.194 \times 10^{-10}$

TABLE V-10 (Cont).

Run No	Temp. °C	P_1 (Psia)	P_2 (Psia)	Flux cc(STP)/ cm^2 sec.	P cm.cc(STP)/ sec.cm^2.cmH_g
88-11	45.0	410.4	12.43	$.739 \times 10^{-5}$	$.182 \times 10^{-10}$
88-12	45.0	410.4	12.43	$.686 \times 10^{-5}$	$.169 \times 10^{-10}$
88-13	45.0	312.4	12.43	$.590 \times 10^{-5}$	$.193 \times 10^{-10}$
88-14	45.0	312.4	12.43	$.546 \times 10^{-5}$	$.179 \times 10^{-10}$
89-1	55.0	732.3	12.39	$.284 \times 10^{-4}$	$.387 \times 10^{-10}$
89-2	55.0	732.3	12.39	$.278 \times 10^{-4}$	$.379 \times 10^{-10}$
89-3	55.0	616.3	12.39	$.231 \times 10^{-4}$	$.376 \times 10^{-10}$
89-4	55.0	616.3	12.39	$.230 \times 10^{-4}$	$.374 \times 10^{-10}$
89-5	55.0	514.3	12.39	$.180 \times 10^{-4}$	$.352 \times 10^{-10}$
89-6	55.0	514.3	12.39	$.177 \times 10^{-4}$	$.346 \times 10^{-10}$
89-7	55.0	413.3	12.39	$.146 \times 10^{-4}$	$.356 \times 10^{-10}$
89-8	55.0	413.3	12.39	$.144 \times 10^{-4}$	$.354 \times 10^{-10}$
89-9	55.0	312.3	12.39	$.125 \times 10^{-4}$	$.411 \times 10^{-10}$
89-10	55.0	312.3	12.39	$.113 \times 10^{-4}$	$.370 \times 10^{-10}$
89-11	55.0	312.3	12.39	$.108 \times 10^{-4}$	$.353 \times 10^{-10}$
89-12	55.0	208.3	12.39	$.647 \times 10^{-5}$	$.324 \times 10^{-10}$
89-13	55.0	208.3	12.39	$.715 \times 10^{-5}$	$.358 \times 10^{-10}$
89-14	55.0	208.3	12.39	$.679 \times 10^{-5}$	$.340 \times 10^{-10}$
89-15	55.0	208.3	12.39	$.698 \times 10^{-5}$	$.350 \times 10^{-10}$

TABLE V-11. PERMEABILITY COEFFICIENTS FOR ETHANE

Sulfolene in Membrane: 18 wt. % Thickness: 2 mils.

Run No	Temp. °C	P_1 (Psia)	P_2 (Psia)	Flux cc(STP)/ cm^2 sec.	P cm.cc(STP)/ $sec.cm^2.cmH_g$
78-4	15.0	214.5	12.52	$.696 \times 10^{-6}$	$.339 \times 10^{-11}$
79-1	25.0	494.4	12.50	$.424 \times 10^{-5}$	$.864 \times 10^{-11}$
79-2	25.0	416.4	12.50	$.323 \times 10^{-5}$	$.786 \times 10^{-11}$
79-3	25.0	322.4	12.50	$.254 \times 10^{-5}$	$.806 \times 10^{-11}$
79-4	25.0	215.4	12.50	$.169 \times 10^{-5}$	$.817 \times 10^{-11}$
79-5	25.0	215.4	12.50	$.144 \times 10^{-5}$	$.697 \times 10^{-11}$
80-1	35.0	495.5	12.58	$.924 \times 10^{-5}$	$.188 \times 10^{-10}$
80-2	35.0	495.5	12.58	$.995 \times 10^{-5}$	$.202 \times 10^{-10}$
80-3	35.0	415.5	12.58	$.865 \times 10^{-5}$	$.211 \times 10^{-10}$
80-4	35.0	415.5	12.58	$.778 \times 10^{-5}$	$.190 \times 10^{-10}$
80-5	35.0	415.5	12.58	$.781 \times 10^{-5}$	$.190 \times 10^{-10}$
80-6	35.0	312.5	12.57	$.490 \times 10^{-5}$	$.160 \times 10^{-10}$
80-7	35.0	312.5	12.57	$.527 \times 10^{-5}$	$.172 \times 10^{-10}$
80-8	35.0	312.5	12.57	$.534 \times 10^{-5}$	$.175 \times 10^{-10}$
80-9	35.0	212.5	12.57	$.419 \times 10^{-5}$	$.206 \times 10^{-10}$
80-10	35.0	212.5	12.57	$.368 \times 10^{-5}$	$.181 \times 10^{-10}$
80-11	35.0	212.5	12.57	$.290 \times 10^{-5}$	$.143 \times 10^{-10}$
80-12	35.0	212.5	12.57	$.407 \times 10^{-5}$	$.200 \times 10^{-10}$
80-13	35.0	212.5	12.57	$.344 \times 10^{-5}$	$.169 \times 10^{-10}$
81-1	45.0	499.3	12.35	$.173 \times 10^{-4}$	$.349 \times 10^{-10}$
81-2	45.0	499.3	12.35	$.193 \times 10^{-4}$	$.389 \times 10^{-10}$
81-3	45.0	499.3	12.35	$.185 \times 10^{-4}$	$.374 \times 10^{-10}$
81-4	45.0	417.3	12.35	$.149 \times 10^{-4}$	$.362 \times 10^{-10}$
81-5	45.0	417.x	12.35	$.145 \times 10^{-4}$	$.353 \times 10^{-10}$

TABLE V-11 (Cont).

Run No	Temp. °C	P_1 (Psia)	P_2 (Psia)	Flux cc(STP)/ cm^2 sec.	P cm.cc(STP)/ sec.cm^2.cmH_g
81-6	45.0	312.3	12.35	$.102 \times 10^{-4}$	$.334 \times 10^{-10}$
81-7	45.0	312.3	12.35	$.983 \times 10^{-5}$	$.322 \times 10^{-10}$
81-8	45.0	213.3	12.35	$.647 \times 10^{-5}$	$.316 \times 10^{-10}$
81-9	45.0	213.3	12.35	$.668 \times 10^{-5}$	$.327 \times 10^{-10}$
81-10	45.0	115.3	12.35	$.321 \times 10^{-5}$	$.307 \times 10^{-10}$
81-11	45.0	115.3	12.35	$.332 \times 10^{-5}$	$.317 \times 10^{-10}$
82-1	55.0	532.3	12.39	$.324 \times 10^{-4}$	$.612 \times 10^{-10}$
82-2	55.0	532.3	12.40	$.321 \times 10^{-4}$	$.608 \times 10^{-10}$
82-3	55.0	423.3	12.40	$.243 \times 10^{-4}$	$.581 \times 10^{-10}$
82-4	55.0	423.3	12.40	$.236 \times 10^{-4}$	$.564 \times 10^{-10}$
82-5	55.0	423.3	12.40	$.236 \times 10^{-4}$	$.565 \times 10^{-10}$
82-6	55.0	313.3	12.39	$.147 \times 10^{-4}$	$.479 \times 10^{-10}$
82-7	55.0	313.3	12.39	$.149 \times 10^{-4}$	$.488 \times 10^{-10}$
82-8	55.0	212.3	12.39	$.114 \times 10^{-4}$	$.560 \times 10^{-10}$
82-9	55.0	212.3	12.39	$.101 \times 10^{-4}$	$.499 \times 10^{-10}$
82-10	55.0	212.3	12.39	$.108 \times 10^{-4}$	$.534 \times 10^{-10}$
82-11	55.0	212.3	12.40	$.102 \times 10^{-4}$	$.503 \times 10^{-10}$
82-12	55.0	114.3	12.39	$.486 \times 10^{-5}$	$.468 \times 10^{-10}$
82-13	55.0	114.3	12.39	$.469 \times 10^{-5}$	$.452 \times 10^{-10}$
82-14	55.0	114.3	12.39	$.486 \times 10^{-5}$	$.468 \times 10^{-10}$
82-15	55.0	114.3	12.40	$.496 \times 10^{-5}$	$.478 \times 10^{-10}$

TABLE V-12. PERMEABILITY COEFFICIENTS FOR ETHYLENE

Sulfolene in Membranes: 18 wt. % Thickness: 2 mils.

Run No.	Temp. °C	P_1 (Psia)	P_2 (Psia)	Flux cc(STP)/ cm^2 sec.	P cm.cc(STP)/ sec.cm^2.cmH_g
71-1	0.0	560.5	12.59	$.161 \times 10^{-5}$	$.289 \times 10^{-11}$
71-2	0.0	508.5	12.59	$.158 \times 10^{-5}$	$.314 \times 10^{-11}$
71-3	0.0	409.5	12.59	$.877 \times 10^{-6}$	$.217 \times 10^{-11}$
71-4	0.0	320.5	12.59	$.858 \times 10^{-6}$	$.274 \times 10^{-11}$
72-1	15.0	720.4	12.59	$.537 \times 10^{-5}$	$.745 \times 10^{-11}$
72-2	15.0	615.4	12.49	$.383 \times 10^{-5}$	$.624 \times 10^{-11}$
72-3	15.0	513.4	12.49	$.328 \times 10^{-5}$	$.643 \times 10^{-11}$
72-4	15.0	412.4	12.49	$.247 \times 10^{-5}$	$.607 \times 10^{-11}$
72-5	15.0	314.4	12.49	$.166 \times 10^{-5}$	$.541 \times 10^{-11}$
73-1	25.0	721.5	12.55	$.103 \times 10^{-4}$	$.143 \times 10^{-10}$
73-2	25.0	624.5	12.55	$.836 \times 10^{-5}$	$.134 \times 10^{-10}$
73-3	25.0	520.5	12.55	$.710 \times 10^{-5}$	$.137 \times 10^{-10}$
73-4	25.0	409.5	12.55	$.446 \times 10^{-5}$	$.110 \times 10^{-10}$
73-5	25.0	315.5	12.55	$.334 \times 10^{-5}$	$.108 \times 10^{-10}$
73-6	25.0	214.5	12.55	$.204 \times 10^{-5}$	$.991 \times 10^{-11}$
73-7	25.0	214.4	12.55	$.207 \times 10^{-5}$	$.101 \times 10^{-10}$
74-1	35.0	734.5	12.60	$.196 \times 10^{-4}$	$.267 \times 10^{-10}$
74-2	35.0	616.5	12.60	$.154 \times 10^{-4}$	$.250 \times 10^{-10}$
74-3	35.0	509.5	12.60	$.116 \times 10^{-4}$	$.229 \times 10^{-10}$
74-4	35.0	413.5	12.60	$.915 \times 10^{-5}$	$.224 \times 10^{-10}$
74-5	35.0	313.5	12.60	$.584 \times 10^{-5}$	$.191 \times 10^{-10}$
74-6	35.0	313.5	12.60	$.600 \times 10^{-5}$	$.196 \times 10^{-10}$
74-7	35.0	212.5	12.60	$.411 \times 10^{-5}$	$.202 \times 10^{-10}$
74-8	35.0	212.5	12.60	$.355 \times 10^{-5}$	$.175 \times 10^{-10}$

TABLE V-12 (Cont).

Run No.	Temp. °C	P_1 (Psia)	P_2 (Psia)	Flux cc(STP)/ cm^2 sec.	P cm.cc(STP)/ sec.cm^2.cmH_g
75-1	45.0	722.4	12.43	$.363 \times 10^{-4}$	$.502 \times 10^{-10}$
75-2	45.0	614.4	12.43	$.286 \times 10^{-4}$	$.467 \times 10^{-10}$
75-3	45.0	516.4	12.43	$.226 \times 10^{-4}$	$.440 \times 10^{-10}$
75-4	45.0	416.4	12.43	$.169 \times 10^{-4}$	$.410 \times 10^{-10}$
75-5	45.0	313.4	12.43	$.115 \times 10^{-4}$	$.377 \times 10^{-10}$
75-6	45.0	217.4	12.43	$.769 \times 10^{-5}$	$.369 \times 10^{-10}$
76-1	55.0	709.4	12.51	$.612 \times 10^{-4}$	$.862 \times 10^{-10}$
76-2	55.0	620.4	12.51	$.522 \times 10^{-4}$	$.844 \times 10^{-10}$
76-3	55.0	521.4	12.51	$.404 \times 10^{-4}$	$.780 \times 10^{-10}$
76-4	55.0	409.4	12.51	$.292 \times 10^{-4}$	$.723 \times 10^{-10}$
76-5	55.0	316.4	12.51	$.210 \times 10^{-4}$	$.678 \times 10^{-10}$
76-6	55.0	218.4	12.51	$.136 \times 10^{-4}$	$.649 \times 10^{-10}$

TABLE V-13. PERMEABILITY COEFFICIENTS FOR 1,3 BUTADIENE

Sulfolene in Membranes: 18 wt. % Thickness: 2 mils.

Run No	Temp. °C	P_1 (Psia)	P_2 (Psia)	Flux cc(STP)/ cm^2 sec.	P cm.cc(STP)/ sec.cm^2.cm.H_g
90-1	38.0	37.5	12.59	$.161 \times 10^{-5}$	$.635 \times 10^{-10}$
90-2	38.0	37.5	12.59	$.202 \times 10^{-5}$	$.798 \times 10^{-10}$
90-3	38.0	37.5	12.59	$.187 \times 10^{-5}$	$.737 \times 10^{-10}$
90-4	38.0	32.5	12.59	$.108 \times 10^{-5}$	$.533 \times 10^{-10}$
90-5	38.0	32.5	12.59	$.107 \times 10^{-5}$	$.530 \times 10^{-10}$
91-1	46.5	39.5	12.60	$.239 \times 10^{-5}$	$.872 \times 10^{-10}$
91-2	46.5	39.5	12.60	$.241 \times 10^{-5}$	$.879 \times 10^{-10}$
91-3	46.5	33.5	12.60	$.154 \times 10^{-5}$	$.725 \times 10^{-10}$
91-4	46.5	33.5	12.60	$.162 \times 10^{-5}$	$.760 \times 10^{-10}$
92-1	55.0	39.5	12.54	$.271 \times 10^{-5}$	$.990 \times 10^{-10}$
92-2	55.0	39.5	12.54	$.279 \times 10^{-5}$	$.102 \times 10^{-9}$
92-3	55.0	33.5	12.54	$.212 \times 10^{-5}$	$.998 \times 10^{-10}$
92-4	55.0	33.5	12.54	$.218 \times 10^{-5}$	$.102 \times 10^{-9}$
92-5	55.0	28.5	12.54	$.166 \times 10^{-5}$	$.103 \times 10^{-9}$
92-6	55.0	28.5	12.54	$.164 \times 10^{-5}$	$.101 \times 10^{-9}$
92-7	55.0	28.5	12.54	$.139 \times 10^{-5}$	$.859 \times 10^{-10}$
92-8	55.0	23.5	12.54	$.970 \times 10^{-6}$	$.872 \times 10^{-10}$
92-9	55.0	23.5	12.54	$.979 \times 10^{-6}$	$.880 \times 10^{-10}$

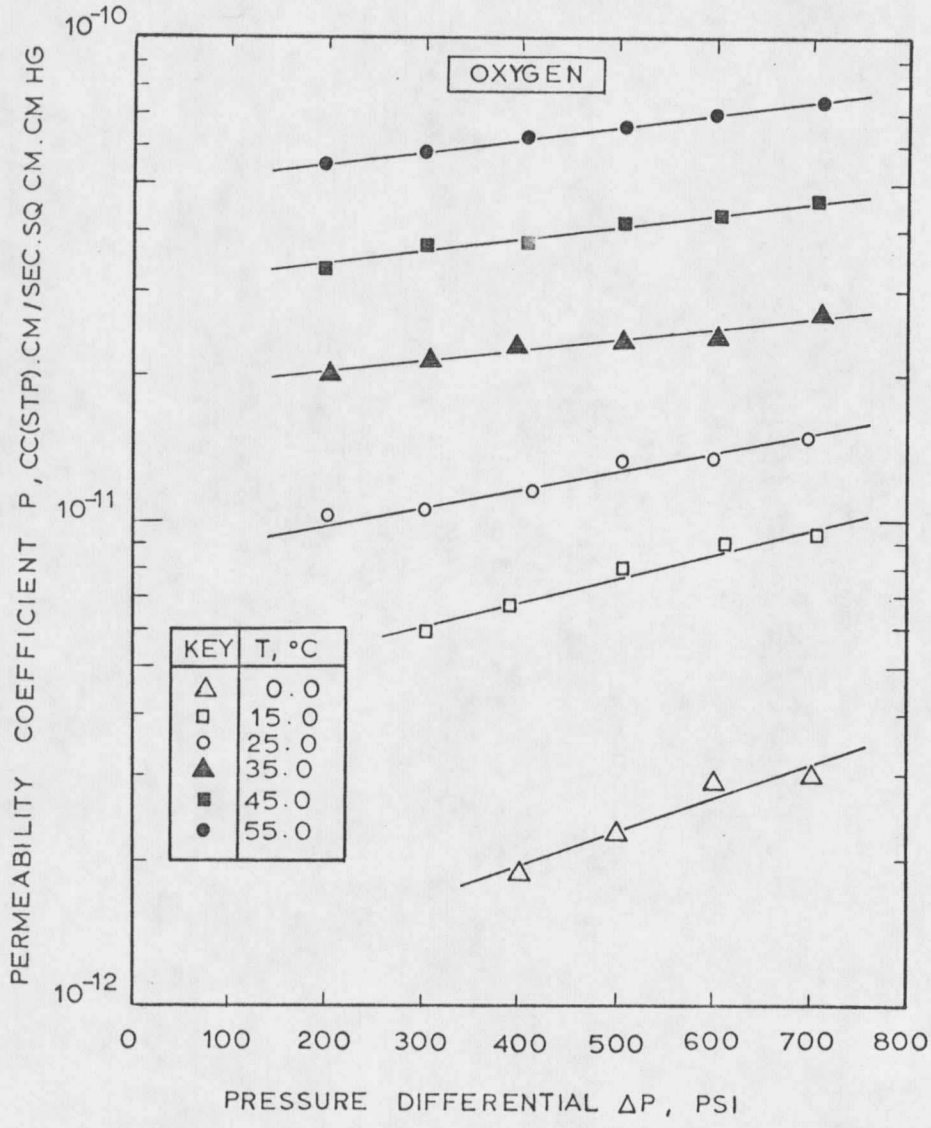

FIGURE V-12. PERMEABILITY COEFFICIENT VS. PRESSURE DIFFERENTIAL FOR OXYGEN

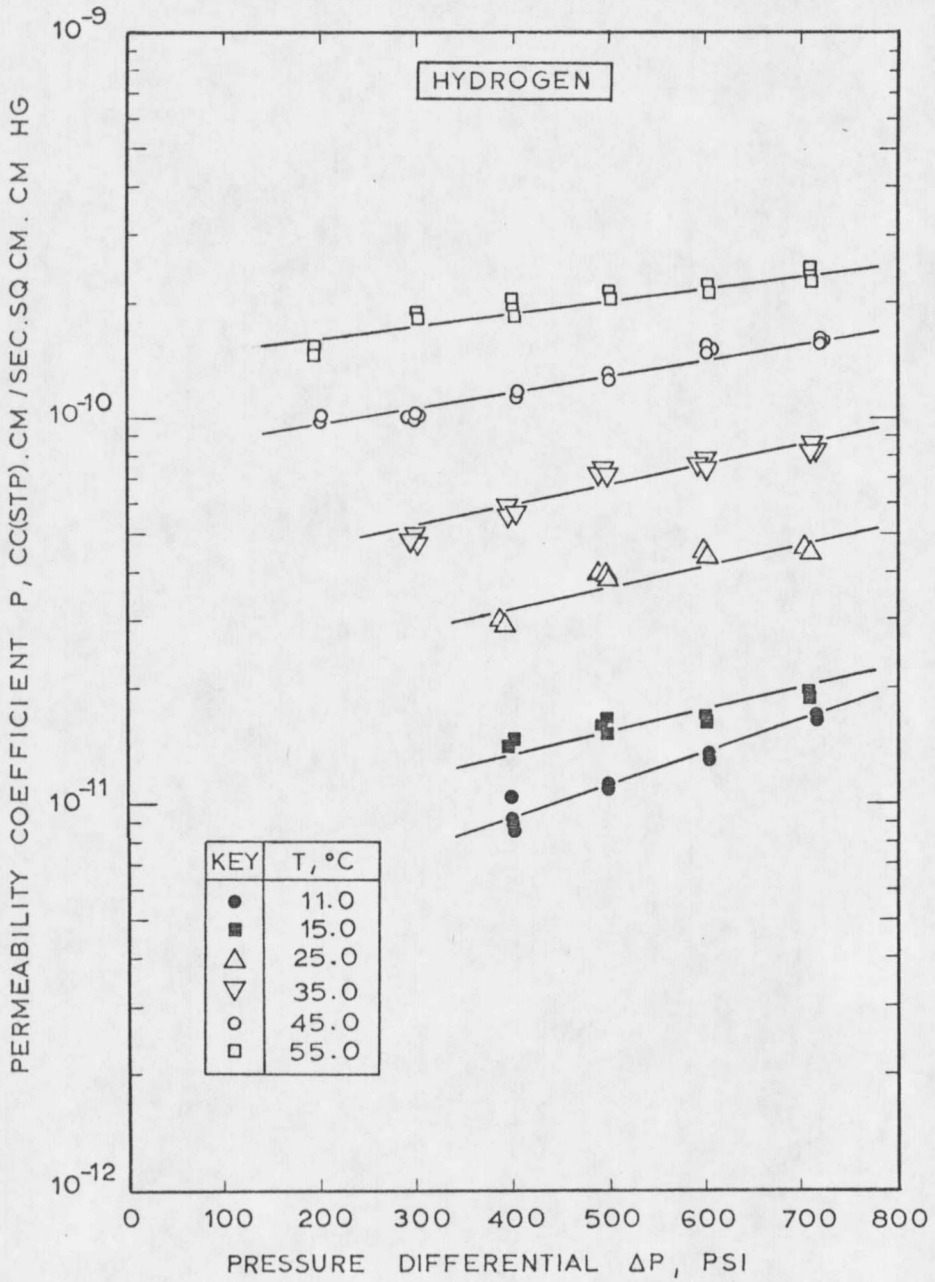

FIGURE V-13. PERMEABILITY COEFFICIENT VS. PRESSURE DIFFERENTIAL FOR HYDROGEN

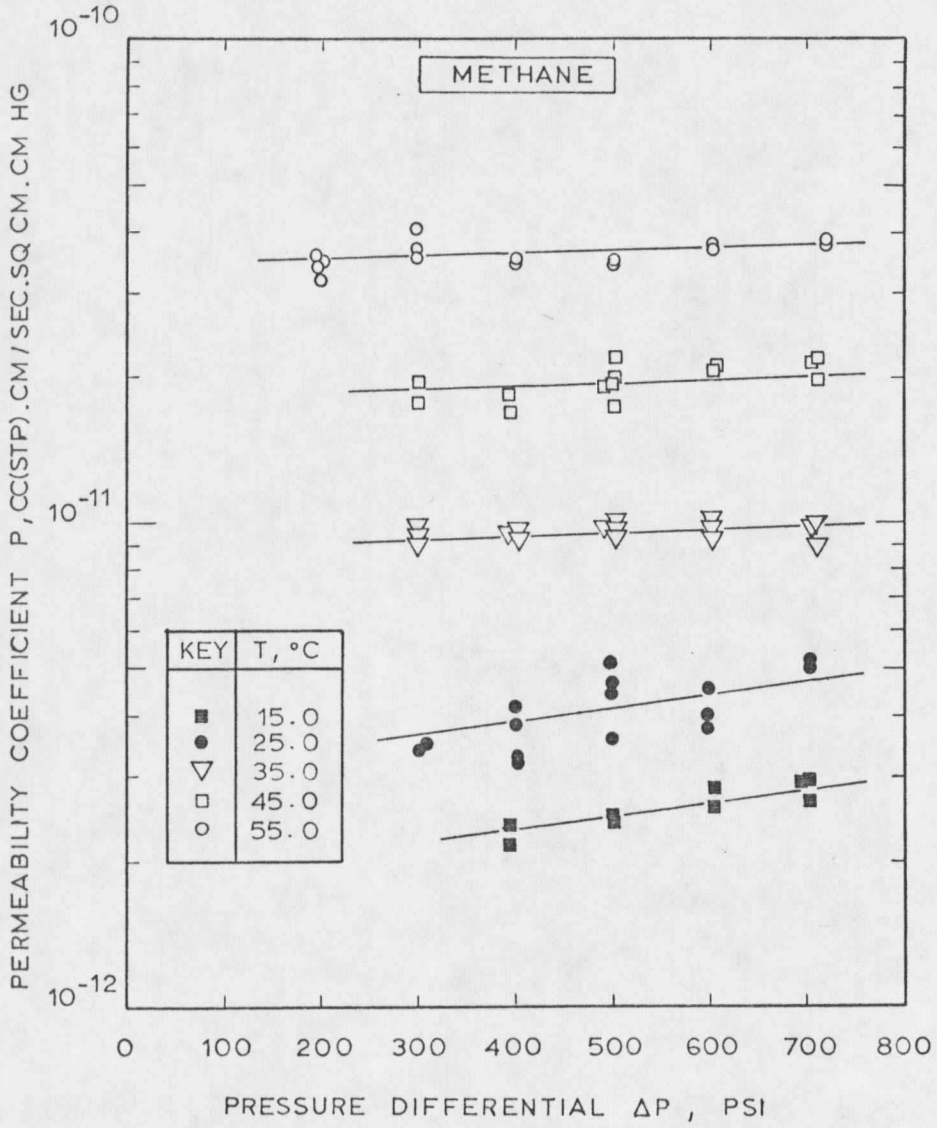

FIGURE V-14. PERMEABILITY COEFFICIENT VS. PRESSURE DIFFERENTIAL FOR METHANE

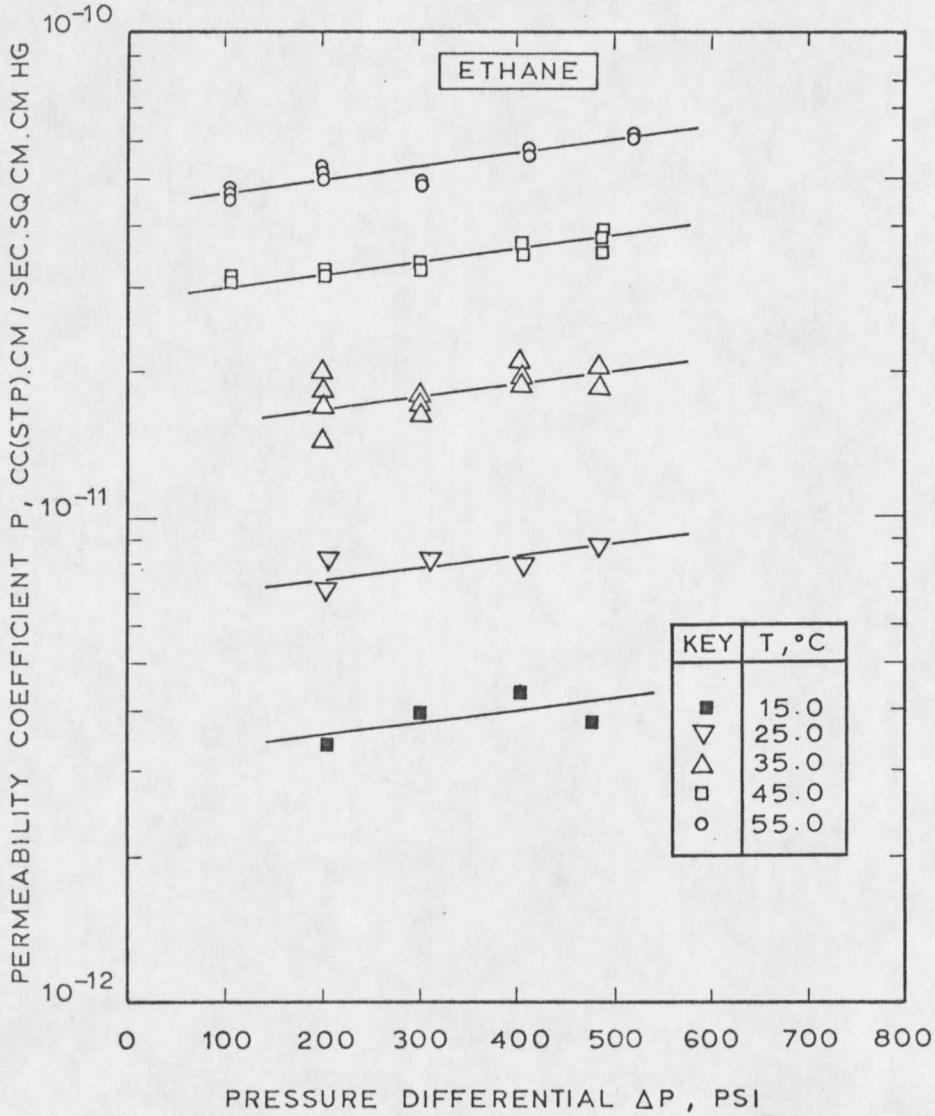

FIGURE V-15. PERMEABILITY COEFFICIENT VS. PRESSURE DIFFERENTIAL FOR ETHANE

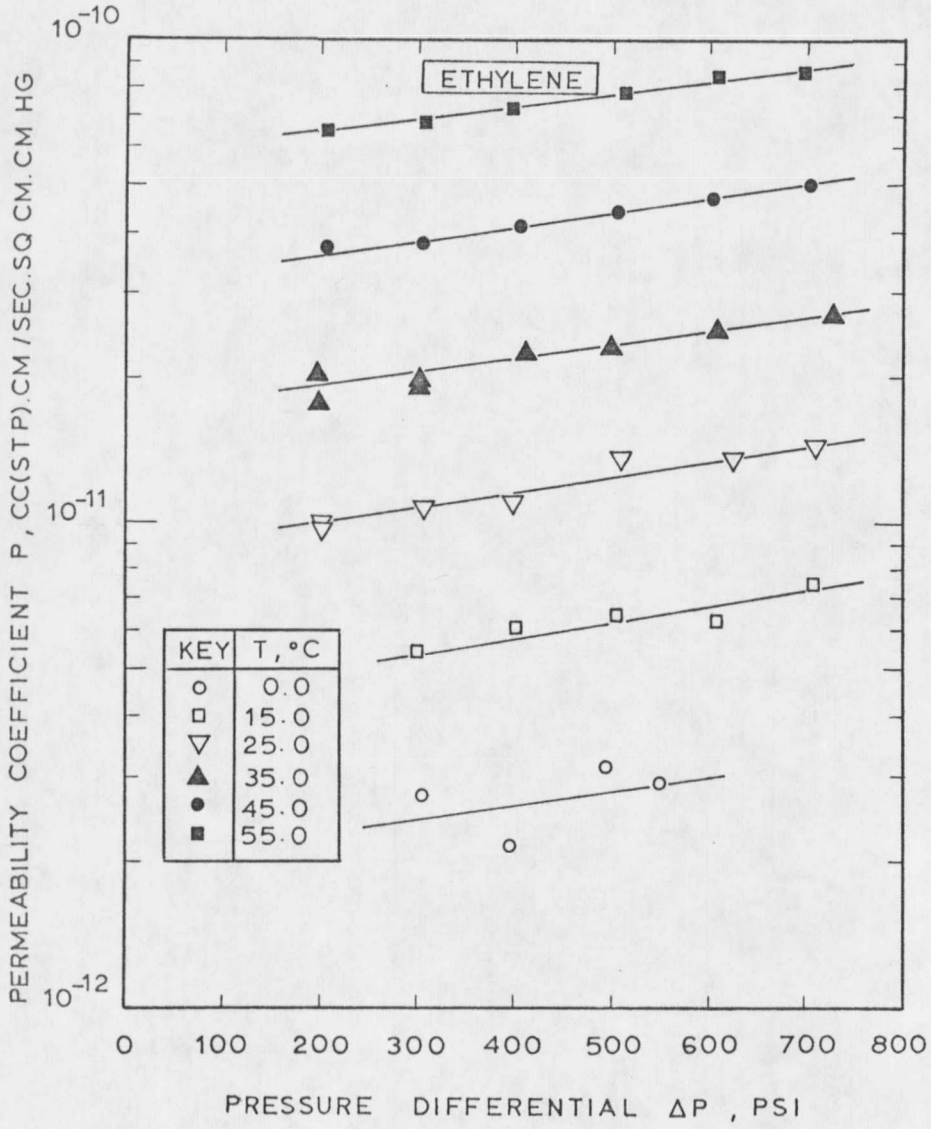

FIGURE V-16. PERMEABILITY COEFFICIENT VS. PRESSURE DIFFERENTIAL FOR ETHYLENE

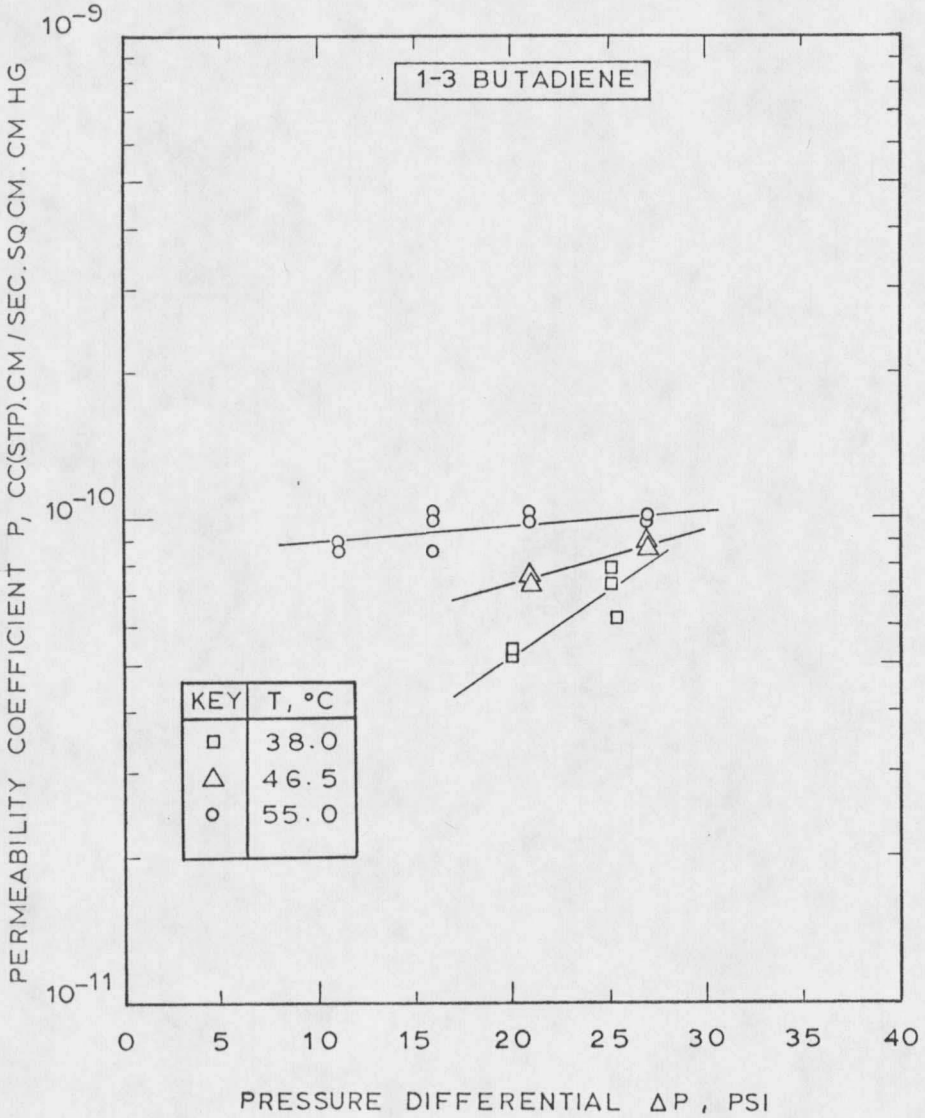

FIGURE V-17. PERMEABILITY COEFFICIENT VS. PRESSURE DIFFERENTIAL FOR 1-3 BUTADIENE

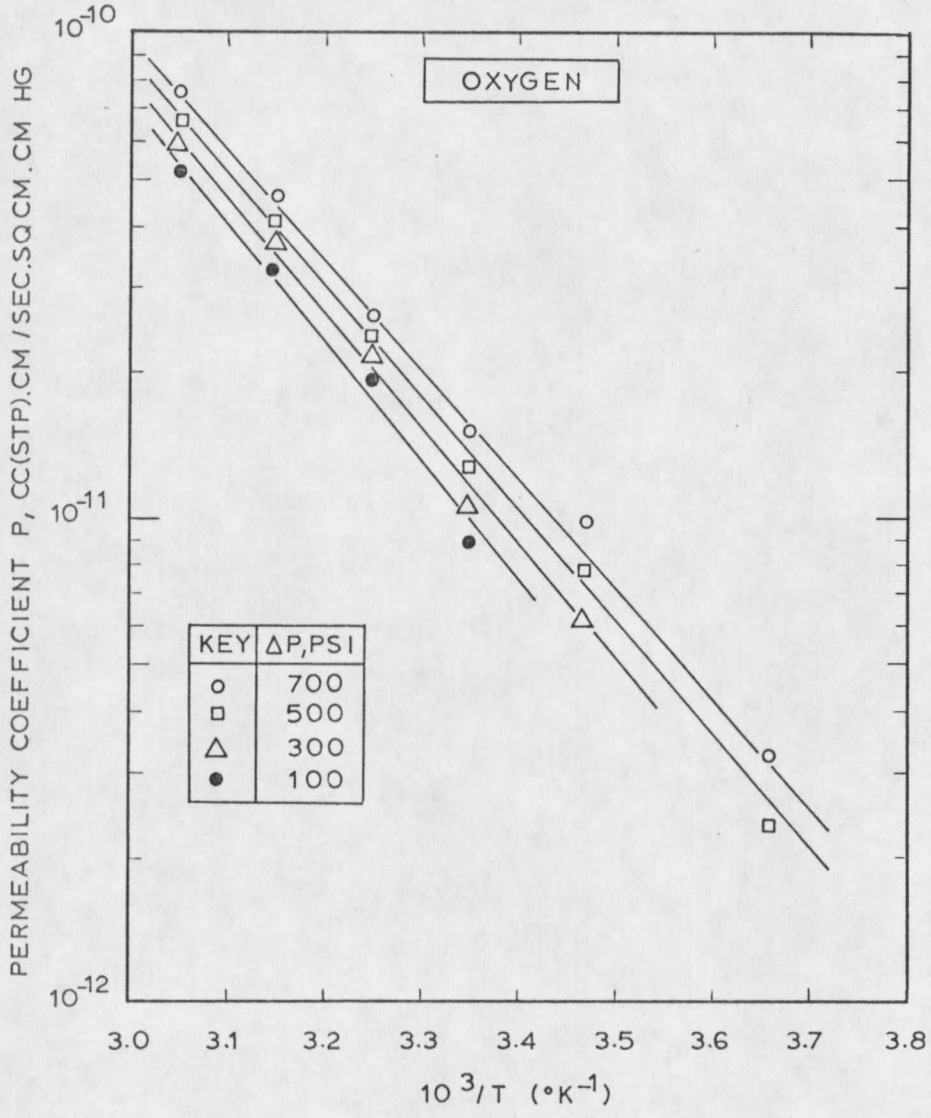

FIGURE V-18. PERMEABILITY COEFFICIENT VS. $10^3/T$ FOR OXYGEN

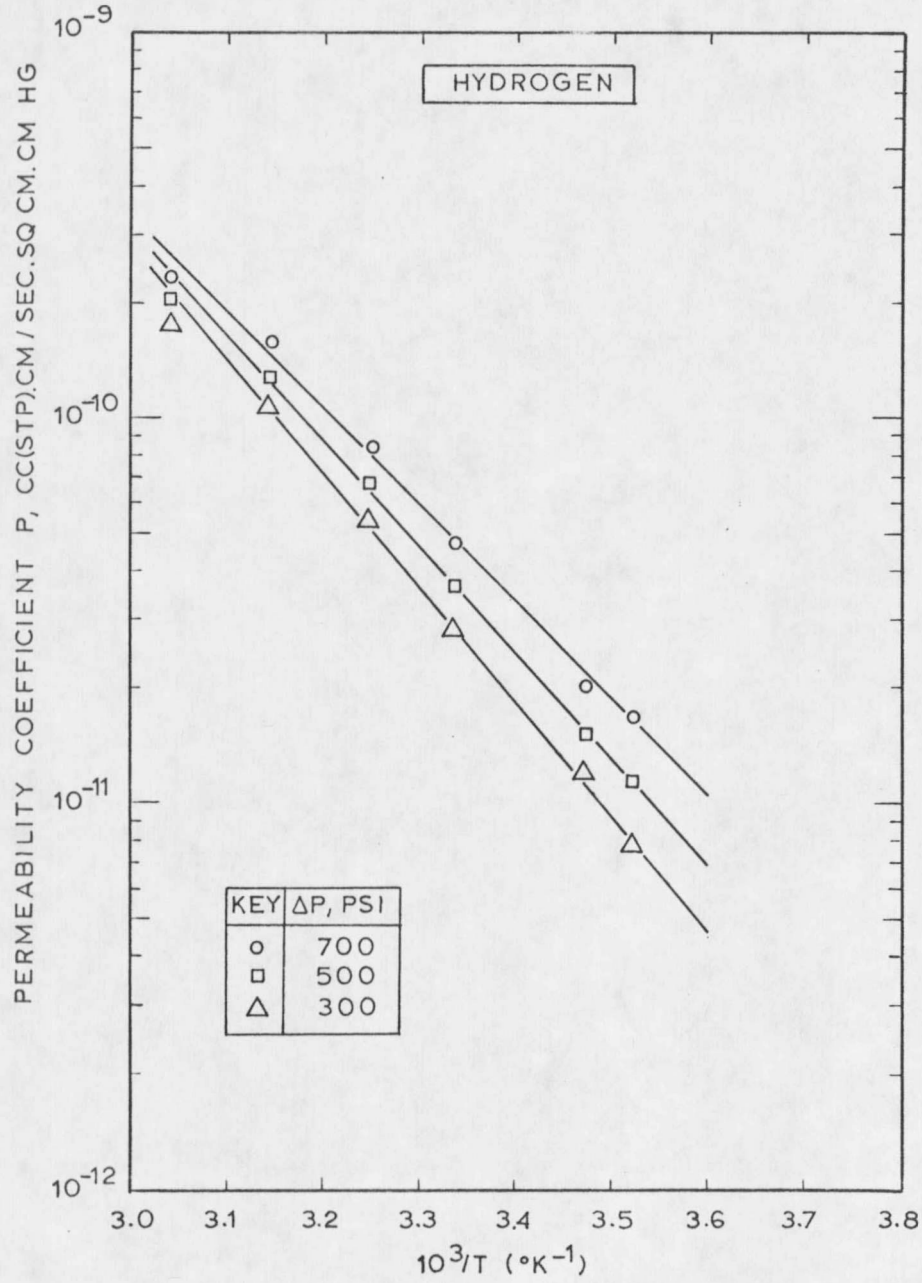

FIGURE V-19. PERMEABILITY COEFFICIENT VS. $10^3/T$ FOR HYDROGEN

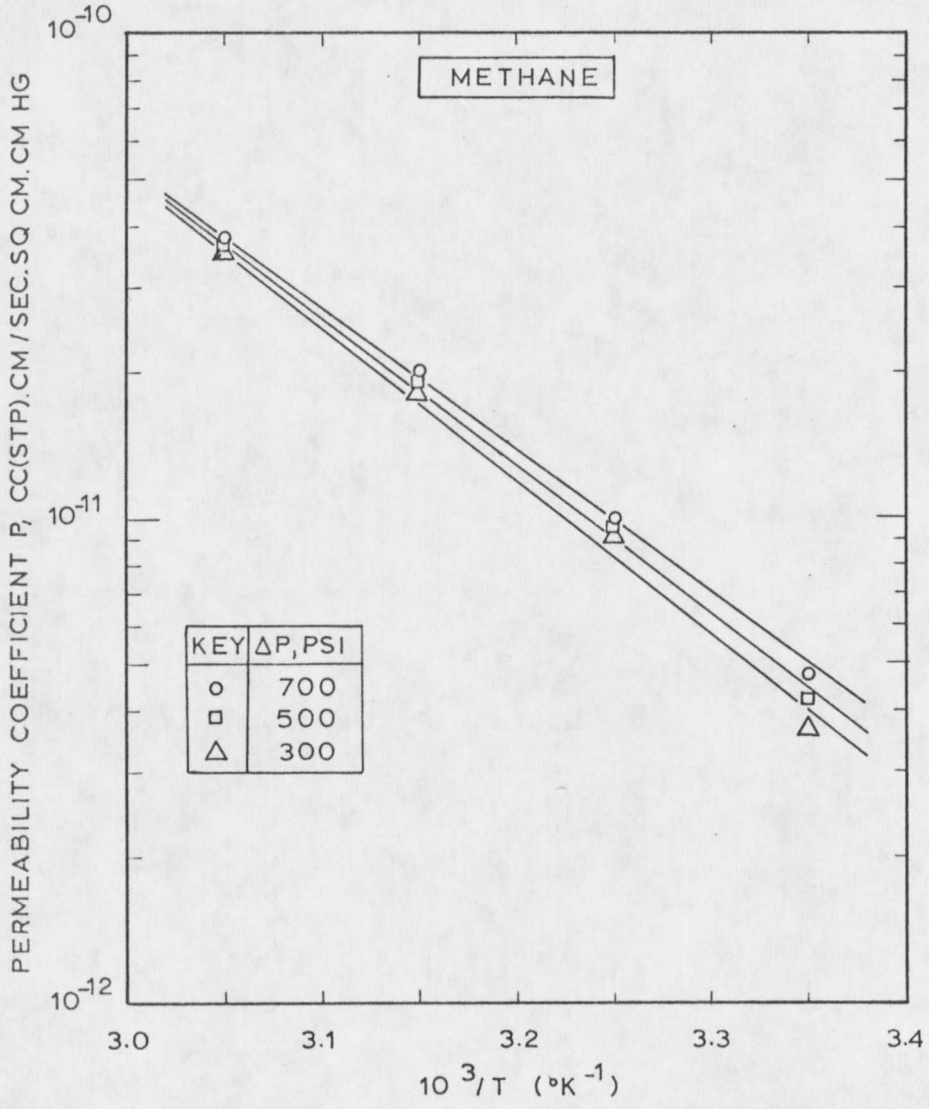

FIGURE V-20. PERMEABILITY COEFFICIENT VS. $10^3/T$ FOR METHANE

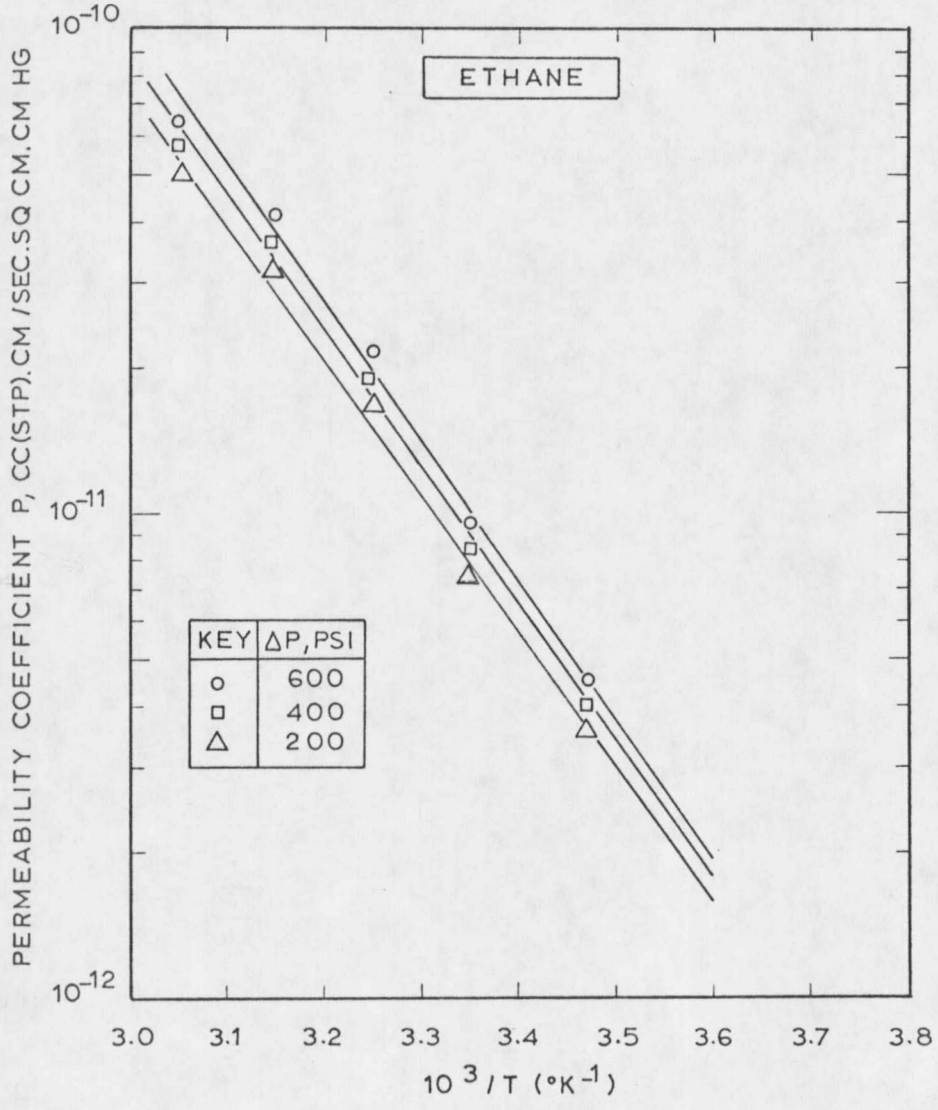

FIGURE V-21. PERMEABILITY COEFFICIENT VS. $10^3/T$ FOR ETHANE.

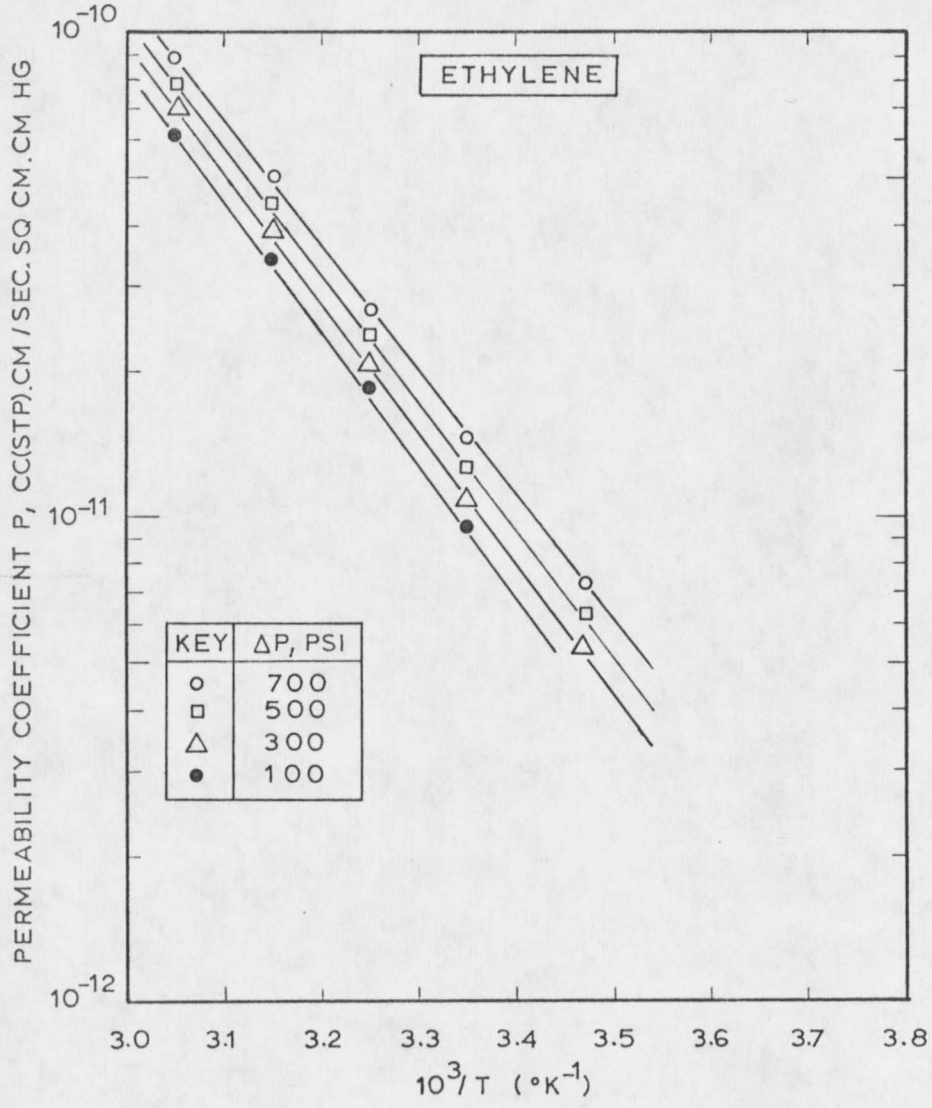

FIGURE V-22. PERMEABILITY COEFFICIENT VS $10^3/T$ FOR ETHYLENE

All the permeability coefficients are of the same order of magnitude. The trend is the same for all cases; the coefficients increase with increasing temperature. The coefficients for hydrogen are the highest in the group under consideration. Then come 1-3 butadiene, ethylene, oxygen, methane in that order. The system seems to be slightly selective to the olefins studied, 1-3, butadiene and ethylene, compared to the other hydrocarbons, methane and ethane.

The behavior of the different gases appear to be diffusivity controlled. The pressure dependence of the permeability coefficients may be explained by a non-linear relationship between the solubility and the pressure. A plasticizing effect due to higher concentrations of sorbed gas in the membrane may also be responsible, at least in part, for such behavior, because of the associated increase in diffusivity. The high permeability coefficient of hydrogen is probably related to the small diameter of its molecule.

G. SEPARATION OF SO_2/N_2 MIXTURES

(1) The Data

The pseudo-permeability coefficients for SO_2 and N_2 and the separation factor α_{SO_2/N_2} were determined in the 0°C to 55°C temperature range and a total pressure range of about 200 psig to 600 psig. The feed gas analyzed 6.5 volume % SO_2. The membrane used contained 18 wt % sulfolene on a solvent free basis and had a thickness

of 2 mils. The feed gas flow rate was changed for the different runs, in order to try to keep a constant SO_2 volume % in the high pressure side of the permeation cell. The data are presented in Table V-14.

(2) Discussion

The pseudo-permeability coefficients for SO_2 and N_2 are plotted in Figure V-23 and Figure V-24 respectively. The separation factor for SO_2 is plotted in Figure V-25. The data in general shows some scattering, that is probably due to the impossibility of keeping the mass transfer parameters constant. The SO_2 concentration in the high pressure side of the membrane is difficult to keep constant. The mass transfer coefficients are functions of temperature and pressure, and probably also of the rate of permeation. Even though the data reflects these facts, they neyertheless show a definite trend in each case. Starting with SO_2, the pseudo-permeability coefficients (Figure V-23) follow the same trend as the permeability coefficients for pure SO_2, that are shown in Figure V-5. They decrease with increasing temperature and increase with increasing pressure. The values obtained are somewhat lower, which is in agreement with the definition of the pseudo-permeability coefficient. This reflects the resistance to mass transfer in the gaseous films in contact with the membrane, which arises when working with gas mixtures. Comparing the pseudo-permeability coefficients for N_2, shown in Figure V-24, with

TABLE V-14. SEPARATION OF SO_2/N_2 MIXTURES

Feed: SO_2 Volume %: 6.5 Sulfolene in Membrane: 18 wt. Thickness: 2 mils.

Run No.	Temp. °C	P_1 (Psia)	P_2 (Psia)	% SO_2 Perm	% SO_2 Vent	Flux cc(STP)/cm^2.sec $SO_2 \times 10^3$	$N_2 \times 10^4$	π cc(STP)cm/ .sec.cm^2.cmH_g $SO_2 \times 10^6$	$N_2 \times 10^{10}$	α SO_2/N_2
111-1	0.0	622.4	12.51	92.15	3.07	.897	.764	.116	.125	370.2
111-2	0.0	515.4	12.50	91.41	3.33	.715	.672	.123	.133	309.1
111-3	0.0	416.4	12.50	91.74	3.98	.673	.606	.129	.149	267.7
111-4	0.0	316.4	12.50	93.71	5.27	.600	.403	.118	.132	267.6
111-5	0.0	220.4	12.50	93.75	6.35	.439	.293	.189	.140	221.2
111-6	0.0	528.4	12.51	92.93	.356	.839	.639	.115	.123	356.0
111-7	0.0	420.4	12.51	94.57	4.19	.964	.553	.164	.135	398.5
111-8	0.0	315.4	12.50	95.50	5.66	.911	.429	.151	.142	353.7
111-9	0.0	215.4	12.47	87.85	5.46	.123	.170	.151	.825	125.3
111-10	0.0	362.4	12.49	94.48	4.42	.656	.383	.152	.109	369.4
112-1	51.0	524.4	12.49	93.45	5.08	.529	.371	.0347	.734	266.2
112-2	15.0	414.4	12.49	92.61	5.24	.284	.227	.0275	.568	226.7
112-3	15.0	317.4	12.47	91.10	5.11	.143	.140	.0291	.458	190.2
112-4	15.0	216.4	12.47	82.60	5.85	.0248	.0523	.0103	.254	76.4
113-1	25.0	528.4	12.41	89.93	4.61	.313	.350	.0232	.683	184.7
113-2	25.0	414.4	12.41	89.37	5.21	.167	.199	.0157	.499	153.0
113-3	25.0	318.4	12.41	87.35	5.76	.0847	.123	.0111	.404	112.9
113-4	25.0	364.4	12.41	87.17	5.09	.110	.161	.0139	.460	126.6

TABLE V-14 (Cont)

Run No.	Temp °C	P_1 (Psia)	P_2 (Psia)	$\%SO_2$ Perm	$\%SO_2$ Vent	Flux cc(STP)/cm^2.sec $SO_2 x10^3$	Flux cc(STP)/cm^2.sec $N_2 x10^4$	π cc(STP)cm/ sec.cm^2.cmH_g $SO_2 x10^6$	π cc(STP)cm/ sec.cm^2.cmH_g $N_2 x10^{10}$	α SO_2/N_2
114-1	35.0	524.4	12.43	86.27	5.22	.193	.307	.0114	.610	114.1
114-2	35.0	418.4	12.43	84.54	5.52	.115	.211	.00900	.526	93.6
114-3	35.0	314.4	12.43	81.16	5.71	.0557	.129	.00697	.432	71.2
114-4	35.0	367.4	12.43	82.01	5.45	.0804	.176	.00805	.502	79.2
115-1	45.0	522.4	12.45	81.59	5.21	.144	.324	.00826	.645	80.6
115-2	45.0	413.4	12.45	81.59	5.49	.0920	.208	.00720	.526	76.1
115-3	45.0	310.4	12.45	76.92	5.53	.0873	.262	.0113	.886	57.0
116-1	55.0	529.5	12.52	76.80	5.07	.132	.399	.00754	.784	67.0
116-2	55.0	413.5	12.52	76.09	5.60	.0798	.251	.00576	.637	53.6
116-3	55.0	311.5	12.52	71.82	5.92	.0442	.173	.00460	.589	40.5

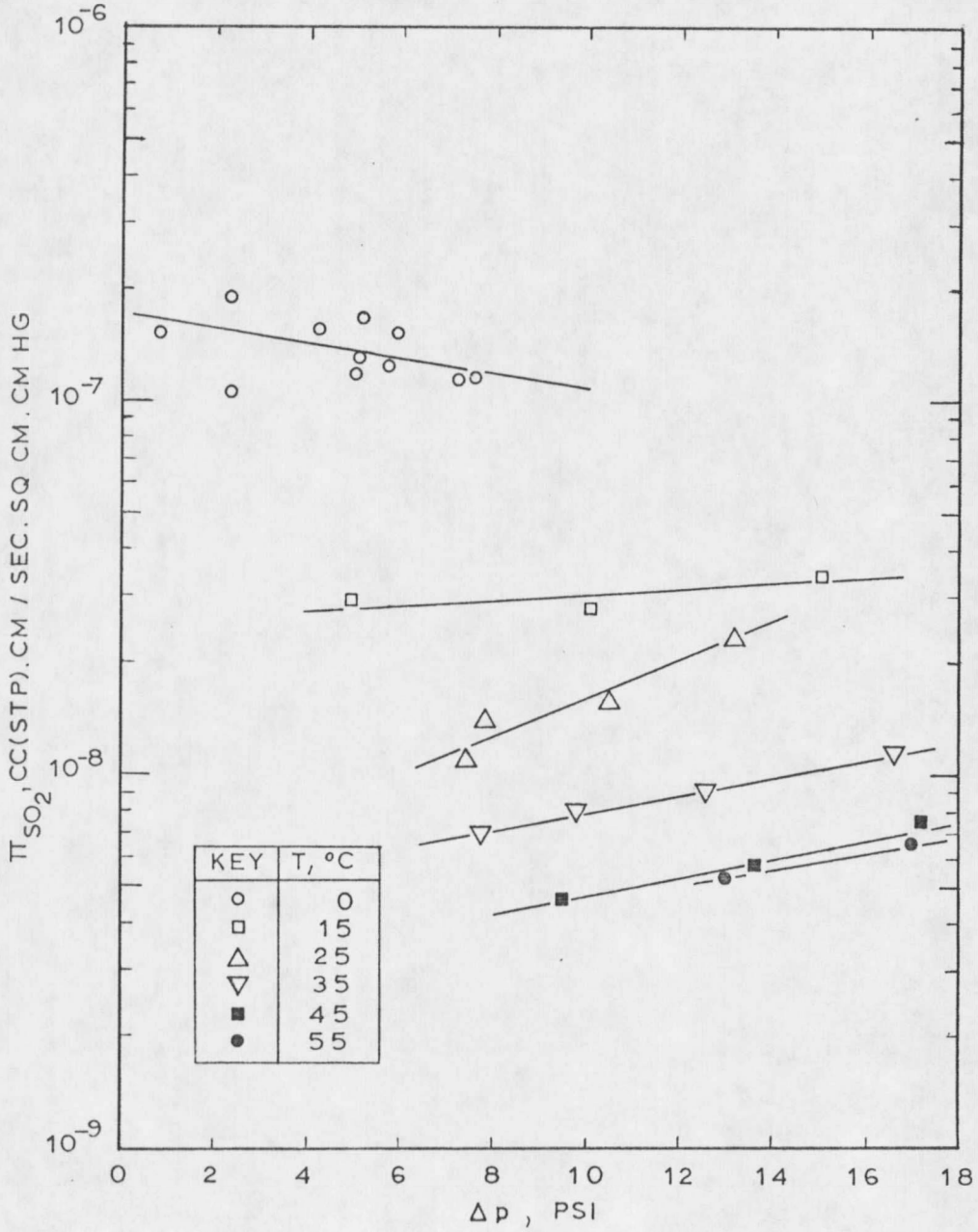

FIGURE V-23. PSEUDO PERMEABILITY COEFFICIENT VS PARTIAL PRESSURE DIFFERENTIAL FOR SO_2

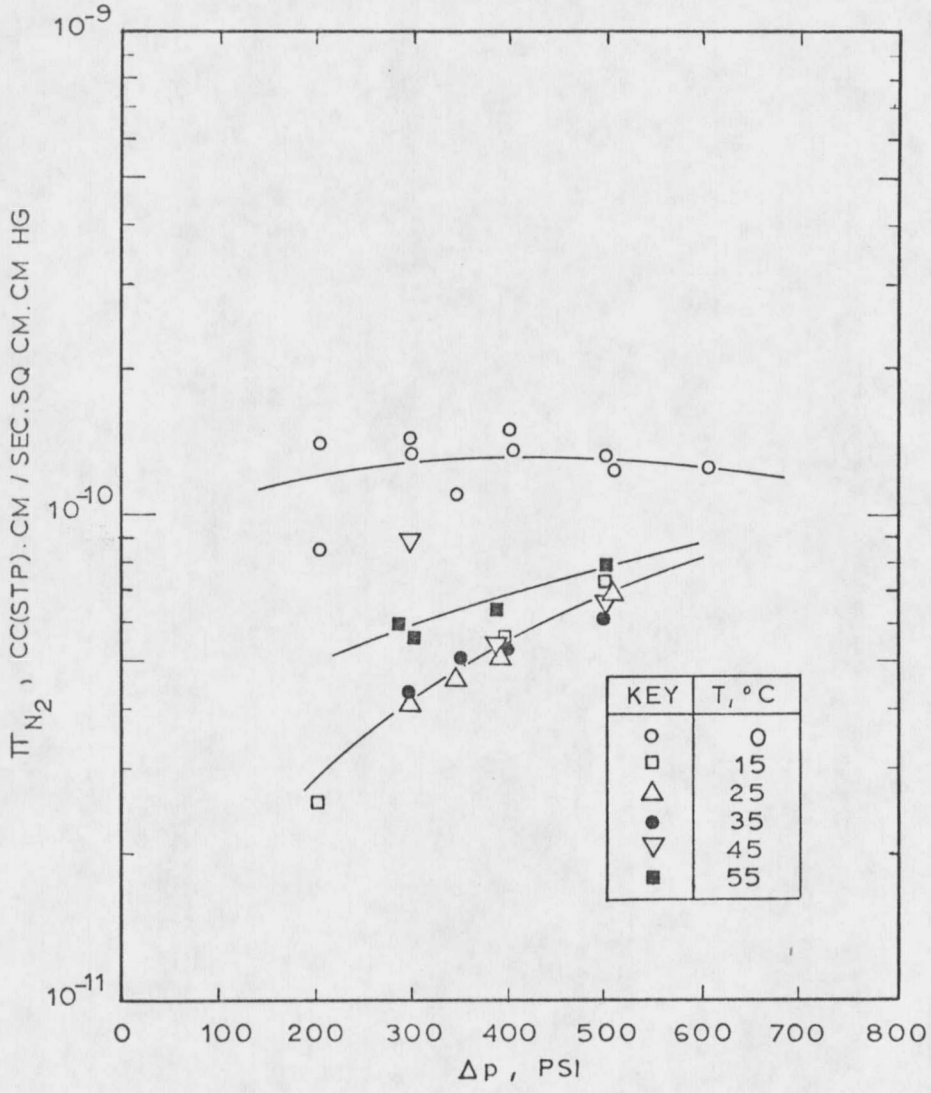

FIGURE V-24. PSEUDO PERMEABILITY COEFFICIENT VS. PARTIAL PRESSURE DIFFERENTIAL FOR N_2

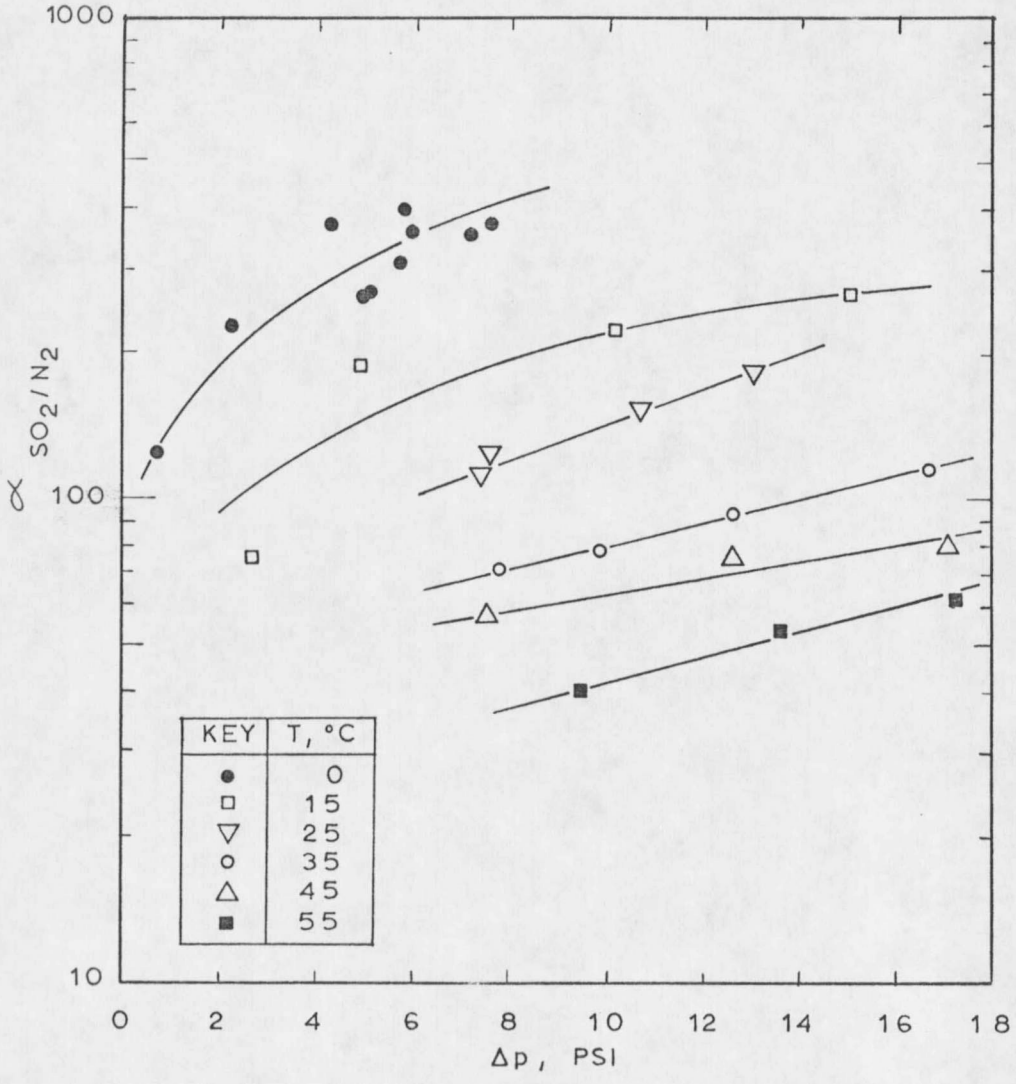

FIGURE V-25. SEPARATION FACTOR α VS. PARTIAL PRESSURE DIFFERENTIAL FOR SO_2

the permeability coefficients determined using pure N_2, there are some interactions between N_2 and the sorbed gas in the membrane. First, the pseudo-permeability coefficients for N_2 are higher than the pure N_2 permeability coefficients, in opposition to what would have been expected if no interactions were present. Second, the temperature dependence of the coefficients is reversed: the pseudo-permeability coefficient for N_2 decreases with increasing temperature up to about 35°C, and then seems to increase. This behavior can probably be explained by the plasticizing effect of SO_2 sorbed in the membrane. It has been demonstrated by Stannet et al. (14) that the diffusivity can increase with increasing sorbed gas concentrations. At lower temperatures, the concentration of sorbed SO_2 in the membrane is higher, and it is also at the lower temperatures that the highest values of the pseudo-permeability coefficients are encountered, as shown in Figure V-24. It appears that at the lower temperatures the transport of N_2 is determined by the concentration of sorbed SO_2 in the membrane. At higher temperatures the solubility of SO_2 decrease considerably, and with it, its plasticizing effect. Thus, at higher temperatures, nitrogen regains its "traditional" behavior, when the plasticizing effect of SO_2 becomes less important.

Turning now to the separation factor for SO_2 (Figure V-25), it can be seen that it increases with decreasing temperature. This is probably due to the fact that the concentration of sorbed SO_2 increases

with decreasing temperature, being apparently a very strong function of temperature. This increase in sorbed SO_2 concentration may cause an increase in the diffusivity of N_2, as discussed previously, but the net effect is a permeate richer in SO_2. As temperature increases, the pseudo-permeability fo SO_2 goes down, because of the lower solubility, and while the N_2 permeability coefficient may decrease because of the diminishing plasticizing effect, it eventually increases because of the increase of its diffusivity with temperature. The net effect is a drop in the separation factor with increasing temperature. From Table V-15, it can be seen that the 18% sulfolene membrane is very selective with respect to SO_2, giving at the same time high permeate fluxes. The best separations are obtained at 0°C. The highest concentration of SO_2 in the permeate was 95.5% for an exhaust gas SO_2 concentration of 5.6%, with permeate flow rates of about 1×10^{-3} cc(STP)/(cm^2.sec.). Upstream pressure was 315 psia.

H. SEPARATION OF CO_2/H_2 MIXTURES

(1) The Data

The pseudo-permeability coefficients for CO_2 and H_2 and the separation factor α_{CO_2/H_2} were determined in the 0°C to 55°C temperature range and at a total pressure range of about 160 psig to 720 psig. Two different feed mixtures were used: 3.3 vol% CO_2 and 48.5 vol. % CO_2. The membrane used contained 18 wt% sulfolene

TABLE V-15. SEPARATION OF CO_2/H_2 MIXTURES

Feed: CO_2 Volume: 48.5% Sulfolene in Membrane: 18 wt% Thickness: 2 Mils.

Run No.	Temp. °C	P_1 (Psia)	P_2 (Psia)	$\%SO_2$ Perm	$\%SO_2$ Vent	Flux cc(STP)/cm^2sec. $CO_2 \times 10^4$	Flux cc(STP)/cm^2sec. $H_2 \times 10^4$	π cc(STP)cm/ sec.cm^2.$cmHg \times 10^9$ CO_2	π cc(STP)cm/ sec.cm^2.$cmHg \times 10^9$ H_2	α CO_2/H_2
100-2	0.0	732.5	12.54	67.44	42.04	.579	.279	.190	.0653	2.86
100-3	0.0	616.5	12.54	68.20	42.10	.380	.177	.149	.0493	2.86
100-4	0.0	517.5	12.54	66.37	43.98	.205	.104	.0919	.0357	2.52
100-5	0.0	422.5	12.54	67.89	44.29	.0988	.0467	.0543	.0198	2.66
101-1	15.0	732.5	12.49	64.17	43.51	.803	.448	.254	.109	2.33
101-2	15.0	622.4	12.49	63.89	44.67	.565	.319	.205	.0922	2.19
101-3	15.0	525.4	12.49	62.82	41.13	.377	.223	.178	.0720	2.42
101-4	15.0	420.4	12.49	65.68	45.26	.237	.124	.128	.0539	2.31
102-1	25.0	737.4	12.50	61.82	42.76	.988	.610	.316	.144	2.17
102-2	25.0	615.4	12.50	60.09	43.35	.659	.438	.250	.125	1.97
102-3	25.0	515.4	12.50	64.11	45.82	.517	.290	.223	.104	2.11
102-4	25.0	413.4	12.50	63.29	45.29	.329	.191	.180	.0847	2.08
102-5	25.0	322.4	12.50	63.07	47.20	.189	.111	.129	.0657	1.91
103-1	35.0	732.4	12.43	60.56	44.48	.127	.826	.391	.202	1.92
103-2	35.0	615.4	12.43	61.72	45.38	.928	.575	.335	.171	1.94
103-3	35.0	514.4	12.43	60.94	43.45	.657	.421	.299	.145	2.03
103-4	35.0	415.4	12.43	63.89	46.98	.478	.270	.251	.123	2.00

TABLE V-15. (Cont).

Run No.	Temp. °C	P_1 (Psia)	P_2 (Psia)	$\%SO_2$ Perm	$\%SO_2$ Vent	Flux cc(STP)/cm^2sec. $CO_2 \times 10^4$	Flux cc(STP)/cm^2sec. $H_2 \times 10^4$	π cc(STP)cm/sec.cm^2.cmH_g $CO_2 \times 10^9$	π cc(STP)cm/sec.cm^2.cmH_g $H_2 \times 10^9$	α CO_2/H_2
103-5	35.0	316.4	12.43	61.75	45.95	.274	.170	.195	.0100	1.90
104-1	45.0	732.3	12.38	62.38	47.01	1.79	1.08	.524	.277	1.87
104-2	45.0	514.2	12.38	62.26	46.92	.985	.597	.414	.219	1.87
104-3	45.0	314.3	12.38	61.34	46.17	.457	.288	.326	.172	1.85
104-4	45.0	210.3	12.38	61.50	47.36	.251	.157	.268	.146	1.78
105-1	55.0	719.3	12.38	56.32	44.29	2.09	1.62	.661	.404	1.62
105-2	55.0	514.3	12.38	56.44	42.35	1.15	.889	.537	.300	1.76
105-3	55.0	315.3	12.38	59.55	46.61	.629	.427	.443	.257	1.69
105-4	55.0	165.3	12.38	59.05	46.67	.231	.160	.325	.189	1.65

TABLE V-16. SEPARATION OF CO_2/H_2 MIXTURES

Feed: CO_2 Volume: 3.3% Sulfolene in Membrane: 18 wt% Thickness: 2 Mils.

Run No.	Temp °C	P_1 (Psia)	P_2 (Psia)	$\%SO_2$ Perm	$\%SO_2$ Vent	Flux cc(STP)/cm^2sec. $CO_2 \times 10^5$	Flux cc(STP)/cm^2sec. $H_2 \times 10^4$	π cc(STP)cm/ sec.cm^2.cmH_g $CO_2 \times 10^9$	π cc(STP)cm/ sec.cm^2.cmH_g $H_2 \times 10^9$	α CO_2/H_2
106-1	10.0	732.4	12.49	4.85	2.93	3.86	.0757	.0181	.0106	1.68
106-2	10.0	529.4	12.48	5.01	3.07	1.66	.0315	.0104	.0618	1.66
107-1	25.0	732.5	12.54	4.40	3.02	.154	.335	.0703	.0472	1.48
107-2	25.0	616.5	12.54	4.59	3.04	.124	.258	.0674	.0434	1.54
107-3	25.0	414.5	12.54	4.84	3.10	6.14	.120	.0492	.0304	1.59
108-1	35.0	742.4	12.49	4.16	2.75	.250	.576	.123	.0797	1.54
108-2	35.0	615.4	12.49	4.39	2.75	.181	.394	.108	.0660	1.62
108-3	35.0	515.4	12.49	4.34	2.85	.149	.328	.103	.0660	1.54
108-4	35.0	312.4	12.49	4.72	2.99	5.51	.111	.0619	.0375	1.61
109-1	45.0	622.3	12.40	4.22	.284	.401	.910	.230	.0151	1.51
109-2	45.0	521.3	12.40	4.17	2.95	.317	.728	.209	.145	1.43
109-3	45.0	423.3	12.40	4.25	2.85	.238	.535	.202	.132	1.51
109-4	45.0	316.3	12.40	4.43	3.05	.160	.345	.173	.115	1.47
110-1	55.0	607.5	12.57	4.13	2.91	.580	1.34	.332	.229	1.44
110-2	55.0	521.5	12.57	4.30	2.91	.510	1.14	.343	.226	1.50
110-3	55.0	409.5	12.57	4.29	3.02	.364	.813	.303	.207	1.44
110-4	55.0	316.5	12.57	4.26	2.94	.254	.571	.285	.190	1.47

on a solvent free basis and had a thickness of 2 mils. The data are presented in Table V-15 and Table V-16.

(2) Discussion

The permeability coefficients for CO_2 are about one order of magnitude greater than those of H_2, as can be observed in Figure V-10 and Figure V-13. Thus it seems possible to obtain a permeate with higher CO_2 concentration by using sulfolene modified membranes. The pseudo-permeability coefficients for CO_2 and H_2 obtained using the CO_2 rich mixture are plotted in Figure V-26 and Figure V-27 respectively.

The separation factors are presented in Figure V-28.

The pseudo-permeability coefficients for CO_2 show the same trend as the permeability coefficients for CO_2 at lower pressures (Figure V-10), and seem to be diffusivity controlled. The values of the coefficients obtained are about one order of magnitude lower than those for the pure gas. This is in agreement with the definition of the pseudo-permeability coefficient, and could be explained in terms of the additional resistances to mass transfer created when using mixtures of gases instead of the pure components.

The pseudo-permeability coefficients for H_2 seem to be slightly higher than the pure gas permeability coefficients. This suggests that the CO_2 sorbed in the membrane changes the transport characteristics of the H_2-sulfolene membrane system. As was the case for SO_2/N_2

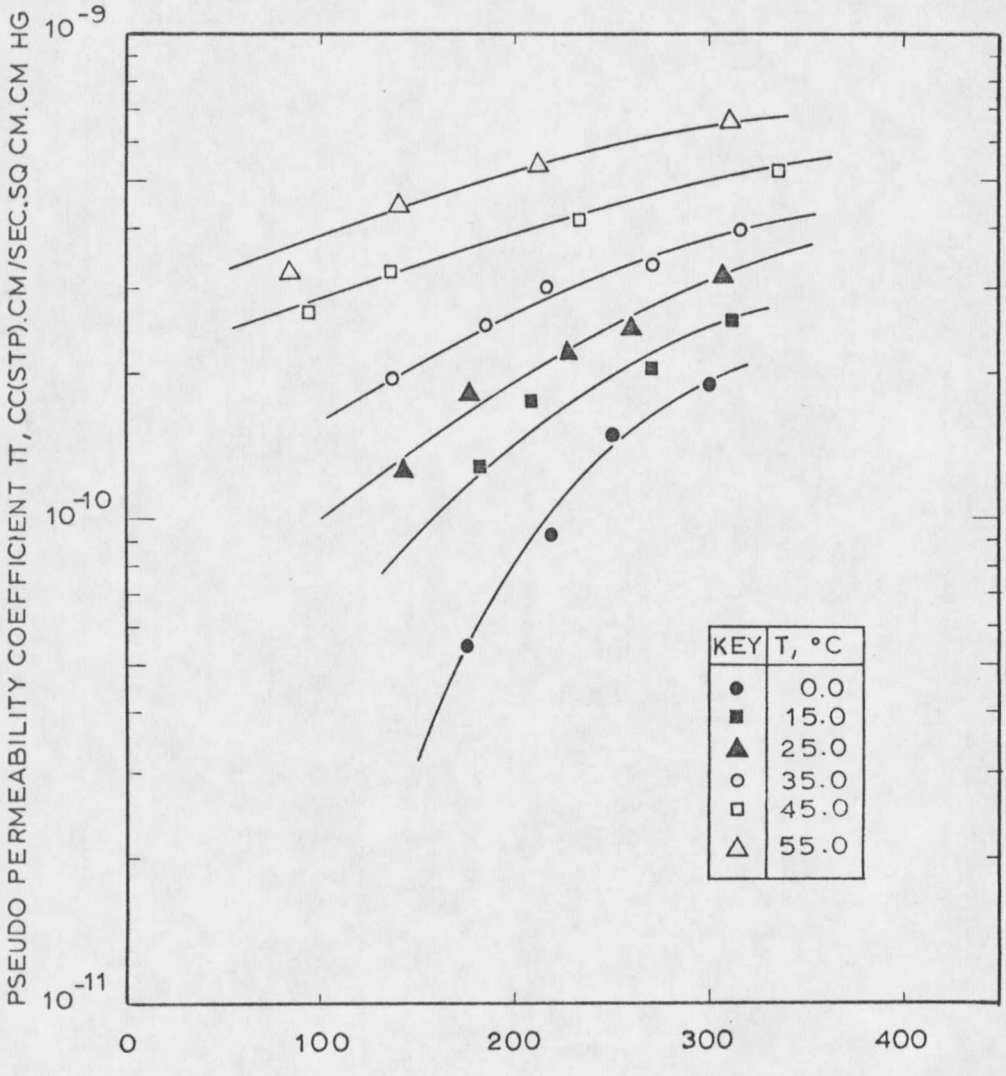

FIGURE V-26. PSEUDO PERMEABILITY COEFFICIENT VS. PARTIAL PRESSURE DIFFERENTIAL FOR CARBON DIOXIDE

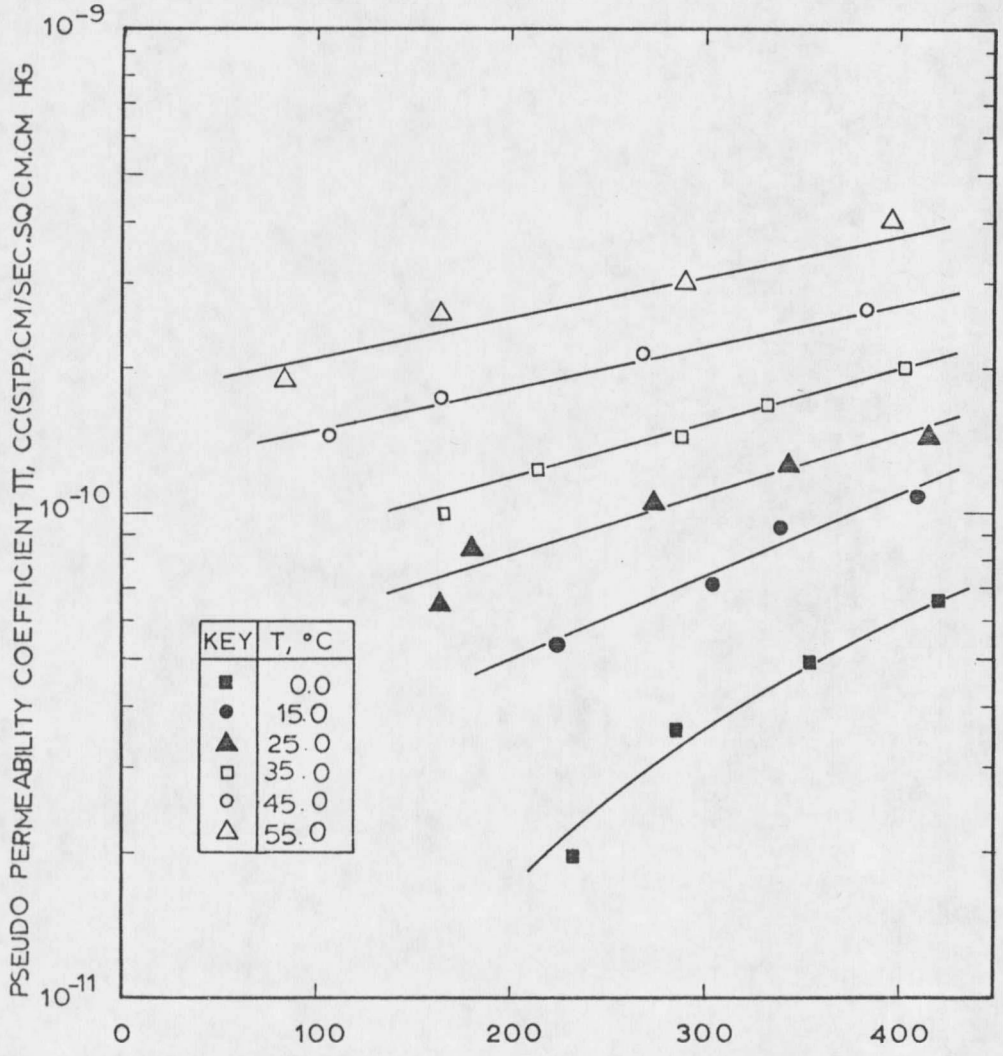

FIGURE V-27. PSEUDO PERMEABILITY COEFFICIENT VS. PARTIAL PRESSURE DIFFERENTIAL FOR HYDROGEN

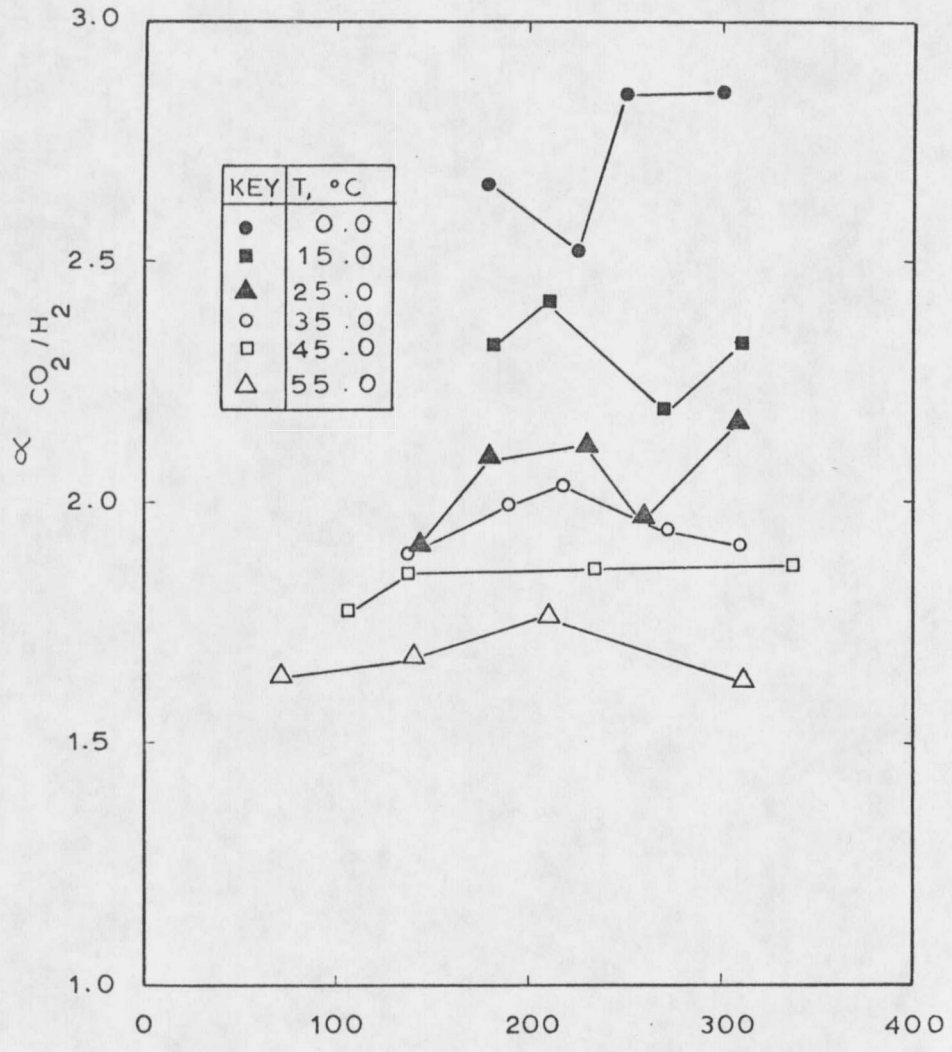

FIGURE V-28. SEPARATION FACTOR α VS. PARTIAL PRESSURE DIFFERENTIAL FOR CARBON DIOXIDE

mixtures, the diffusivity of the less permeable gas, in this case H_2, seems to increase with the concentration of the more permeable component, in this case CO_2, due to plasticizing effects. Basically the same conclusions are derived by analysis of the lean CO_2 mixture results. These data are plotted in Figure V-29 and Figure V-30. In this case, however, the plasticizing effects are much weaker, probably because of the very low CO_2 content of the feed gas (3.3 vol. %). It is interesting to note that the permeability coefficients for hydrogen are almost exactly the same as the permeability coefficients obtained with pure H_2 (Figure V-13). This suggests that the plasticizing effect of sorbed CO_2 at this low concentrations may be negligible.

The separation of CO_2/H_2 mixtures is more efficient at lower temperatures and higher CO_2 partial Pressures. This conclusions could have been expected by inspection of the permeability coefficients of the pure components (Figure V-10 and Figure V-13). The maximum difference in the permeability coefficients of CO_2 and H_2 occurs at lower temperatures and higher pressures. Based on this, the effectiveness of the separation of CO_2/H_2 mixtures may increase considerably by increasing the partial pressure of CO_2 beyond the values tested in this study. For the range of pressures considered, the highest separation factor obtained was 2.86 at 0°C, with a total pressure of about 732 psia and with 42 vol. % CO_2 in the exhaust gas. The permeate analyzed about 67.5% CO_2.

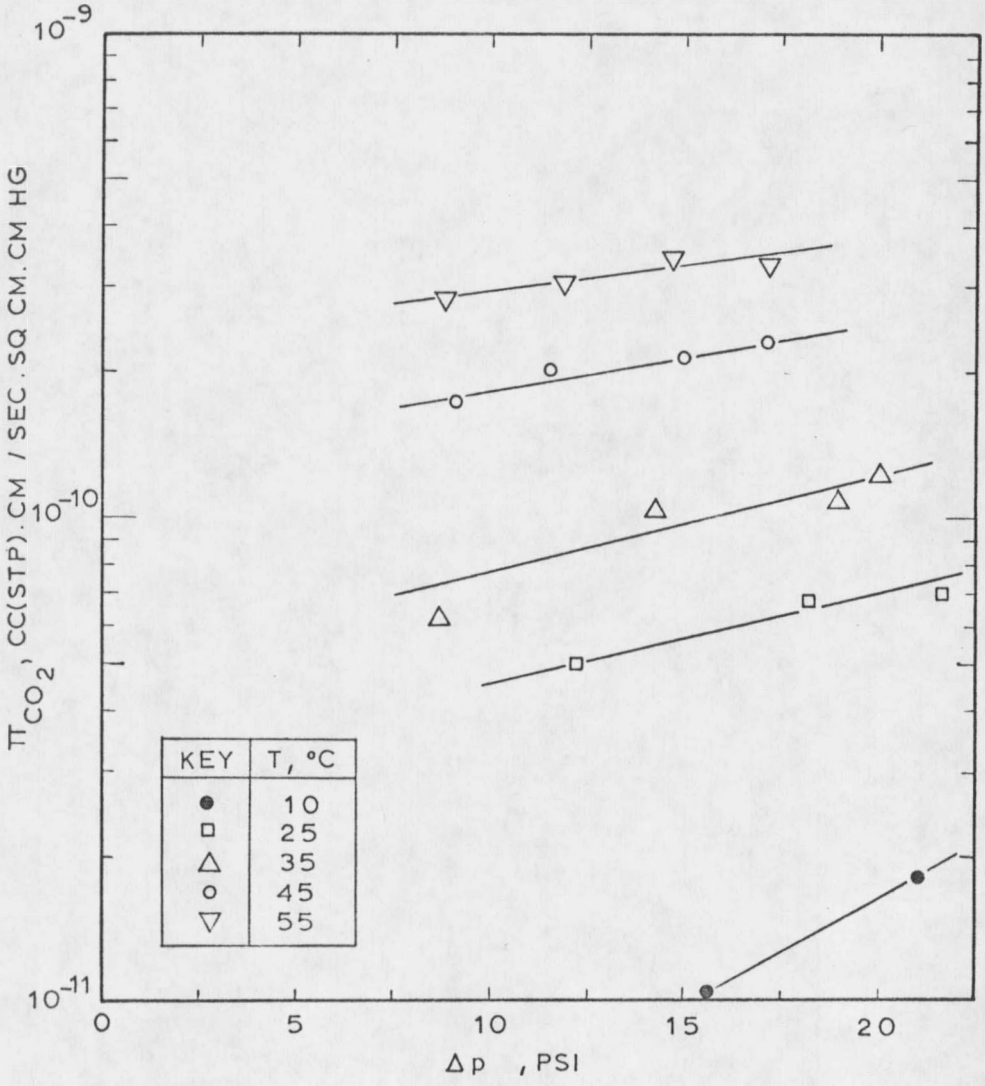

FIGURE V-29. PSEUDO PERMEABILITY COEFFICIENT VS. PARTIAL PRESSURE DIFFERENTIAL FOR CO_2

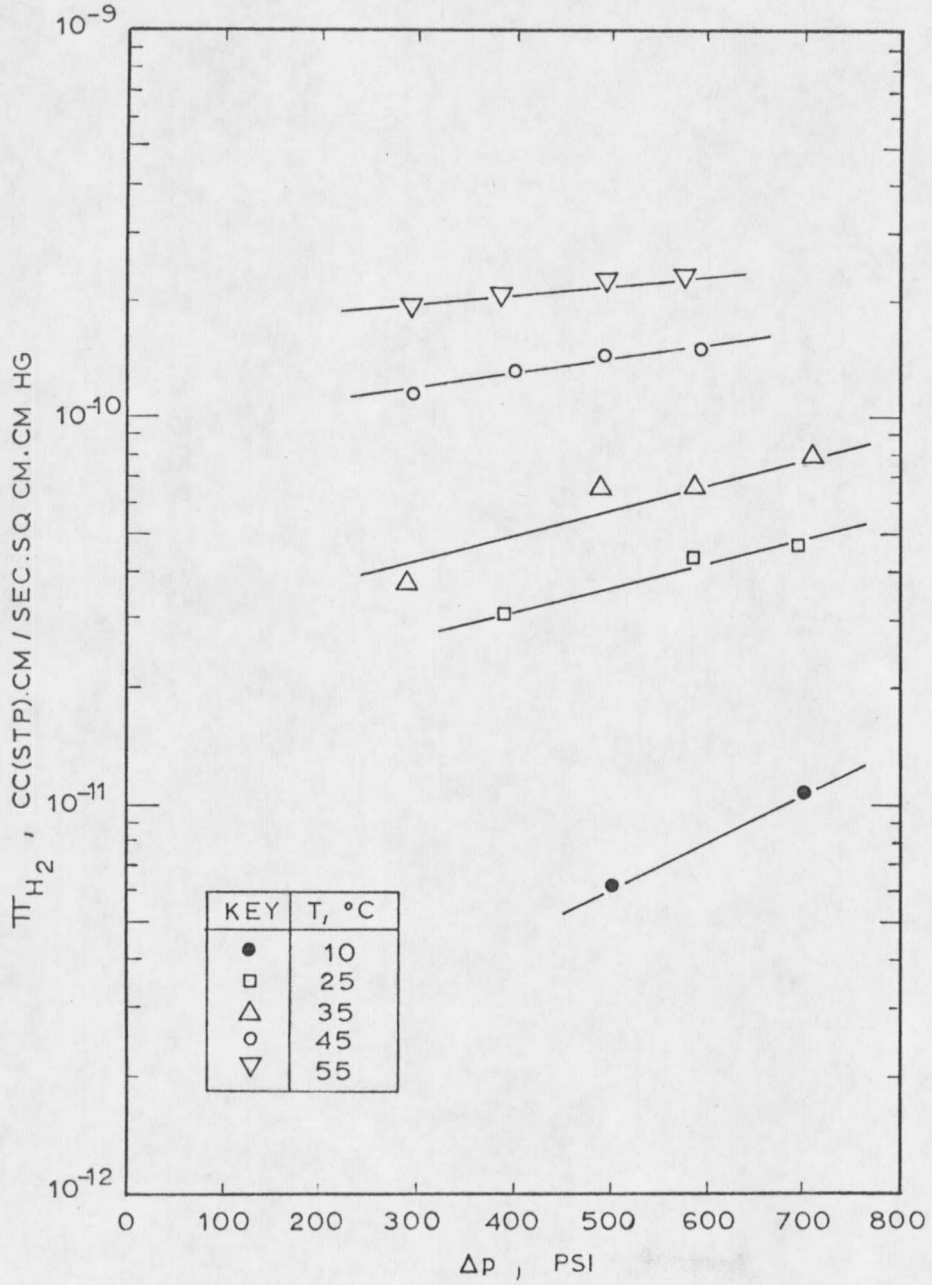

FIGURE V-30. PSEUDO PERMEABILITY COEFFICIENT VS. PARTIAL PRESSURE DIFFERENTIAL FOR H_2

I. ANALYSIS OF ERRORS

The reliability of the permeability measurements could be affected by various possible sources of experimental error, the most important being:

1. Change in temperature of the gas contained in the lines connecting the constant temperature enclosure and the measuring device: the temperature was not allowed to change more than 0.1°C, but even this small temperature change could introduce an error of about 10% for the slower measurements, taking into account the volume of the permeate to be about 20 cc. This was true for gases like N_2 at the lowest temperature tested. For faster runs this error was negligible because the operation was almost perfectly isothermal.
2. Non-uniform film thickness: Multiple measurement of the films used were made with a precision micrometer. The average thickness difference was about 5% (based on 2mils membrane thickness).
3. For some gases, like CO_2, a net mass transfer was observed through the mercury slug. This effect was probably important for very low permeation rates, but became negligible for higher permeate flow rates.

CONCLUSIONS AND RECOMMENDATIONS

A. CONCLUSIONS

1. A permeation apparatus suitable for the determination of permeability coefficients of gas membrane systems has been developed. The apparatus is capable of operating at super-atmospheric pressures and super and sub-ambient temperatures.

2. Sulfolene modified vinylidene fluoride membranes were found to be very efficient membranes for the separation of sulfur dioxide from gaseous mixtures. The most effective separation was obtained with a 2 mils thick, 18 wt % sulfolene membrane on a solvent free basis. The permeation parameters for this membrane compare favorably with those reported in the literature for the separation of sulfur dioxide.

3. The permeability coefficient for sulfur dioxide were found to be four orders of magnitude greater than those for nitrogen, carbon monoxide, argon, oxygen, methane, ethane, ethylene and 1,3 butadiene; about 3 orders of magnitude greater than that of hydrogen and about two orders of magnitude greater than that of carbon dioxide.

4. The permeability coefficients for sulfur dioxide and carbon dioxide exhibit a non-linear exponential dependence on temperature and pressure. The dissolved gases exert a pronounced plasticizing influence on the membrane, which

results in permability coefficients being highly dependent upon the sorbed gas concentration.

5. The permeability coefficients for oxygen, hydrogen, methane, ethane, ethylene and 1,3 butadiene exhibit also exponential dependence on pressure and temperature.

6. The permeability coefficients for nitrogen, carbon monoxide and argon were found to be independent of pressure. The temperature dependence is of the exponential type.

7. The best separations of sulfur dioxide from sulfur dioxide-nitrogen mixtures were obtained at the lowest temperature tested and for the higher values of the partial pressure of sulfur dioxide. The sorbed gas exerts a pronounced plasticizing influence on the membrane, influence that is translated in pseudo-permeability coefficients for nitrogen that are higher than those determined using the pure gas, effect that lowers the degree of separation for this binary mixture. In spite of this, very good separations can be achieved. A 95.5 vol. % SO_2 permeate was obtained for an exhaust gas SO_2 concentration of 5.6 vol. %, with permeate flow rates of about 1×10^{-3} cc(STP)/cm^2.sec, at 0°C and 315 psia upstream pressure.

8. The separation of CO_2 from a CO_2/H_2 mixture was found to be feasible. The best results were obtained at the lower

temperatures and for the higher values of the upstream CO_2 partial pressure. The highest separation factor obtained was 2.86, at 0°C with a total pressure of about 732 psia and with 42 vol % CO_2 in the exhaust gas. The permeate analyzed 67.5% CO_2. The dissolved gas exerts a plasticizing influence in the membrane, the net effect being pseudo-permeability coefficients for H_2 higher than those obtained with the pure gas.

B. RECOMMENDATIONS

1. Even though the permeation apparatus possesses adequate sensitivity for determining the permeability coefficients even for very slightly soluble gases, the accuracy could be further improved by placing the whole permeation apparatus in a constant temperature enclosure.
2. Other techniques of making membranes should be investigated, techniques that allow higher concentrations of modifier in the membrane. Drying of the membrane at very low pressures and at low temperatures could prove useful. Also the drying of the membrane by selective diffusion of the solvent into another solvent, in which the polymer is not soluble, is also possible. Membranes of good consistency were made by immersion in water of a glass plate with the membrane

solution spread over it.

3. The search must be continued for a better modifier for SO_2 separations. The solubility of SO_2 in the chemical gives an initial information on its potential use as a modifier. Chemicals with high SO_2 solubilities and compatible physical characteristics should be tested systematically.

APPENDIX

NOMENCLATURE

c	Total molar concentration, moles/L^3
c_i	Molar concentration of component A, moles/L^3
D_{ij}	Binary diffusivity for system i-j, L^2/t
J_i^*	Molar flux of species i relative to the molar average velocity, moles/tL^2
K	Overall mass transfer coefficient, moles/tL^2
k_1	Constant
k_2	Constant
$k_{x,loc}$	Local mass transfer coefficient for the feed side of the permeation cell, moles/tL^2
$k^{\cdot}_{x,loc}$	Local mass transfer coefficient in high mass transfer for the feed side of the permeation cell, moles/tL^2
$k_{y,loc}$	Local mass transfer coefficient for the permeate side of the permeation cell, moles/tL^2
m_i	Solubility constant for species i in a Henry's law type relationship
N_i	Molar flux with respect to stationary coordinates, moles/L^3
P	Total pressure F/L^2
P_i	Permeability coefficient of component i, $L^3.L/t.L^2.F/L^2$, defined in equation III-15.
P_o	Reference value of the permeability coefficient, $L^3.L/t.L^2.F/L^2$
p_i	Partial pressure of i F/L^2
r	Ratio N_{Bo}/N_{Ao} for A binary mixture A-B

T	Absolute temperature
W_i	Molar flow rate of species i, Moles/t
x_i	Mole fraction of species i in feed side of the permeation cell
y_i	Mole fraction of species i in permeate side of the permeation cell
z	Rectangular coordinate, L

SUBSCRIPTS

1	High pressure side of permeation cell
2	Low pressure side of permeation cell
A	Component A
B	Component B
o	Interface
b	Bulk Stream

GREEK LETTERS

α_i	Separation factor of species i
π_i	Pseudo-permeability coefficient of species i, $L^3.L/t.L^2.F/L^2$, defined in equation III-21.

BIBLIOGRAPHY

1. Stern, S. A., Proceedings of the Symposium on Membrane Processes in Industry, Southern Research Institute, Birmingham, Alabama, May, 1969, pg. 196

2. Stern, S. A., T. F. Sinclair; P. J., Garris, N.P. Vahldieck, and P. M. Mohr, Ind. Eng. Chem., 57, 49 (1965)

3. Robb et al., U. S. Patent No. 3,335,545, as cited in W. J. Ward III, Liquid Membrane for Sulphur Dioxide Extraction, U. S. Patent No. 3,503,186

4. Ward, W. J., U. S. Patent No. 3,396,510 as cited in W. J. Ward III, Liquid Membrane for Sulphur Dioxide Extraction, U. S. Patent No. 3,503,186

5. Ward, W. J., U. S. Patent No. 3,503,186, Liquid Membrane for Sulphur Dioxide Extraction

6. Seibel, D. R. and F. P. McCandless, "Separation of Sulfur Dioxide and Nitrogen by Permeation Through A Sulfolane Plasticized Vinylidene Fluoride Film", Ind. Eng. Chem. Pro, Vol 13, No. 1 pp. 76-78

7. Tajar, J. G. and I. F. Miller, "Facilitated Versus Non-Faciliated Permeation Through Polymer Membranes", AIChE Symposium in Houston, Texas, 1971, No. 76.

8. Bird, R. B., W. E. Stewart, E. N. Lightfoot, "Transport Phenomena", John Wiley & Sons, Inc., 1966, Pg. 638

9. Bird, R. B., W. E. Stewart, E. N. Lightfoot, "Transport Phenomena", John Wiley & Sons, Inc., 1966, Pg. 639-640.

10. Evnochides, S. K., "The Transport of Gases Through Polymeric Membranes", Ph.D. Thesis, Chemical Engineering Department, University of Houston, Texas, 1970, pg. 9

11. Evnochides, S. K., "The Transport of Gases Through Polymeric Membranes", Ph.D. Thesis, Chemical Engineering Department, University of Houston, Texas, 1970, pg. 10

12. Evnochides, S. K., "The Transport of Gases Through Polymeric Membranes", Ph.D. Thesis, Chemical Engineering Department, University of Houston, Texas, 1970, pg. 23

13. Li, N. N. and E. J. Henley, "Permeation of Gases Through Polyethylene Films at Elevated Pressures", AIChE Journal 10, 666 (1964).

14. Stannet, V. M., Szwarc, R. L., Bhangara, J. A. Meyer, A. W. Meyers, and E. E. Rogers, "Permeability of Plastic Films and Coated Paper to Gases and Vapors", Techical Association of the Pulp and Paper Industry (1962).

MONTANA STATE UNIVERSITY LIBRARIES
3 1762 10011806 4

D378
Z19
cop.2

Zavaleta, Ronanth
Selective permeation throughmodified vinylidene fluoride membranes

DATE	ISSUED TO

D378
Z19
Cop.2